Riparian Buffer Landscape Effects on Groundwater Flow Paths and Nitrate Occurrences in Groundwater near Streams of the Eastern Shore of Virginia

Paul Garret Probasco
Ocean City, New Jersey

M.S. Hydrogeology, Rensselaer Polytechnic Institute, 2003
B.S. Geological Sciences, Rutgers University, 2000

A Thesis presented to the Graduate Faculty
of the University of Virginia in Candidacy for the Degree of
Master of Science

Department of Environmental Sciences

University of Virginia
May, 2010

Janet P Herman

Todd Scanlon

Abstract

Elevated concentrations of nitrate occur in groundwater throughout the United States due to the widespread application of nitrogenous fertilizers associated with agricultural land uses. Forested stream buffers, which separate upland agricultural areas from stream channels, are recognized for their importance as locations of groundwater nitrate removal through plant uptake and denitrification. An understanding of the groundwater hydrology of the buffer subsurface is important in being able to predict where denitrification can occur, since the groundwater hydrology determines the locations in which groundwater with elevated nitrate will intercept available supplies of organic matter. Previous studies have identified differences in the pattern of groundwater flow through riparian floodplains within stream buffers, which was related to differences in their ability to remove nitrate by denitrification. In this study, the effect of forested buffer topography on groundwater flow paths and nitrate occurrences in groundwater near streams of the Eastern Shore of Virginia was investigated. A field and groundwater modeling-based approach of five buffer-stream sites was undertaken to address the objectives of this study. Observations of groundwater nitrate, hydraulic head and soil/sediment characteristics were collected in transects oriented approximately perpendicular to the stream channel at each site. Groundwater sampling results indicate groundwater inputs to the buffer at each site generally contain elevated nitrate, with monitoring wells located near the agricultural field-buffer boundary having mean nitrate concentrations ranging from 0.0 to 7.1 mg/L. The mean nitrate concentration for the outer monitoring well at one site (4.6 mg/L) does not reflect nitrate occurrences beneath

the streambed, where a mean nitrate concentration of 12.4 mg/L was observed at a depth of 0.88 m below the streambed. A semi-normal distribution of elevated nitrate was observed for hillslope piezometers, which contrasted with a bimodal distribution of nitrate for riparian floodplain piezometers. For the riparian floodplain piezometers, a group with relatively low nitrate concentrations was observed along with a second group having elevated nitrate concentrations. The results of the MODFLOW groundwater flow modeling indicate riparian floodplains have an effect on groundwater flow paths, with a downward deflection of the shallow groundwater flow paths generally occurring at the hillslope-floodplain transition. At one buffer site, the downward deflection of groundwater flow paths at the hillslope-floodplain transition agreed with observations of relatively low mea nitrate concentrations ($\leq$ 0.4 mg/L) in shallow floodplain groundwater (< 2 m below ground surface) and observations of elevated mean nitrate concentrations (3.6 to 4.1 mg/L) in the relatively deep floodplain groundwater ($\geq$ 2 m below ground surface). A clear relationship between groundwater flow paths and nitrate occurrences at sites with relatively narrow riparian floodplains was not obtained. Based on the observations and groundwater modeling results from this study, a lack of elevated nitrate may be observed in shallow groundwater (< 2 m below ground surface) within relatively extensive riparian floodplains of the Eastern Shore of Virginia due to a by-pass of groundwater beneath the riparian floodplain sediments.

Acknowledgments

My project could not have been completed without funding from outside organizations and agencies, and for their support I am grateful. Specifically, this project was funded by a U.S. Department of Education Graduate Assistance in Area of National Need (GAANN) fellowship award P200A030055 (P.I. Teresa Culver), and a graduate student research grant from the Geological Society of America. In addition, logistical support for field activities was provided by the Anheuser-Busch Coastal Research Center with funding from the National Science Foundation (DEB 0621014, P.I. Karen McGlathery) for the Virginia Coast Reserve Long-Term Ecological Research program.

I would like to thank my advisor, Janet Herman, for her help and advice throughout my project, as well as the other members of my committee, Aaron Mills and Todd Scanlon. I am very grateful for the guidance provided by Aaron Mills for much of my fieldwork, and the assistance from Todd Scanlon with groundwater model development.

Numerous graduate and undergraduate students helped me with my project. I am very thankful to all who endured the biting insects and poison ivy that was abundant at my field sites during the summer months. Graduate students that gave up their time to assist me in the field include Dirk Koopmans, Adam Benthem, Sean McLoughlin and Kirby Webster, and undergraduate students who provided fieldwork help include Nathan Farrar, Javier Longoria and Daniel Michaelson. George McFadden provided me a lot of help both in the field and in the lab, and Arden Spencer Cox assisted me with numerous lab analyses. I also must acknowledge Sam Flewelling for his willingness to discuss

research topics with me and to help me in running the ion chromatograph. I am also very thankful for the help of Joe Battistelli and Kristina Reid Black in the lab.

Finally, I am very grateful and appreciative of all my friends and family who provided me so much encouragement during the difficult times during my graduate program. It is their support which really helped me see this project through to completion.

Table of Contents

Abstract ii
Acknowledgments iv
Table of Contents vi
List of Tables viii
List of Figures ix
Introduction 1
1.1 Background literature 1
1.2 Research Questions 10
1.3 Study Site 11
2 Methods 16
2.1 Groundwater, Surface Water, and Sediment Sampling and Analysis 16
2.2 Soil Boring Investigation 22
2.3 Hydraulic conductivity measurements 24
2.4 Surveying 26
2.5 Numerical groundwater model development 27
2.5.1 Model objectives and selection 27
2.5.2 Model description 27
2.5.3 Site-specific model setup 32
2.5.4 MODFLOW output post-processing 35
2.6 Landscape and depth-based NO_3^--N distributions 36
3 Results 37
3.1 Streambed sediment characteristics and porewater NO_3^--N 37
3.2 Phillips Creek hillslope-riparian soil and sediment composition 40
3.3 Buffer topography and landscape 42
3.4 Hydraulic conductivities determined from slug tests 48
3.5 Groundwater and surface water NO_3^--N 50
3.6 Phillips Creek floodplain site DOC results 53
3.7 Groundwater dissolved oxygen, sulfide and NO_3^--N field analytical results 55

3.8 Groundwater modeling results 55
3.9 In-stream piezometer vertical hydraulic gradients observations 61
4 Discussion 63
Bibliography 74
Appendix A – Groundwater model input parameters 78
Appendix B – Soil and sediment core logs 83
Appendix C – Photographs of soil and sediment cores 109
Appendix D – Piezometer and monitoring well slug test water level recordings 122
Appendix E – Groundwater and surface water NO_3^--N results 125
Appendix F – Field dissolved oxygen, nitrate-N and sulfide data 135

List of Tables

Table		Page
1	Forested buffer and stream site characteristics	15
2	Streambed sediment core identifications and sampling dates	18
3	Vertical and horizontal hydraulic conductivity (K) measurements of streambed sediment cores	39
4	Buffer slopes	47
5	Landscape categorization of buffer piezometers	48
6	Hydraulic conductivities determined by slug tests	49
7	Average NO_3^--N concentrations at groundwater and surface water sampling locations	51
8	DOC analytical results for PC floodplain site groundwater samples collected on 30 January 2009	54
9	Volumetric percent discrepancies computed by MODFLOW for each site groundwater flow simulation	61
10	Vertical hydraulic head gradients of in-stream piezometers	62
E.1	Cobb Mill Creek floodplain groundwater and surface water NO_3^--N (mg/L)	126
E.2	Phillips Creek upland groundwater and surface water NO_3^--N (mg/L)	128
E.3	Phillips Creek floodplain groundwater and surface water NO_3^--N (mg/L)	129
E.4	Coal Kiln groundwater and surface water NO_3^--N (mg/L)	132
F.1	Field DO, NO_3^--N and S^{2-} analytical results	136

List of Figures

Figure		Page
1	Map of Eastern Shore of Virginia with locations of three stream sites	14
2	Cobb Mill Creek	19
3	Phillips Creek	19
4	Coal Kiln	19
5	Phillips Creek floodplain site with locations of soil boring points	23
6(a-g)	Streambed porewater NO_3^--N and organic matter profiles at study sites	38
7(a-b)	Organic matter concentrations with median depth in streambed sediment cores from (a) Phillips Ck. floodplain and (b) Coal Kiln	40
8	Cross-sectional view of subsurface at Phillips Creek floodplain site	41
9(a-b)	Total organic content of soil/sediment in cores located near (a) the hillslope/floodplain boundary, and in (b) cores located on the hillslope	42
10	Cobb Mill Creek hillslope site with piezometer locations and surface topographic contours shown	43
11	Cobb Mill Creek floodplain site with surveyed points and topographic profile	44
12	Phillips Creek floodplain site with surveyed points and topographic profile	45
13	Phillips Creek upland site with surveyed points and topographic profile	46
14	Coal Kiln site with surveyed points and topographic profile	47

Figure		Page
15	Mean piezometer-based NO_3^--N concentration distributions for the Cobb Mill Creek hillslope site and the four other sites investigated in this study	53
16(a-b)	Mean NO_3^--N distributions for piezometers by (a) landscape and (b) depth	54
17	Steady-state, hydraulic head contours of subsurface at CMC hillslope site	56
18(a-b)	Steady-state, groundwater flow paths determined from MODFLOW and MODPATH (a), and groundwater flow vectors based on MODFLOW output for the CMC floodplain site (b)	57
19(a-b)	Steady-state, groundwater flow paths determined from MODFLOW and MODPATH (a), and groundwater flow vectors based on MODFLOW output for the PC upland site (b)	58
20(a-b)	Steady-state, groundwater flow paths determined from MODFLOW and MODPATH (a), and groundwater flow vectors based on MODFLOW output for the PC floodplain site (b)	59
21(a-b)	Steady-state, groundwater flow paths determined from MODFLOW and MODPATH (a), and groundwater flow vectors based on MODFLOW output for the CK site (b)	60
22(a-d)	Close-up view of groundwater flow vectors in and near floodplain sediments at (a) CMC floodplain, (b) PC upland, (c) PC floodplain and (d) CK	68
A.1	CMC floodplain hydraulic conductivity zones	79
A.2	PC upland hydraulic conductivity zones	80
A.3	PC floodplain hydraulic conductivity zones	81
A.4	Coal Kiln hydraulic conductivity zones	82
D.1	Water level recording of slug tests completed at CMC floodplain on 14 July 2009	123

Figure		Page
D.2	Water level recording of slug tests completed at PC floodplain site on 16 July 2009	123
D.3	Water level recording of slug tests completed at PC floodplain and upland sites on 16 July 2009	124
D.4	Water level recording of slug tests completed at Coal Kiln on 18 July 2009	124

Introduction

1.1 Background literature

Occurrences of elevated nitrate concentrations in groundwater are recognized throughout the United States (Hamilton and Helsel, 1995). The high mobility of the nitrate ion, combined with the widespread application of manure and synthetic nitrogenous fertilizers, causes nitrate to be a common groundwater contaminant. Nitrate in groundwater is a concern because it can impair drinking water quality where the unconfined aquifer is the source of water supply, and because it can lead to decreased surface water quality for surface water bodies that are groundwater fed. Nitrate that reaches streams and rivers can eventually be transported to estuaries, where it can contribute to the eutrophication and subsequent onset of hypoxia and anoxia in these N-limited aquatic systems (Paerl, 1997). Increases in N loading to estuaries from groundwater and other anthropogenic sources have caused eutrophic conditions to develop in the majority of estuaries in the United States (Bricker et al., 2007).

In humid regions of the United States, groundwater is the major source of streamflow, and groundwater and surface water in these regions can therefore be considered a single hydrologic system (Winter et al., 1999). Within these systems, groundwater flow can in a general way be described as movement from upland areas of recharge to lowland areas of discharge (Freeze and Cherry, 1979), which typically coincide with surface water bodies. In between the areas of recharge and discharge, groundwater flows through subsurface soils and either unconsolidated sediments or bedrock fractures, where dissolved species can interact with the aquifer materials. The

extent to which dissolved species interact with aquifer materials has a large effect on the concentrations of these dissolved species in groundwater-fed streams.

Nitrate that is transported in upland soil water to the water table has the potential to be removed from groundwater prior to being discharged to surface water. Early studies of nitrate fate in agricultural watersheds recognized the ability of riparian forests to remove nitrate from groundwater before it discharged to stream channels (Lowrance et al., 1984; Peterjohn and Correll, 1984; Lowrance, 1992). In the studies by Lowrance et al. (1984) and Peterjohn and Correll (1984), nitrate removal was identified through a mass balance approach, in which N mass inputs to riparian forests were observed to exceed N mass losses in streamflow. Lowrance (1992) observed nitrate removal in groundwater by decreases in the ratio of nitrate to chloride along a groundwater flow path. Plant uptake was identified as a removal mechanism by Lowrance et al. (1984) and Peterjohn and Correll (1984) through biomass measurements in the riparian forest, with the remainder of nitrate losses being attributed to denitrification, the microbial transformation of nitrate to gaseous N under anaerobic conditions. Denitrification is a multi-step reaction that can be represented by the following net equation (unbalanced):

$$NO_3^- + C_{org} \rightarrow CO_2 + H_2O + N_2 \qquad (1).$$

Early denitrification measurements in riparian forest studies consisted of measuring denitrification potential, or the maximum rate at which microorganisms can reduce nitrate to nitrous oxide under laboratory conditions, along vertical profiles from the surface (Groffman et al., 1992; Lowrance, 1992). In the studies by Groffman et al. (1992) and

Lowrance (1992), measurements of denitrification potential were not in agreement with observed losses of subsurface nitrate.

Riparian forests, or zones, commonly refer to the forested strips of land located between upland agricultural fields and stream channels (Lowrance, 1992). From an ecological standpoint, riparian zones represent the area of land adjacent to a stream channel that has interactions with both the terrestrial and aquatic environments (Gregory et al., 1991). Terrestrial interactions include inputs of sediment to the riparian forest from upland areas by overland flow, and biogeochemical cycling of nutrients derived from upland sources through overland or groundwater flow. Aquatic interactions include delivery of terrestrial sediments and nutrients to the stream channel, and deposition of sediment on the land surface from stream flooding events. For the latter case, the portion of land adjacent to the stream channel that comprises the floodplain represents the lateral extent of the riparian zone. A more general term to describe the wooded area between agricultural fields and a stream channel would be a buffer, which includes a hillslope portion and possibly a riparian floodplain portion. In this paper, the hillslope will be considered a separate landscape from the relatively flat floodplain.

For nitrate to be removed by denitrification, it is critical for groundwater with elevated nitrate to intercept supplies of organic matter (Hill, 1996). This removal mechanism is desirable because it produces a net removal of N from the aquatic system, and not just a temporary storage in biomass that occurs with plant uptake. At many stream sites, the organic-rich streambed sediments often are the location where nitrate is removed by denitrification before groundwater discharges to surface water (Galavotti,

2004; Gu et al., 2007; Domagalski et al., 2008). Other studies have identified the occurrence of denitrification where nitrate in groundwater intercepts organic matter supplies in the hillslope and floodplain portions of a forested buffer (Vidon and Hill, 2004a), or at locations where groundwater with elevated nitrate interacts with reduced mineral deposits (*e.g.* glauconitic minerals, pyrite) in sediments of an unconfined aquifer (Bohlke and Denver, 1995; Tesoriero et al., 2000). For unconfined aquifers without reduced mineral deposits, which are generally much more prevalent than aquifers with reduced minerals, identifying labile organic matter occurrences becomes highly important for predicting where nitrate removal by denitrification could occur. Organic matter may be very localized and difficult to spatially predict (Gold et al., 1998), or it may be associated with recognizable landscape changes, such as the transition from an upland to riparian landscape, which can facilitate development of biogeochemical "hot-spots" (McClain et al., 2003).

The ability of groundwater hydrology to drive nitrate removal at a stream-side buffer requires an understanding of the underlying hydrogeology. The underlying hydrogeology determines the general direction and velocity of groundwater flow through the subsurface, which can affect the extent to which nitrate can be removed by denitrification. The direction of groundwater flow through the buffer subsurface determines if groundwater with elevated nitrate will intercept available supplies of organic matter, and the velocity of groundwater flow is inversely proportional to its residence time, which can control the extent to which nitrate is removed by denitrification in sandy, organic-rich streambed sediments (Gu et al., 2007).

The ability of buffer hydrogeology to control nitrate removal in turn requires knowledge of several hydrogeologic variables, including aquifer depth, hydraulic conductivity and in unconfined aquifers, the water table gradient. A useful approach that can be taken to understand how these hydrogeologic variables affect groundwater flow is to consider the groundwater head distribution within a two-dimensional, "vertical slice" view of the buffer subsurface. This approach to interpreting groundwater flow is justified where topographic gradients normal to valley contours are greater than longitudinal gradients associated with streams (Toth, 1963). Tóth (1963) used a theoretical approach to determine the effects of aquifer thickness and topography on groundwater flow paths for a hypothetical undulating land surface. The results from his study indicate both local and regional flow systems will develop within a hypothetical unconfined aquifer system, with local flow systems having relatively short and shallow flow paths, and deep flow systems having relatively long and deep flow paths. In a riparian zone setting, groundwater within the unconfined aquifer includes shallow, local flow systems that originated from recharge on the buffer slope adjacent to the riparian zone (Hill, 2000), and deep flow systems of greater length where the source of water is recharge in relatively distant, upland areas compared to the shallower flow systems (Tesoriero et al., 2000). The shallow and deep groundwater flow paths within the riparian zone subsurface can also have distinct differences in nitrate concentration (Hill, 1990).

More recently, several field-based studies have been conducted to improve our understanding of groundwater hydrology within hillslope and riparian landscapes, with an interest in how the hydrology relates to nitrate transport (Burt et al., 1999; Vidon and

Hill, 2004b; Angier et al., 2005). Vidon and Hill (2004b) investigated the groundwater hydrology of eight riparian zone sites in southern Ontario, Canada, that are comprised of glacial sediments and have a range in topography from relatively flat riparian to hillslope-dominated. They observed that when upland groundwater and the stream channel were hydrologically connected, groundwater flow paths within a 2-D vertical plane were parallel or upward to the land surface for all sites in their study. In seven of their eight sites, 90% or higher nitrate removal occurred in groundwater flowing laterally toward the stream channel, with the landscape variables affecting the distance required for 90% nitrate removal being the thickness of the surficial aquifer, the upland-riparian zone land slope, and the composition of the soils and subsurface sediments (Vidon and Hill, 2004c). Where upward groundwater flow occurred, discharge of groundwater to the land surface was observed at some riparian zone sites (Vidon and Hill, 2004b). A discharge of groundwater to the land surface was also observed by Angier et al. (2005) along a first-order stream in the mid-Atlantic coastal plain of Maryland. Groundwater seeps within riparian zones that produce small rivulets can be important sources of nitrate in stream water when these rivulets discharge directly to the stream channel (Vidon and Hill, 2004c; Angier et al., 2005).

Other authors report deflection of groundwater flow paths at the hillslope-floodplain boundary due to sharp differences in hydraulic conductivity between hillslope materials and the fine-grained floodplain sediments (Burt, 1997; Burt et al., 1999). The movement of groundwater at the hillslope-floodplain boundary in a downward direction to more permeable sediments can allow groundwater to by-pass the denitrification

potential of the floodplain sediments (Burt et al., 1999). An upward deflection of groundwater flow paths at the hillslope-floodplain boundary can also occur, as was modeled by Puckett et al. (2002) for a riparian zone site in Minnesota. The presence of upward-dominated groundwater flow within the riparian floodplain may cause misinterpretation of the nitrate removal ability of riparian floodplain sediments, with differences in groundwater redox chemistry across a floodplain being due to differences in groundwater age, and not from reactions occurring as groundwater moves horizontally through the floodplain sediments (Puckett et al., 2002). The ability of groundwater to by-pass riparian floodplain sediments is also controlled by the depth to the confining unit underlying the surficial aquifer, with a relatively shallow confining unit causing groundwater with elevated nitrate to flow closer to reduced floodplain sediments than it would with a relatively deep confining unit. Within the outer coastal plain of the mid-Atlantic, the thickness of the unconfined aquifer has been identified as a key constraint on the occurrence of by-pass flow, and subsequently, the nitrate removal ability of riparian buffers (Lowrance et al., 1997).

The Delmarva Peninsula comprises much of the outer coastal plain of the mid-Atlantic region and has occurrences of elevated nitrate in groundwater throughout the peninsula (Hamilton and Helsel, 1995; Denver et al., 2004). The natural background concentration of NO_3^--N in shallow groundwater of the Delmarva Peninsula, which provides a reference for identifying occurrences of elevated NO_3^--N, is 0.4 mg/L (Hamilton et al., 1993). Denver et al. (2004) reported a median nitrate concentration (as N) of 5.4 mg/L in samples from 29 wells located in the surficial aquifer of agricultural

areas within the peninsula. Agriculture is a major land use in this region, representing 48% of the landcover (Denver et al., 2004), and is, therefore, the major source of nitrate in groundwater due to the application of manure and synthetic fertilizers to meet crop N requirements. The sandy texture of soils in this region also contributes to the widespread occurrence of nitrate in groundwater because they typically are aerobic and have a relatively high permeability. Aerobic conditions in soil prevent losses of nitrate through denitrification, and the permeable nature of sandy soils allows nitrate to be transported to the saturated zone before being taken up by plants or denitrified by microorganisms in the root zone.

The Eastern Shore of Virginia covers the southern portion of the Delmarva Peninsula and has been the site of previous studies on the hydrologic and biogeochemical mechanisms controlling the fate of nitrate in groundwater near low-order non-tidal streams (Speiran, 1996; Gu, 2007; Gu et al., 2007; Gu et al., 2008). Gu (2007) investigated nitrate transport and delivery to Cobb Mill Creek, where a forested hillslope is present along the study reach and separates the stream channel from upland agricultural areas. Nitrate-N remains elevated in groundwater throughout the subsurface of the hillslope at this site, with NO_3^--N present at a concentration of approximately 12 mg/L in groundwater samples collected one meter below the streambed (Gu et al., 2007; Gu et al., 2008). The groundwater-surface water interface at this site is the critical location for nitrate removal, as organic-rich streambed sediments provide conditions favorable for denitrification (Galavotti, 2004). Groundwater discharge to surface water occurs through the streambed sediments at this site, and the extent of nitrate removal in groundwater by

denitrification is controlled by the rate of groundwater flow through the streambed sediments (Gu et al., 2007). In a study by Speiran (1996) of Walls Landing Creek in the Eastern Shore of Virginia, the forested buffer that separates the stream channel from the upland agricultural field consists of a hillslope and riparian floodplain portion. Groundwater NO_3^--N concentrations were noticeably different with depth at the riparian floodplain of this site, with NO_3^--N not detected in groundwater sampled at 1.1 m below ground surface (bgs), but detected at 13-14 mg/L in groundwater at 2.0 m bgs (Speiran, 1996).

Although recent studies have improved our understanding of the effects buffer landscape (*i.e.*, topography, subsurface sediment texture and aquifer thickness) has on nitrate attenuation in groundwater, there is still a lack of agreement as to how much of a N sink riparian floodplains can provide. While a downward deflection of groundwater flow away from floodplain sediments was reported by Burt et al. (1999), Vidon and Hill (2004c) report occurrences of horizontal groundwater flow and nitrate removal within riparian floodplain landscapes. In the conceptual model by Vidon and Hill (2004c) for nitrate removal in riparian zones, no distinction is made in the N removal function of relatively flat riparian zones (slope <5%) with relatively thick aquifers (>6 m) from that of riparian zone sites with intermediate aquifer thickness (2-6 m). The N removal function of relatively flat riparian zone sites with an aquifer thickness <2 m would be small due to discontinuous groundwater inputs to the riparian zone (Vidon and Hill, 2004c). For wooded buffer sites like those in the Eastern Shore of Virginia, where unconfined aquifer thickness is generally greater than 6 m, the conceptual model for

nitrate removal in riparian zones by Vidon and Hill (2004c) states that buffers with a land surface slope >5% will function as a small N sink due to the potential for elevated nitrate in groundwater to by-pass riparian sediments, while buffers with a land surface slope <5% will function as a small to medium N sink. The range in the magnitude of the N sink function of buffers with a slope <5% in their study is attributed to the greater range in groundwater inputs to buffers with gently sloping land surfaces compared to the buffers with steeper slopes (Vidon and Hill, 2004c).

1.2 Research Questions

The relatively thick (>6 m) unconfined aquifer of the Eastern Shore of Virginia allows subsurface inputs of groundwater to stream buffers to be maintained year-round. In this region, buffer topography and both the texture and lithology of soils and subsurface sediments are the landscape variables that could affect groundwater nitrate occurrences in the riparian zone. Buffers in the Eastern Shore of Virginia vary between hillslope and floodplain landscapes, where differences in topography can influence the texture and lithology of soils and subsurface sediments. Although differences in buffer topography and both soil and subsurface sediment characteristics may clearly be present between hillslope and riparian floodplain landscapes, there is still difficulty in being able to predict how riparian floodplains in the Eastern Shore of Virginia affect the occurrence of elevated NO_3^--N in groundwater. To improve our understanding of how buffer topography affects nitrate in groundwater, the following research questions were developed:

- What is the effect of forested stream buffer topography on groundwater flow paths?
- How do differences in forested stream buffer topography and possibly groundwater flow paths relate to nitrate occurrences in groundwater near streams of the Eastern Shore of Virginia?

A field measurement and groundwater modeling-based approach of five unique forested buffer-stream sites was undertaken to address these research objectives. The first research question addresses the need to establish the subsurface hydrologic framework at each site, and the second research question builds on the first by relating the subsurface hydrology to observations of nitrate in groundwater within each site.

1.3 Study Site

The focus of this study is the Eastern Shore of Virginia, which geologically represents the eastern portion of a seaward thickening wedge of unconsolidated sedimentary deposits (Mixon, 1985). The sedimentary wedge is comprised of alternating layers of coarse and fine-grained sediments that range in age from early Cretaceous to Holocene, and originated in transgressive and regressive marine environments (Meng and Harsh, 1988). The stratigraphy of sedimentary deposits also relates to the hydrogeology of this region, with fine-grained sediments functioning as the confining unit to the surficial, unconfined aquifer. The topography in this region is relatively flat, with upland areas occurring in the central part of the Delmarva Peninsula at elevations of 35 to 60 feet above sea level (asl), and lowland areas on the west and east sides of the peninsula which gradually slope toward the Chesapeake Bay and Atlantic Ocean, respectively (Mixon, 1985). Land use in the region reflects the rural nature of the region, and is mainly a mixture of agriculture and forested land uses, with localized areas of urban development

around towns. Climatologically, the Eastern Shore of Virginia is characterized by warm, humid summers and mild winters. The average annual precipitation, based on data from the NOAA station in Painter, Virginia, is 43.35 inches per year (NOAA, 2004).

The geology and hydrogeology of the Eastern Shore of Virginia includes unconsolidated, sandy Quaternary sediments that are part of the surficial, unconfined aquifer of the region known as the Columbia aquifer (Meng and Harsh, 1988; Richardson, 1994). Geologically, there are two formations which comprise the Columbia aquifer in the study area – the Butlers Bluff Member of the Nassawadox Formation and the Wachapreague Formation. The Butlers Bluff Member of the Nassawadox Formation, which represents most of the study area, covers the upland, eastern side of the southern portion of the Eastern Shore of Virginia and is comprised of a fine to coarse pebbly sand (Mixon, 1985). Bordering the Nassawadox Formation to the east and in horizontal alignment is the Wachapreague Formation (units not vertically stacked). The Wachapreague Formation includes two separate units - an upper unit of medium to coarse gravelly sand, and a lower unit of fine to very fine sand mixed with clay and silt (Mixon, 1985). The thickness of the Columbia aquifer varies within the Eastern Shore of Virginia, and is controlled by the land surface topography and the elevation of the underlying Upper Yorktown confining unit (Richardson, 1994). In a study of the unconfined aquifer properties near Oyster, Virginia (southern Eastern Shore of Virginia), Hubbard et al. (2001) determined a mean hydraulic conductivity (K) value of 5.53×10^{-3} cm s^{-1} for aquifer sediments. Burger and Belitz (1997) measured K values in sediment cores collected from the wall of a borrow pit in Oyster, Virginia, and determined slightly

greater K values were present in the horizontal direction compared to the vertical direction in most cores, with anisotropic ratios ranging from 1.33 to 1.57. Recharge to the Columbia aquifer is reported to vary spatially, and studies of baseflow measurements indicate net recharge ranges from 3.5 to 16.5 inches per year (Speiran, 1996). The Columbia aquifer is an important resource in the Eastern Shore of Virginia because it is used for domestic water supply (Denver et al., 2004).

Five wooded buffer-stream sites were selected in this study to represent the variability present in both the width and topography of the forested stream buffers that are present within the larger study area of the Eastern Shore of Virginia. Topographic differences at each forested buffer-stream site will be defined in this study by a distinction between upland/hillslope landscapes, and riparian floodplain landscapes. The five forested buffer sites are located at Cobb Mill Creek, Phillips Creek and Coal Kiln stream (Figure 1), with two separate sites designated for Cobb Mill Creek and Phillips Creek. Cobb Mill Creek contains a hillslope buffer site (investigated previously) and a second site located upstream of the hillslope site where the forested buffer transitions from a hillslope to floodplain landscape. Phillips Creek includes one site that predominantly contains an upland forest landscape within the stream buffer, and a second site located downstream of the upland forest site that contains both a hillslope and floodplain. The sites at Cobb Mill Creek (CMC) and Phillips Creek (PC) will be referenced herein as the CMC hillslope, CMC floodplain, PC upland, and PC floodplain sites. The Coal Kiln (CK) site contains a vegetated buffer with a hillslope and floodplain portion. At the CMC floodplain, PC floodplain and CK sites, the floodplain represents

Figure 1. Map of Eastern Shore of Virginia with locations of three stream sites.

roughly half of the forested buffer between the agricultural field and stream channel. The widths of each buffer, expressed as the distance of a straight line drawn normal to topography and extending from the agricultural field-woods boundary to the stream channel, range from 8 m at Coal Kiln to 90 m at the CMC floodplain site. A tile drain outlet was observed in the stream bank at Coal Kiln located south of the stream channel; as a result, the buffer on the north side of the stream channel was investigated to avoid engineered effects on groundwater flow through the stream buffer. Tile drains were not observed at Cobb Mill Creek and Phillips Creek.

Although noticeable differences in buffer topography and width are present among the sites in this study, the hydrogeology of each study site is similar due to the Columbia aquifer being the single surficial, unconfined aquifer of the Eastern Shore of

Virginia (Richardson, 1994). Being part of a single unconfined aquifer, the subsurface sediments at each study site are likely to be very similar and comprised of predominantly unconsolidated sands. A site-wide similarity in the characteristics of the unconfined aquifer sediments is further supported by the similarity in the underlying Quaternary geologic formations in the study region. At the Cobb Mill Creek and Phillips Creek sites, the subsurface sediments are part of the Butlers Bluff Member of the Nassawadox Formation, while the subsurface sediments at the Coal Kiln site are located at the boundary between the Nassawadox and Wachapreague Formations (Mixon, 1985). Characteristics of each forested buffer-stream site, including stream order, width, topography, vegetation and aquifer thickness, are summarized in Table 1.

Table 1. Forested buffer and stream site characteristics.

Site	Stream order	Width (m)	Vegetation type	Aquifer thickness (m)
Cobb Mill Ck. hillslope	2nd	70	Mixed deciduous/evergreen	10[a]
Cobb Mill Ck. floodplain	2nd	70	Mixed deciduous/evergreen	10
Phillips Ck. upland	1st	16	Mixed deciduous/evergreen	12.8[b]
Phillips Ck. floodplain	1st	35	Mixed deciduous/evergreen	12.8
Coal Kiln	2nd	8	Scrubby wooded/herbaceous	15.5

Table notes: a: Cobb Mill Creek site aquifer thickness is from (Hubbard et al., 2001).
b: Phillips Creek and Coal Kiln aquifer thickness values were determined using the upper elevation of the Yorktown confining unit observed at the nearest USGS borehole to each site (Richardson, 1994), and the elevation of the land surface at each site from a 30 m USGS digital elevation model (DEM).

2 Methods

2.1 Groundwater, Surface Water, and Sediment Sampling and Analysis

Field site instrumentation and investigation began in March 2007 and continued through July 2009. Initial field activities at each site included installation of piezometers, collection of streambed sediment porewater samples, and collection of sediment cores at the location of porewater sampling. Porewater samples were obtained by pushing a 0.3 cm diameter stainless steel mini-drive point piezometer (MDPP) with pointed tip into the streambed at multiple depths. Porewater samples were generally collected at depths of 5 cm, 10 cm, 20 cm, 30 cm, 40 cm, 50 cm and 60 cm below the streambed. Aqueous samples were obtained with use of a plastic syringe that was connected to the MDPP with Tygon tubing. At the location of vertical porewater sampling, a sediment core was subsequently collected for characterization of sediment texture and organic matter content. Sediment cores were collected by hammer driving an approximately 1 m length, 7.6 cm diameter Schedule 40 PVC pipe with beveled edge at its base into the streambed. The length of the retrieved sediment cores ranged from 0.5 to 1.0 m. During later field events, deeper streambed sediment cores (~1.5 m length) were obtained at the Phillips Creek floodplain and Coal Kiln sites by hammer driving 7.6 cm diameter aluminum pipe into the streambed. In both cases, cores were capped at the top, brought to the surface, and then capped at the base prior to being transported back to the laboratory for sediment analysis.

Sediment samples were obtained from streambed sediment cores for organic content analysis. As part of the sediment sampling for organic matter, water in sediment

cores was initially drained. For the two sediment cores collected during the March 2007 field event, water above the top of sediment in each core was removed by siphoning. Water in subsequent sediment cores was removed by gravity draining at the base of each core. Sediment grab samples were collected from the cores in ~1 m length PVC casing by drilling 1.75 cm diameter holes into the PVC casing at specific depths below the top of sediment. Grab samples were taken beginning at 5 cm below top of sediment, then at 10 cm below top of sediment, and then every 10 cm until the base of the core was reached. For the ~1.5 m length sediment cores collected in aluminum casing, each core was vertically halved, and then sectioned at 10 cm length increments into plastic bags. Sediment in the plastic bags was homogenized, and then an aliquot of sediment from each bag was obtained for organic content analysis. Organic content was determined by weight loss on ignition. Specifically, sediment samples were dried overnight at 105°C, and then 2 to 3 g of dried sediment was placed onto pre-ashed aluminum dishes. The aluminum dishes with dried sediment were then placed in a muffle furnace at 500°C for 24 h, then re-weighed. Sediment characteristics (color, texture) of the recovered sediment in each core were determined by hand-sample analysis. Photographs were also taken of each core. The number and sampling dates of sediment cores collected at the CMC floodplain, PC upland, PC floodplain and CK sites are included in Table 2.

Each field site was instrumented with piezometers and monitoring wells to obtain data on groundwater head and chemistry. Piezometers were initially installed into the streambed and stream bank at each site, with later installations of piezometers and monitoring wells occurring throughout the forested buffer. Each piezometer was

Table 2. Streambed sediment core identifications and sampling dates.

SITE	CORE ID	DATE COLLECTED
CMC floodplain	CMC 3/5/07*	5 March 2007
PC upland	PCPW2*	11 July 2007
	PCPW3*	7 August 2007
PC floodplain	PC 3/5/07*	5 March 2007
	PC 2/2/08	2 February 2008
CK	CK 6/2/07*	2 June 2007
	CKPW2*	12 July 2007
	CKPW3*	8 October 2007
	CK 2/2/08	2 February 2008

Notes: The * notes a porewater NO_3^--N profile was also obtained at location of sediment core. Core identifications include the abbreviated stream site and either the date the sediment core was collected or the porewater (PW) number associated with the sediment core.

constructed of 2.54 cm diameter PVC riser with 0.24 cm diameter holes drilled into the base of each piezometer in bands of 2.54 to 10.16 cm length. Solid PVC points were attached to the base of each piezometer, and threaded caps were used to seal the top of each piezometer between gauging and sampling events. Piezometers were installed to depths of approximately one and two meters below the streambed or water table by hammer driving each piezometer with a steel rod. Monitoring wells consisted of 2.54 cm diameter PVC screen with 0.025 cm slot size. Monitoring wells were also fitted with solid PVC points at the base, threaded caps at the top, and driven into the subsurface by steel rod hammering. Monitoring well depths ranged from 1.13 to 10.02 m bgs. Following installation, piezometers and monitoring wells were developed with use of a peristaltic pump and polyethylene tubing to remove fine-grained sediments from each monitoring point. Maps of each site, showing land cover and field instrumentation, are provided in Figures 2 through 4. Multiple groundwater and surface water gauging and sampling events were completed at each site. The earlier sampling period of the CMC

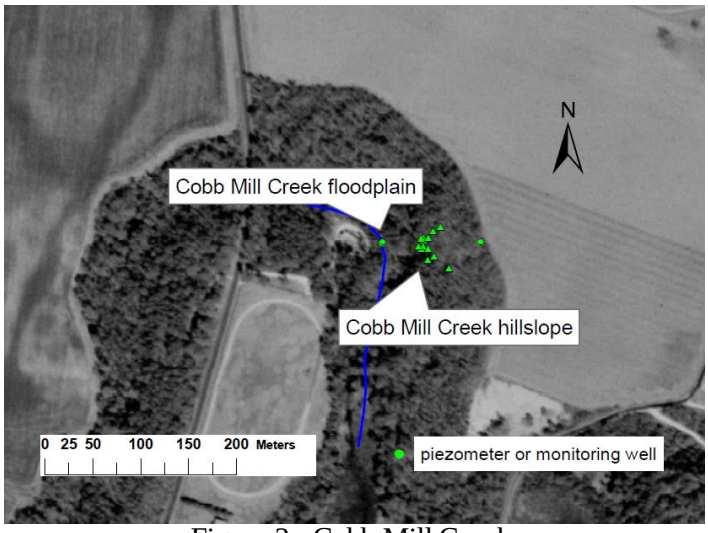

Figure 2. Cobb Mill Creek.

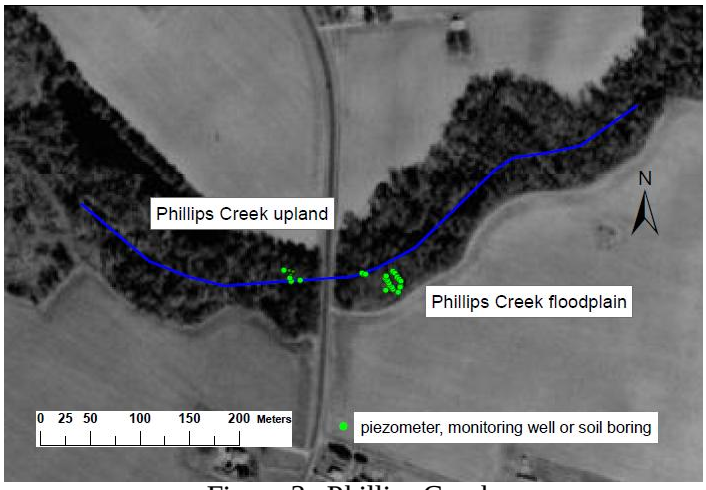

Figure 3. Phillips Creek.

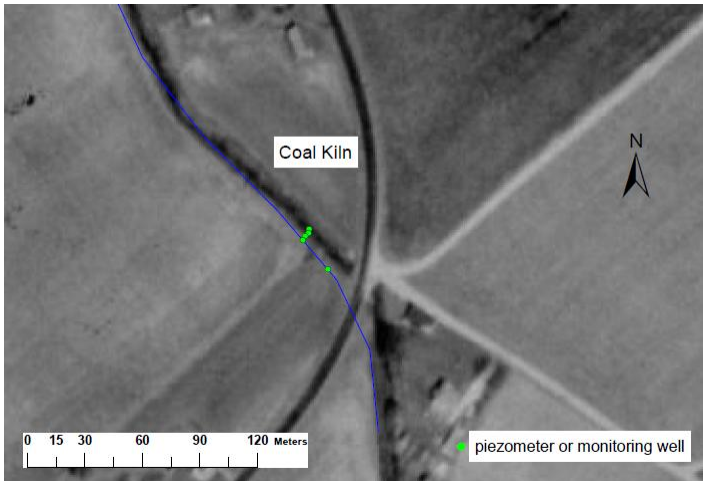

Figure 4. Coal Kiln.

hillslope site reflects the earlier time period of the previous investigations at this site (Galavotti, 2004; Gu, 2007), and details of the sampling and analytical methods used in these studies are found in the cited references. It is noted that the methods used to obtain data in the earlier Cobb Mill Creek hillslope studies are similar to the methods described below for this study. In this study, groundwater head was gauged at each piezometer and monitoring well by measuring the distance from the top of casing to the groundwater surface with use of a Solinst water level indicator. Stream head was gauged by tape measuring the distance from the top of casing of a stream piezometer to the stream water surface. Piezometers and monitoring wells were purged prior to sampling to remove stagnant water from each monitoring point. Groundwater purging and sampling was conducted by use of a peristaltic pump connected to polyethylene tubing. Surface water samples were obtained by submerging glass or plastic sampling vials directly in the stream channel. Aqueous samples (porewater, groundwater and surface water) were stored and transported on ice to the laboratory for dissolved anion analysis. Aqueous samples collected between the 3 March 2007 and 3 February 2008 sampling events were centrifuged at 10,000 rpm for 20 minutes to remove particulate matter. Aqueous samples collected after the 3 February 2008 event were filtered in the field using 0.45 μm Whatman PES Puradisc filters.

To determine the dissolved organic carbon (DOC) content of shallow groundwater at the PC floodplain site, groundwater samples were collected from buffer and in-stream piezometers at the PC floodplain site on 30 January 2009 and analyzed for DOC. Filtered groundwater samples were collected in 40 mL amber glass vials

containing 0.78 mL of pre-added H_3PO_4 preservative. Samples were transported back to the laboratory, where they were analyzed for DOC 11 days later on a Teledyne-Tekmar Phoenix 8000 total organic carbon (TOC) analyzer. An ultraviolet radiation-persulfate oxidation method was used by the TOC analyzer to oxidize DOC to CO_2, which was subsequently detected on a nondispersive infrared (NDIR) detector.

Field and laboratory methods were used to analyze aqueous samples for anions. In the field, unfiltered aqueous samples from the PC upland, PC floodplain and CK sites were colorimetrically analyzed for dissolved oxygen using a Chemetrics dissolved oxygen test kit. Field colorimetric analysis of sulfide (Chemetrics) was completed at the PC floodplain site based on detection of a sulfide odor during purging of a floodplain piezometer located ~3.5 m from the stream channel at this site. Nitrate-N was analyzed in the field at the PC floodplain and CK sites using a 0-3 ppm Chemetrics nitrate-N kit to provide an indication of where elevated nitrate-N occurs in groundwater within the buffer zone of each site.

Filtered aqueous samples were analyzed for NO_3^--N using ion chromatography. Samples collected between the 5 March 2007 and 3 February 2008 events were analyzed on a Dionex ion chromatograph with a 0.1 M Na_2CO_3 and 0.1 M $NaHCO_3$ eluent solution, and a suppressor solution containing 0.028 N H_2SO_4. Samples collected between the 31 July 2008 and 22 August 2008 events were analyzed on a Dionex ICS 3000 ion chromatograph with a 0.018 M KOH eluent solution and an electrolytic suppressor system. Samples collected between the 30 January 2009 and 19 July 2009 events were analyzed on a Dionex ICS 2000 ion chromatograph with a 0.023 M KOH

eluent solution and an electrolytic suppressor system. The detectors for each instrument were electrical conductivity detectors. Concentrations of NO_3^--N were quantified by conducting a linear regression of NO_3^--N standard peak heights or areas to concentrations, with a minimum R^2 value of 0.99 for each instrumental analysis. Instrument-specific method detection limits were determined using laboratory blank samples and 1 mg/L NO_3^--N standards.

2.2 Soil Boring Investigation

A soil boring investigation was conducted at the Phillips Creek floodplain site to characterize the subsurface soil/sediment lithology and organic matter concentrations present within the transition from a hillslope to floodplain landscape at this site. Two transects of soil borings, oriented approximately perpendicular to the buffer topographic contours, were established with lengths of 16.2 and 14.3 m. Each transect line was divided equally into eight sub-intervals, and then a pin flag was randomly placed within each sub-interval (Figure 5). This sampling design was used to allow subsurface organic matter concentrations to be compared along variable distances within the transect. A 6620-DT Geoprobe rig with a 1.5 m length plastic-lined, open steel sampler was used to obtain 4.4 cm diameter soil/sediment cores. Two vertically-sequential cores were collected at each boring location, with the soil/sediment recovery tending to decrease with a decrease in ground surface elevation. The decrease in recovery at the relatively low elevation points was due to the water table being relatively shallow at low elevation points; moreover, the sandy texture of the subsurface prevented the boreholes from staying open below the water table. The ends of each core were sealed with rubber

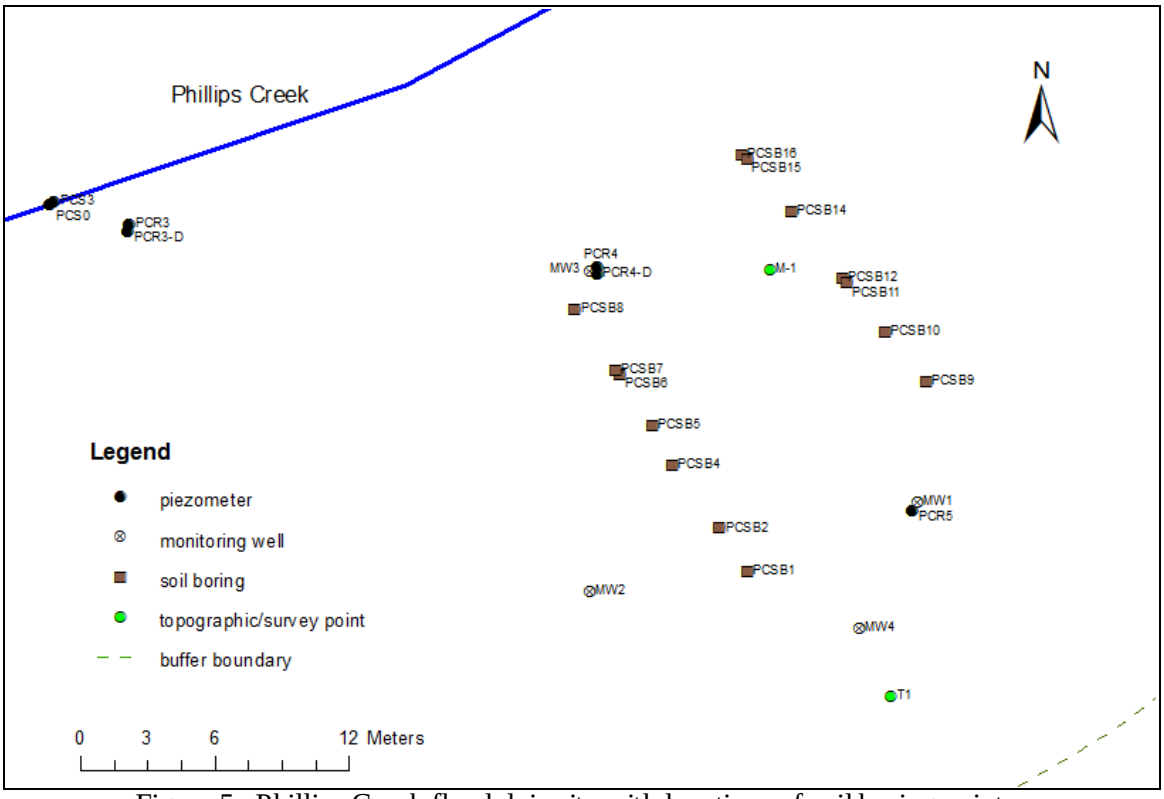

Figure 5. Phillips Creek floodplain site with locations of soil boring points.

stoppers and/or duct tape, and transported back to UVA for logging and organic matter analysis. Additionally, an attempt was made to complete soil borings across the buffer at Coal Kiln, but the steepness of the hillslope at this site prevented access by the Geoprobe rig. Instead, two soil borings were completed at the upgradient edge of the buffer at this site.

Organic matter concentrations were determined for soil and subsurface sediment samples obtained from the PC floodplain site cores using the same procedures discussed earlier for streambed sediment cores. Organic matter profiles were obtained from cores collected on the portion of one transect near the floodplain-hillslope boundary (soil boring points PCSB-14, 15 and 16) and from cores located on the upper hillslope portions of both transects (soil boring points PCSB-2 and 10). A two-sample t test was used to

test for the presence of a significant difference in soil/sediment organic matter concentrations between the floodplain-hillslope and upper hillslope locations. Organic matter concentrations in soil/sediment samples collected from the same elevation interval along the transects were selected for the t test. Differences in soil/sedimentary organic matter were considered significant at the $p<0.05$ level.

2.3 Hydraulic conductivity measurements

The hydraulic conductivities of streambed sediments were determined using a falling head permeameter method. The vertical hydraulic conductivities of 0.5-1.0 m length sediment cores were determined before horizontal sub-samples were collected for hydraulic conductivity measurements. To prepare each individual sediment core for a falling head permeameter measurement, the core was placed vertically upright onto a laboratory bench, and holes were drilled into the bottom and top caps of each core to allow barbed plastic fittings to be attached. Water in each core was gravity drained, and then tubing was connected from the bottom barbed fitting to a glass burette positioned on a ring stand above the core. Tap water was then added to each core through the burette until the pore spaces and headspace were completely filled with water. Hydraulic conductivity was then measured by recording the time elapsed between the initial and reduced values of head in the burette. The hydraulic conductivity could then be computed using the following equation:

$$K = \frac{a * L}{A * t} \ln\left(\frac{h_0}{h_1}\right) \qquad (2)$$

where a is the cross-sectional area of the burette (L^2), A is the cross-sectional area of the core (L^2), L is the length of sediment in the core (L), t is the time interval between the initial and reduced head, and h_0 and h_1 are the initial head and reduced head values, respectively (L).

The horizontal sediment core sub-samples enabled multiple measurements of horizontal hydraulic conductivity to be collected at different depths in a sediment core. Each sub-sample was obtained by drilling an approximately 2.5 cm diameter hole into the PVC casing of a sediment core at a specified depth below the sediment surface. A de-tipped, 10 mL plastic syringe was then pushed completely into the core sediment and used to pull a sediment sample from the core. Void spaces in the syringe were filled with glass wool, and both ends of the syringe were then sealed with rubber stoppers. Hydraulic conductivity of sediment in each horizontal sub-sample was measured using the falling head permeameter method discussed previously.

Rising-head slug tests were used to obtain hydraulic conductivity data of subsurface sediments within the riparian and hillslope buffers of the CMC floodplain, PC upland, PC floodplain and CK sites. The hydraulic conductivity of the CMC hillslope subsurface was determined as part of the groundwater model development in a previous study (Gu et al., 2008). Slug tests at piezometers and monitoring wells were completed by first measuring the depth to water in each monitoring point to determine the static water level. Solinst Levelogger pressure transducers, programmed to record level at a frequency of one measurement per second, were then lowered to the base of a monitoring point. A 2 cm diameter, 56 cm length slug was then lowered into the monitoring point

until it was either completely or partially submerged. It is noted that at some monitoring points, friction between the slug and inner casing of the monitoring point prevented the slug from being completely submerged. The water level was allowed to return to its near-static condition, and then the slug was pulled. After allowing time for the water level to rise, the pressure transducer was pulled from the monitoring point. Water level data recorded by the pressure transducer was subsequently used to produce plots of drawdown over time for the rising head portion of the slug tests, which could then be evaluated to determine hydraulic conductivity using the Bouwer and Rice slug test method (Bouwer and Rice, 1976; Bouwer, 1989). A range in hydraulic conductivity values was determined for one piezometer located at the PC floodplain site based on difficulty in selecting a single static water level during the slug test at this point. As a result, lower and upper static water levels were used in the data analysis to compute upper and lower hydraulic conductivity values.

2.4 Surveying

Piezometers, monitoring wells, buffer topography and soil boring points were surveyed with a Pentax Total Station instrument in July 2009. An arbitrary, defined coordinate system was used at each site, as accuracy in the relative horizontal and vertical locations of surveyed points was critical in this study. A transect-based approach to surveying was completed at each site based on the goal of incorporating surveyed groundwater monitoring and topographic point data into 2-D vertical plane representations of each site. Surveyed transects were oriented approximately

perpendicular to buffer topographic contours and the stream channel. Surveyed point data was imported into ArcGIS software for generation of site maps.

2.5 Numerical groundwater model development

2.5.1 Model objectives and selection

Groundwater modeling was conducted in this study to gain an understanding of the direction and magnitude of groundwater flow within the unconfined aquifer of each forested buffer-stream site. A steady-state, two-dimensional, vertical cross-section modeling approach was taken, and the USGS groundwater modeling programs MODFLOW and MODPATH were selected to quantify groundwater flow at each site. MODFLOW is a three-dimensional, finite difference numerical groundwater modeling code that computes the distribution of groundwater head and flow within a defined model grid (Harbaugh, 2005). MODPATH is a semi-analytical particle tracking code that uses the flow output from MODFLOW to compute flow path line coordinates within a model grid (Pollock, 1994). The graphical user interface ModelMuse (Winston, 2009) was used as a pre-processer for preparing the input data used by MODFLOW and MODPATH.

2.5.2 Model description

MODFLOW computes groundwater head and flow using a block-centered approach, in which a block diagram representing a groundwater system is divided into a series of rectangular grid cells arranged in rows, columns and layers. Although MODFLOW was developed for 3-D applications, the output from the model in two dimensions was selected for this study. With this modeling objective, the fundamental

equation of groundwater flow that forms the basis of computations in MODFLOW can be expressed as:

$$\frac{\partial^2 h_x}{\partial x^2} K_x + \frac{\partial^2 h_z}{\partial z^2} K_z + W = S_s \frac{dh}{dt} \qquad (3)$$

where $h_{x,z}$ is hydraulic head in the x or z directions (L), $K_{x,z}$ is hydraulic conductivity in the x or z directions (L T^{-1}), W is flow into or out of the cell due to an external source or sink (L T^{-3}), and S_s is the specific storage of a grid cell (L^{-1}). The derivative terms on the left-hand side of Eqn. 3 are derived from the application of Darcy's Law (Q=KA*dh/dl) to the conservation of mass (dQ/dx=0). Because the derivative terms are an expression of flow (Q), Eqn. 3 can also be expressed as:

$$\sum Q = S_s \frac{\Delta h}{\Delta t} V \qquad (4)$$

where Q is flow into or out of a grid cell and V is the volume of the grid cell. In a 2-D framework, flow between adjacent grid cells can be represented schematically using the convention shown below (from MODFLOW).

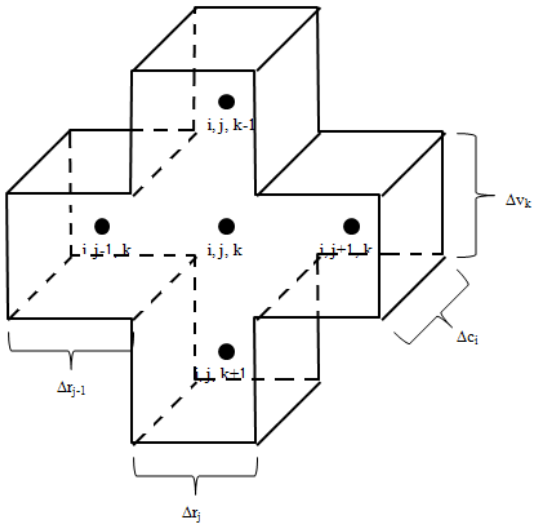

In the above figure, the central nodes of each rectangular block are represented by the i, j, and k indices, where flow in the horizontal, x direction is expressed using the j index, and flow in the vertical, z direction is expressed with the k index. The grid cell dimensions in the x, y and z directions are represented by the Δr_j, Δc_i and Δv_k terms, respectively. The finite difference equation for flow (q) across the grid cell face from the i, j-1, k cell to the i, j, k cell is:

$$q_{i,j-1/2,k} = K_x \Delta c_i \Delta v_k \left(\frac{h_{i,j-1,k} - h_{i,j,k}}{\Delta r_{j-1/2}} \right) \qquad (5)$$

where K_x is the horizontal hydraulic conductivity. Flow across the upper grid cell face from the i, j, k-1 node toward the i, j, k node is expressed as:

$$q_{i,j,k-1/2} = K_z \Delta c_i \Delta r_j \left(\frac{h_{i,j,k-1} - h_{i,j,k}}{\Delta v_{k-1/2}} \right) \qquad (6)$$

where K_z is the vertical hydraulic conductivity. Similar equations can be written for flow across the other two grid cell faces:

$$q_{i,j+1/2,k} = K_x \Delta c_i \Delta v_k \left(\frac{h_{i,j+1,k} - h_{i,j,k}}{\Delta r_{j+1/2}} \right) \qquad (7)$$

$$q_{i,j,k+1/2} = K_z \Delta c_i \Delta r_j \left(\frac{h_{i,j,k+1} - h_{i,j,k}}{\Delta v_{k+1/2}} \right) \qquad (8).$$

The flow into or out of a grid cell from external sources or sinks, W, can be represented in a general way as:

$$W_{i,j,k} = \sum a_{i,j,k} h_{i,j,k} + \sum b_{i,j,k} \qquad (9).$$

The *a* term in the above equation represents a head-dependent flow term ($L^2 T^{-1}$), and *b* represents a head-independent flow term ($L^3 T^{-1}$). Examples of external sources and sinks include constant head boundaries, recharge and pumping wells.

The unconfined nature of groundwater flow in this study was simulated by specifying that the wet/dry status of grid cells be convertible. Under a convertible setting, wetting parameters specified by the MODFLOW user, in addition to hydraulic head values of wet grid cells adjacent to dry cells, are used to determine when a cell that is dry becomes wetted (Harbaugh, 2005). In this study, a grid cell was converted from dry to wet once an adjacent grid cell hydraulic head reached a value of 0.25 m above the base of the dry grid cell. This value was selected based on the thickness of the upper layer of each site model being ~0.5 to 1 m, and through a general trial and error process.

In MODFLOW, the backward differences method is used to approximate the time derivative of head on the right-hand side of Eqn. 3:

$$\frac{dh}{dt} \cong \left(\frac{h_{i,j,k}{}^{m} - h_{i,j,k}{}^{m-1}}{t_m - t_{m-1}} \right) \qquad (10).$$

Under steady-state conditions, a single time step can be used, with no specified change in head over this time step. The backward difference method is advantageous in transient-type flow equations in that solutions obtained are unconditionally stable (Harbaugh, 2005; Hornberger and Wiberg, 2005). Substituting the finite difference approximations to the groundwater flow terms shown in Eqns. 4 through 9 into the original groundwater flow equation (Eqn. 3), the following equation is produced to compute groundwater head at the grid cell with central node i, j, k:

$$K_x \Delta c_i \Delta v_k \left(\frac{h_{i,j-1,k} - h_{i,j,k}}{\Delta r_{j-1/2}} \right) + K_z \Delta c_i \Delta r_j \left(\frac{h_{i,j,k-1} - h_{i,j,k}}{\Delta v_{k-1/2}} \right) + K_x \Delta c_i \Delta v_k \left(\frac{h_{i,j+1,k} - h_{i,j,k}}{\Delta r_{j+1/2}} \right) +$$
$$K_z \Delta c_i \Delta r_j \left(\frac{h_{i,j,k+1} - h_{i,j,k}}{\Delta v_{k+1/2}} \right) + W_{i,j,k} = \left(\frac{h_{i,j,k}^{m} - h_{i,j,k}^{m-1}}{t_m - t_{m-1}} \right) \quad (11).$$

Similar equations are generated for each other individual grid cell present in the model, producing a system of equations to be solved numerically to obtain the distribution of groundwater head within the model. To check the accuracy of the solved head distribution, MODFLOW also computes cell-by-cell flow budgets for the model. A properly constructed model would have a very low percent discrepancy between the inflow and outflow at its hydrologic boundaries.

The strongly implicit procedure (SIP) method was selected as the solver technique used by MODFLOW in this study. The SIP method uses an iterative approach to obtain a solution to the system of groundwater head equations, in which the computed values of head are incrementally modified until a specified head closure criterion is achieved. A head closure criterion of 1×10^{-4} m was used in this study for each site model. As a general description, the SIP method uses a matrix division approach to solve for head during each iteration, although unlike in a direct Gaussian elimination method, additional factors, or parameters are added to the matrix to reduce the computational demand associated with solving the system of equations (Remson et al., 1971). The number of parameters used to modify the matrix can vary, with five considered to be generally acceptable (Harbaugh, 2005). A seed value is used to compute the values of the SIP parameters, with the value of the seed in this study being generated automatically by

MODFLOW. The automatically generated seed value may not be the optimal value for convergence on a correct solution, as was observed on occasion in this study. Optimal seed values were obtained by a trial and error process, with the objective being to obtain iterations in which the maximum head change per iteration was moderate in the positive and negative directions. Seed values were adjusted if the iterative solution contained large positive and negative oscillations, or were flat (*i.e.*, very small) in one particular direction (Harbaugh, 2005).

2.5.3 Site-specific model setup

Site-specific, vertical plane models of groundwater flow were constructed for the CMC floodplain, PC upland, PC floodplain and CK sites. A groundwater flow model for the CMC hillslope site was generated as part of a separate, earlier study (Gu et al., 2008). Because MODFLOW is designed to handle 3-D applications, rectangular block models were created for each site, with the vertical "slice" taken from the center of the block model. From a vertical, cross-sectional view of each model, the upper land surface boundary was initially defined in ArcGIS before setting up the model in ModelMuse. The line that represents this upper land surface boundary was established as the line normal to topographic contours that connects the outermost upgradient monitoring well at a site to the stream channel. Land surface elevation values along this groundwater model transect line were obtained from surveyed monitoring or topographic points located along or near this line. The length of the model in the other horizontal direction (parallel to the stream channel) was made equal to the length of the groundwater transect line. The depth

to the lower boundary of each model was based on the stream-site unconfined aquifer thickness (Table 1).

Once the outer boundaries of a rectangular block model were defined, the block model was discretized into rows, columns and layers to form the model grid cells. The grid cell sizes in the horizontal directions (x and y) were made uniform for a single site, with horizontal grid cell length values varying from 0.25 m at the CK site (relatively narrow buffer) to 1.0 m at the CMC floodplain site (relatively wide buffer). A 0.5 m horizontal grid cell length was used at the PC upland and PC floodplain sites. For the CMC floodplain site, a 1.0 m grid cell length was selected to keep the number of grid cells, and therefore the number of computations required during model simulation, from being unnecessarily high. A 0.25 m grid cell length was selected for the CK site model to provide enough grid cells within the model to define horizontal differences in hydraulic conductivity with adequate resolution.

Layer discretization at each site was not uniform but varied according to observed differences in subsurface lithology and hydraulic conductivity, as well as published data on aquifer hydraulic conductivity. In general, layer thicknesses ranged from approximately one to two meters, with surface layers often having a thickness ≤ 1 m. Layers were thinner near the land surface where more data on hydraulic conductivity was available, and in the case of streambed sediments, where hydraulic conductivity could undergo marked changes in depths < 1 m from the streambed. Within each model cross-section, grid cells were separated into zones that represent differences in hydraulic conductivity. The location of the zone boundaries was subjective, but was set either at

the midpoint between two piezometers with observed differences in hydraulic conductivity, or based on expected changes to hydraulic conductivity within shallow layers due to an upland-riparian landscape transition.

Constant head hydrologic boundary conditions, recharge and porosity were also specified in the groundwater flow models. Both the upgradient and stream head boundaries were specified with mean values from one or more gauging events, with mean upgradient head values representing the mean water table elevation of the upgradient monitoring well installed at a site, and mean stream head values representing the mean of stream water level measurements taken from in-stream piezometers. Exceptions occurred at the CMC floodplain site and the PC floodplain site due to a lack of available groundwater head data at the upgradient or stream end points of the transect lines that defined the model upper surface. For the CMC floodplain site model, the mean water table elevation from the hilltop well located at the CMC hillslope site was used as the upgradient constant head boundary at this site. For the PC floodplain site model, the stream head boundary was extrapolated from the mean water table gradient determined from three monitoring wells installed in the forested buffer at this site. A porosity of 0.30 was used for each stream-buffer site. Recharge was applied to the entire upper surface of each model, with values ranging from 3×10^{-9} m s^{-1} to 8×10^{-9} m s^{-1}. These recharge values reflect the low to average values of average annual baseflow reported for streams located within the southern portion of the Delmarva peninsula (Speiran, 1996). The recharge value used in a groundwater flow model was not a sensitive parameter, as any decreases in water supplied by recharge could be accounted for by increases in

groundwater flow at the upgradient constant head boundary. Site-specific constant head, hydraulic conductivity and SIP solver values used as input for each MODFLOW groundwater flow model are provided in Appendix A. In addition, the boundaries of hydraulic conductivity zones used in each model are illustrated in Appendix A.

2.5.4 MODFLOW output post-processing

The groundwater flow data generated by MODFLOW for individual grid cells was used in MODPATH to produce groundwater flow path lines for each site-specific model. Flow path data produced by MODPATH contains the coordinates of particle paths in the model, which were subsequently plotted using MODPATH-Plot. The approach taken by MODPATH to compute flow path lines is semi-analytical, in that the finite-difference approximation based flow output from MODFLOW is combined with equations that compute particle flow path line coordinates from the x, y and z components of the groundwater velocity field (Pollock, 1994).

Darcian flow vectors were generated and plotted for each site using MODFLOW cell-by-cell flow output and the areas of grid cell faces. Specifically, the x component of Darcian flow ($L\ T^{-1}$) was determined by dividing the flow across the front face of a grid cell face by the front face area, and the z component of Darcian flow was determined by dividing the flow across the lower grid cell face by the lower grid cell area. These computations were completed for each grid cell within a model, producing matrices of the components of Darcian flow. These matrices, along with the z coordinates of model grid cells, were imported into Matlab and used to produce 2-D plots of Darcian flow vectors for each site. The relatively high density of grid cell nodal points at the PC

floodplain and CMC floodplain sites made viewing the flow vectors difficult. Consequently, only half of the horizontal and vertical flow components were used to produce flow vector plots for these two sites.

2.6 Landscape and depth-based NO_3^--N distributions

Piezometers installed in the buffer of each site were categorized by landscape type (hillslope/upland or riparian floodplain) and depth below ground surface to evaluate the effects of landscape and depth on mean NO_3^--N at each piezometer. Depth was categorized as being shallow (< 2 m bgs) or deep (≥ 2 m bgs). The criteria used to distinguish landscape type were the buffer land surface slope and soil texture. A noticeable break in land surface slope at the transition from the riparian floodplain to hillslope was able to be observed at each site containing these two landscapes. Observations of soil characteristics made during piezometer installation were qualitatively used to assess landscape type for piezometers located at the transition from a relatively flat to hillslope topography. The amount of fine-grained material present in soils at this transition zone was compared to soils encountered in the more apparent riparian and hillslope portions of the transect to categorize landscape type. The arbitrary 2 m depth used to distinguish shallow and deep piezometers in this study is based on the field instrumentation approach used in this study, in which piezometers were installed at depths of one or two meters below the water table or streambed. The depth below ground surface was used instead of depth below water table because it is a relatively fixed reference point compared to the water table.

3 Results

3.1 Streambed sediment characteristics and porewater NO_3^--N

The profiles of streambed porewater NO_3^--N and streambed sedimentary organic matter (OM) concentrations from the CMC floodplain, PC upland, PC floodplain and CK sites do not have a regular pattern (Figure 6(a-g)). The irregularity in the pattern of NO_3^--N and sedimentary OM from these four sites contrasts with observations from the CMC hillslope site, where NO_3^--N routinely decreased within the upper 20 cm of organic-rich streambed sediments. A negative relationship between porewater NO_3^--N and sediment OM was observed, however, in a profile obtained from the PC upland site on 11 July 2007 (Fig. 6d). In the six other profiles of NO_3^--N and sediment OM from this study, NO_3^--N already occurred at low concentrations (≤ 0.7 mg L^{-1}) at the base of the profiles. In these six profiles, NO_3^--N was generally low throughout the profiles, although NO_3^--N did increase in the upward direction in a profile obtained from Coal Kiln on 2 June 2007 (Fig. 6c). Descriptions of sediment color and texture from hand sample analyses are provided in Appendix B, and photographs of streambed sediment cores are provided in Appendix C.

Entire-core vertical hydraulic conductivity and sub-core horizontal hydraulic conductivity measurements were collected from Phillips Creek upland and Coal Kiln sediment cores, with values being predominantly in the range of 10^{-2} to 10^{-3} cm s^{-1} (Table 3). These values are consistent with their composition being mostly a fine to medium sand (Fetter, 1994). A relatively low horizontal hydraulic conductivity of 2.0×10^{-6} cm s^{-1} was measured at the 40 cm depth of the PCPW2 sediment core, which can be

a

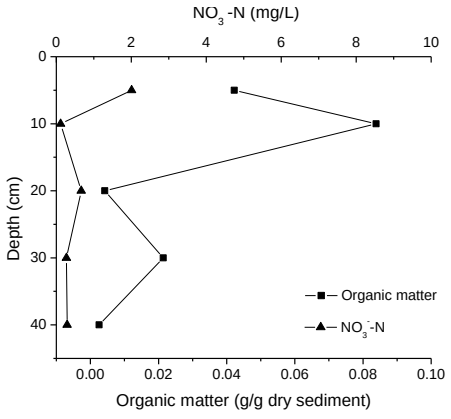

Cobb Mill Ck. floodplain – 5 March 2007

b

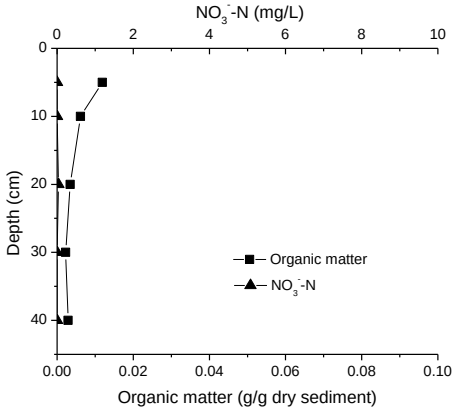

Phillips Ck. floodplain - 5 March 2007

c

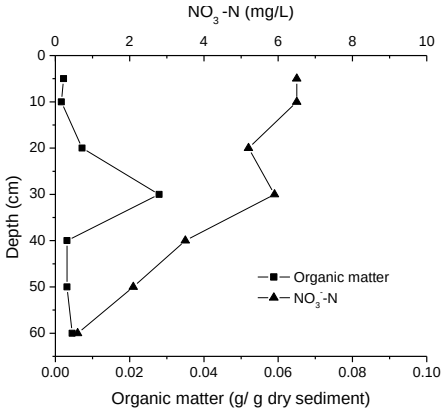

Coal Kiln – 2 June 2007

d

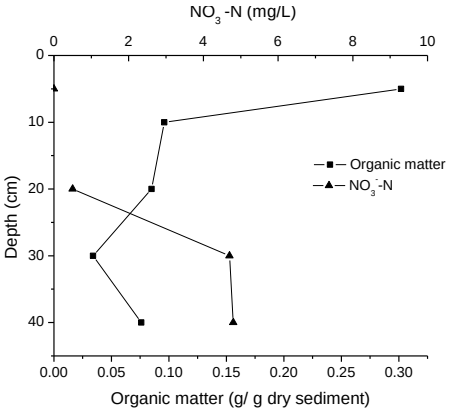

Phillips Ck. upland – 11 July 2007

e

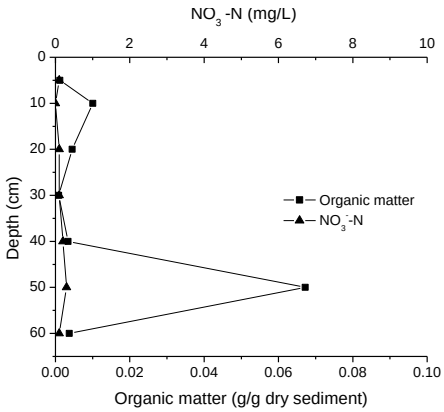

Coal Kiln – 12 July 2007

f

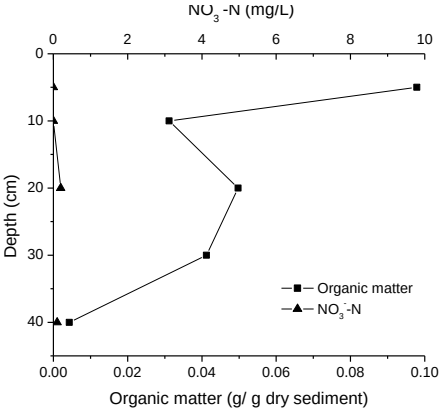

Phillips Ck. upland – 7 August 2007

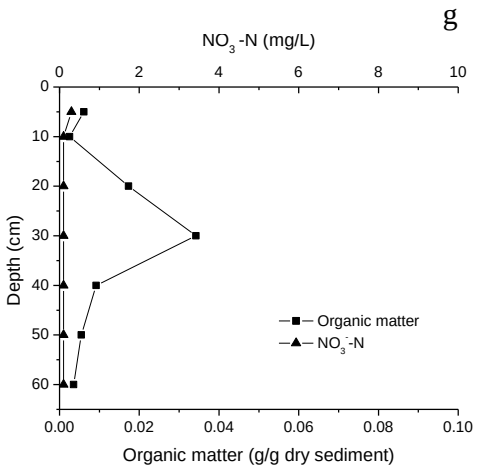

Figure 6(a-g). Streambed porewater NO_3^--N and organic matter profiles at study sites. The study site and sampling date of each porewater profile and sediment core are included in the profile captions.

Note: A site-date labeling system was used in this figure, and not the core identifications listed in Table 2, to present the results more clearly.

Table 3. Vertical and horizontal hydraulic conductivity (K) measurements of streambed sediment cores. Depth below sediment surface noted for horizontal K measurements.

Site	Core ID	Vertical K cm s^{-1}	Horizontal K cm s^{-1}
Coal Kiln	CK 6/2/07	2.4×10^{-3}	10 cm: 1.8×10^{-2} 30 cm: 2.1×10^{-3} 60 cm: 5.2×10^{-3}
	CKPW2	----------	10 cm: 2.1×10^{-2} 40 cm: 2.6×10^{-2} 50 cm: 5.5×10^{-3} 70 cm: 1.1×10^{-2}
	CKPW3	9.2×10^{-3}	10 cm: 1.7×10^{-2} 30 cm: 1.1×10^{-2} 40 cm: 5.6×10^{-3} 60 cm: 5.3×10^{-3}
Phillips Ck.	PCPW2	----------	10 cm: 6.7×10^{-3} 40 cm: 2.0×10^{-6}
	PCPW3	5.7×10^{-5}	20 cm: 1.5×10^{-3} 40 cm: 8.4×10^{-3}

explained by the presence of a silty, organic-rich layer at this depth (Fig. 6d, Appendix B).

Organic-rich sediments were observed in the 34 to 71 cm depth interval from a 1.5 m length streambed sediment core collected at the PC floodplain site (Appendices B and C, Figure 7a). A buried, organic-rich sediment layer was not observed in a similar length core collected from the streambed at Coal Kiln (Fig. 7b), which has relatively organic-rich sediments near the surface only. The vertical profile of organic matter shown in Figure 7b is similar to profiles of organic matter observed in streambed sediment cores collected at the Cobb Mill Creek hillslope site (Galavotti, 2004).

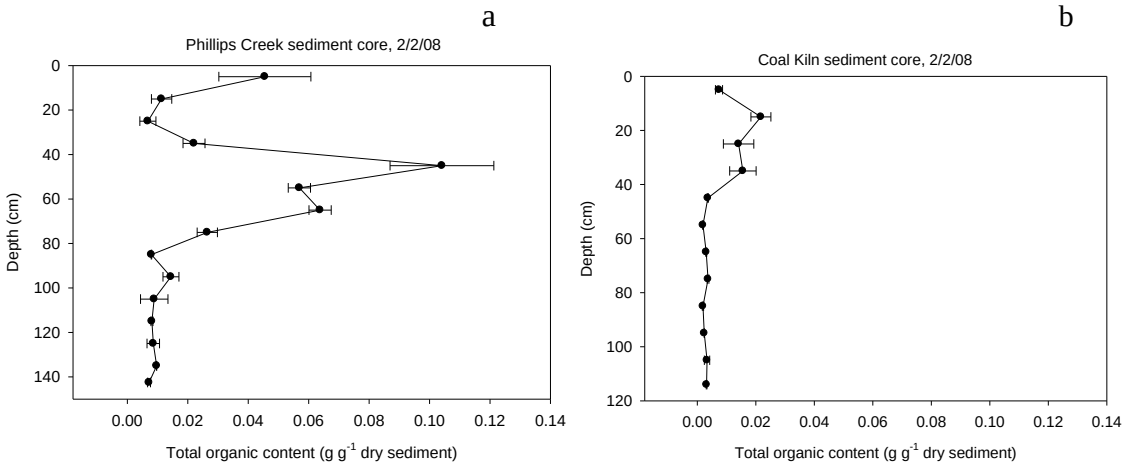

Figure 7(a-b). Organic matter concentrations with median depth in streambed sediment cores from (a) Phillips Ck. floodplain and (b) Coal Kiln. Error bars represent the standard error of replicate OM measurements from a depth interval.

3.2 Phillips Creek hillslope-riparian soil and sediment composition

A cross-sectional view of the subsurface at the Phillips Creek floodplain site indicates the presence of a 15 to 30 cm thick A soil horizon underlain by layers of sandy parent material (Figure 8). The subsurface sedimentary deposits include two laterally

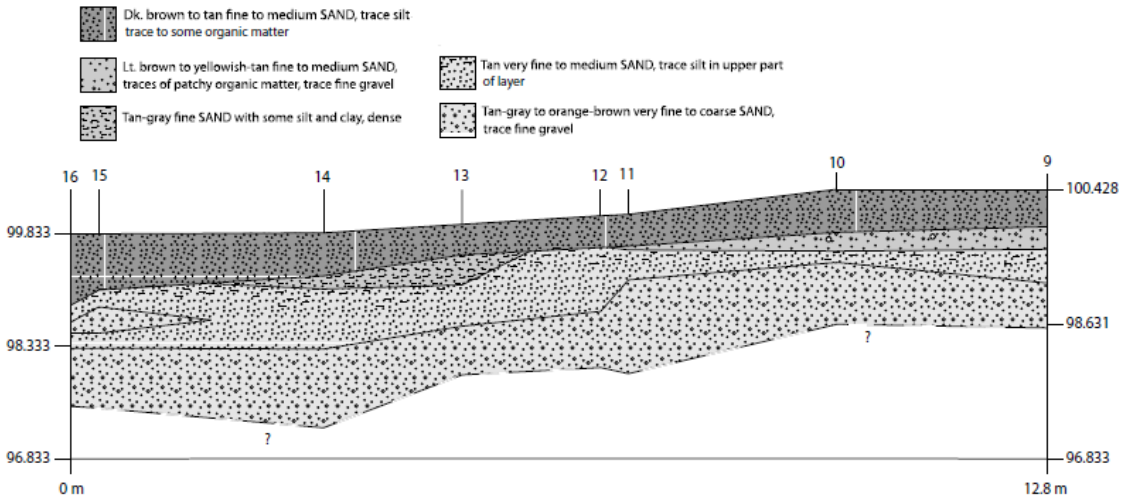

Figure 8. Cross-sectional view of subsurface at Phillips Creek floodplain site. Numbers on top of cross-section refer to locations of soil boring points.

extensive layers with more localized deposits of slightly different texture. A flattening of the surface topography between PCSB-13 and PCSB-14, combined with the observation of a silty, clayey sand deposit in this portion of the transect, are indicative of a shift from a hillslope to riparian floodplain landscape. Observations of soil and sediment characteristics from these cores, as well as others collected during the soil boring investigation, are included in Appendix B. Photographs of these soil/sediment cores are included in Appendix C.

The distribution of organic matter in soil/sediment cores collected along both soil boring transects are shown in Figure 9(a-b). At the 99.0 to 99.4 m depth interval, slightly higher organic matter concentrations appear to be present in cores collected at the hillslope-floodplain transition (PCSB 14,15 and 16) than in cores collected at the hillslope (PCSB-2, 10). A t-test comparison of mean organic matter concentrations within the 98.8 to 99.6 m elevation interval, which is roughly the maximum elevation interval organic matter concentrations were quantified in both core groups, was

conducted. Results of the t test indicate organic matter does not differ significantly between the hillslope and hillslope/floodplain sampling groups.

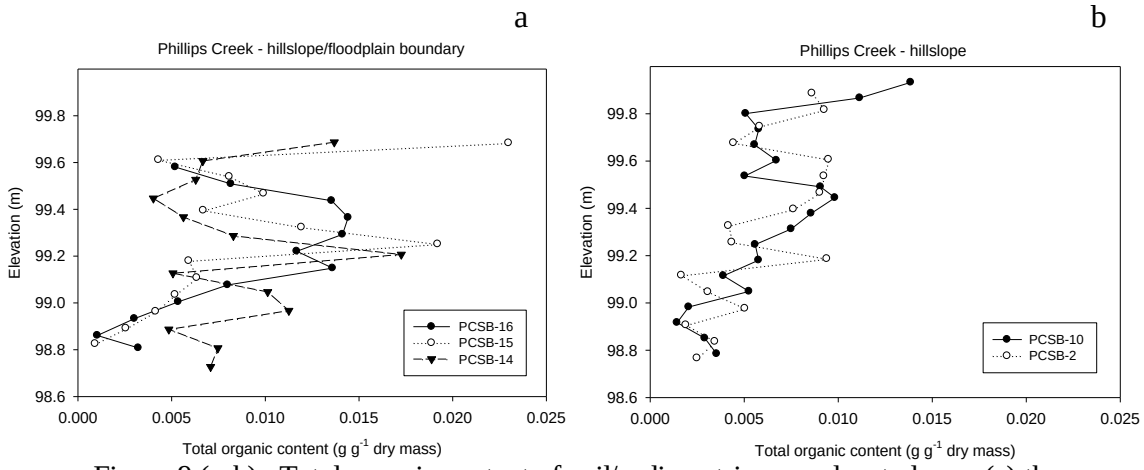

Figure 9 (a-b). Total organic content of soil/sediment in cores located near (a) the hillslope/floodplain boundary, and in (b) cores located on the hillslope. Elevation values are referenced to arbitrary site datum.

3.3 Buffer topography and landscape

Buffer topography along the groundwater model transect line, buffer boundaries and locations of piezometers and monitoring wells at each site are shown in Figures 10 to 14. The entire thickness of the unconfined aquifer is shown in each topographic profile, with the vertical scale set equal to the horizontal scale in the topographic profiles. Average buffer slope values are reported in Table 4, and ranged from 4.1% at the PC floodplain site to 19.7% at the CMC hillslope site. With the exception of the CMC hillslope site, buffer slope was computed as the difference in elevation between the upgradient endpoint of the groundwater model transect line and the floodplain land surface near the stream channel, divided by the distance of the groundwater model transect line. At the CMC hillslope site, where a floodplain is not present, slope was computed as the difference in elevation between the 7.5 m above sea level contour and

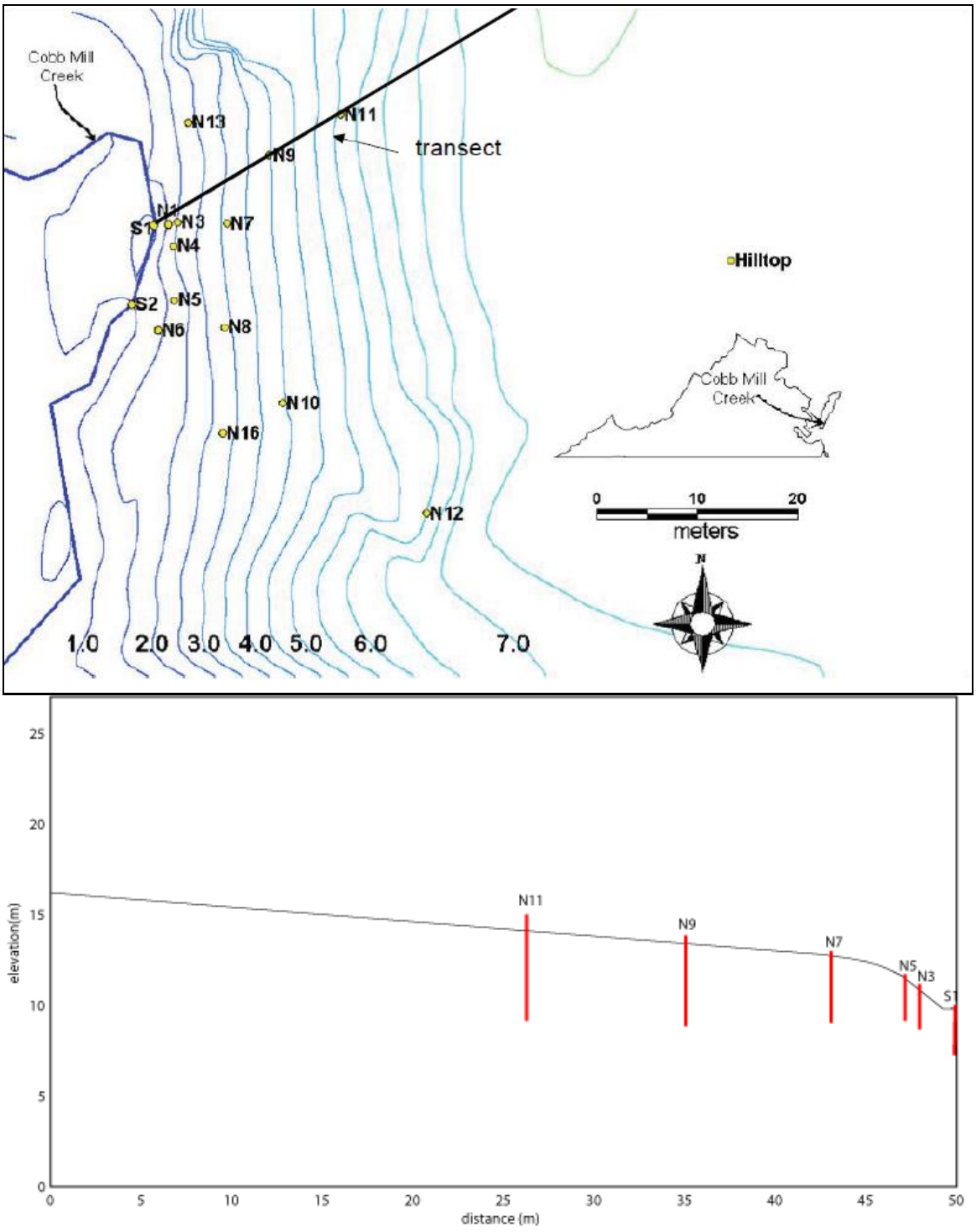

Figure 10. Cobb Mill Creek hillslope site with piezometer locations and surface topographic contours shown. The topographic profile of the transect line is shown below. Figure courtesy of Chuanhui Gu.

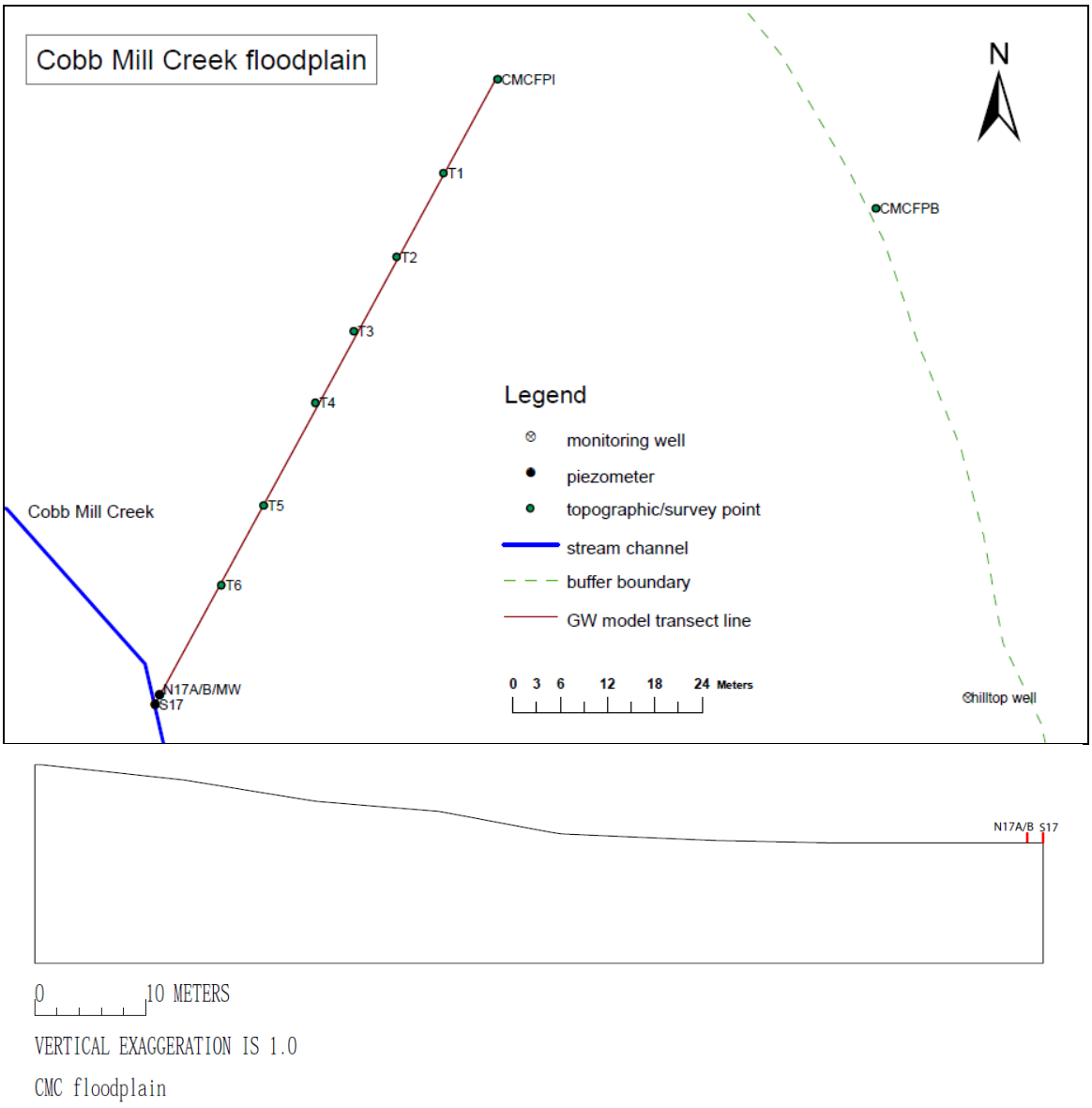

Figure 11. Cobb Mill Creek floodplain site with surveyed points. The topographic profile of the groundwater model transect line is shown below, along with locations of piezometers that are on the transect line.

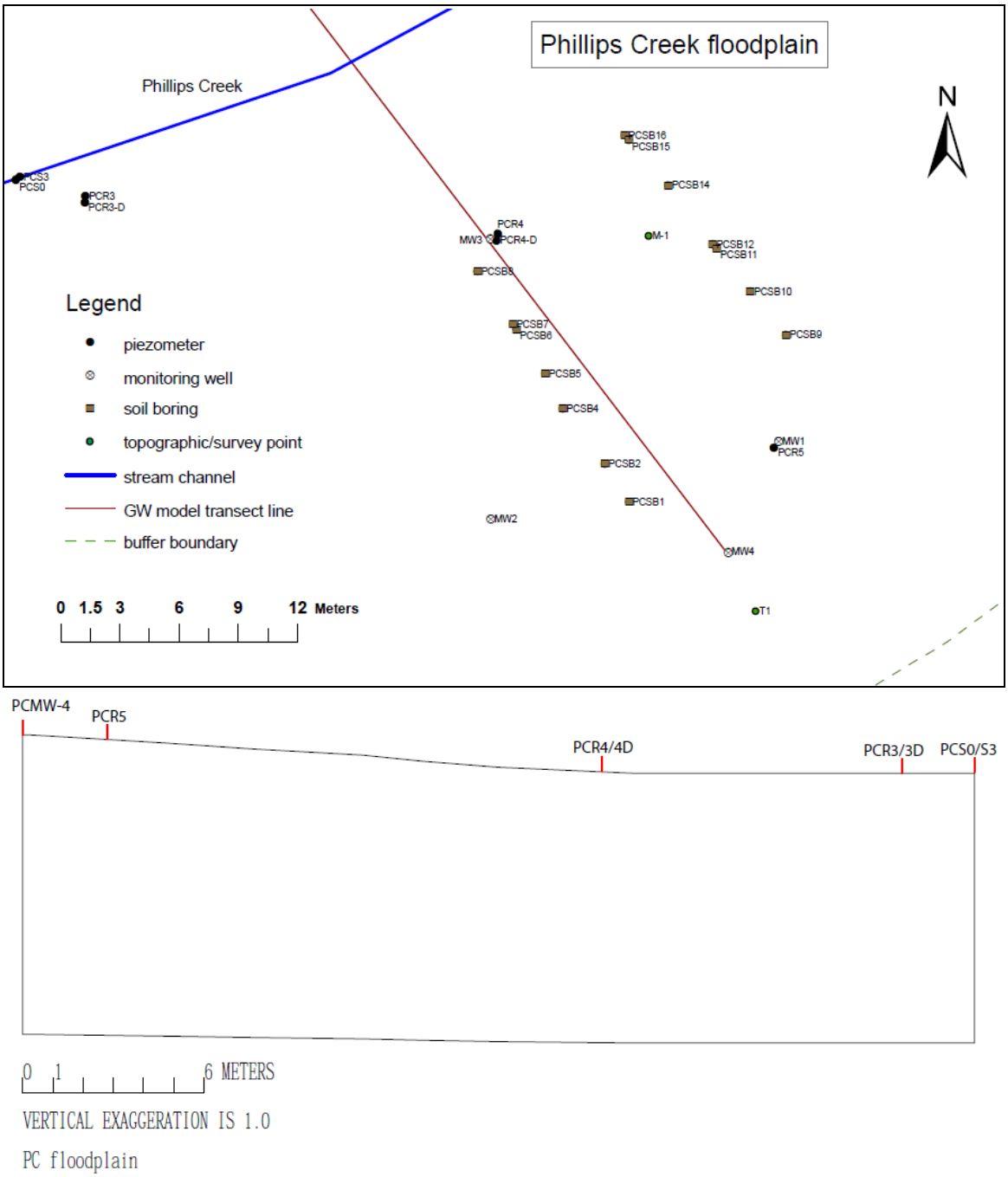

Figure 12. Phillips Creek floodplain site with surveyed points. The topographic profile of the groundwater model transect line is shown below, along with locations of piezometers that are on or extrapolated to the transect line.

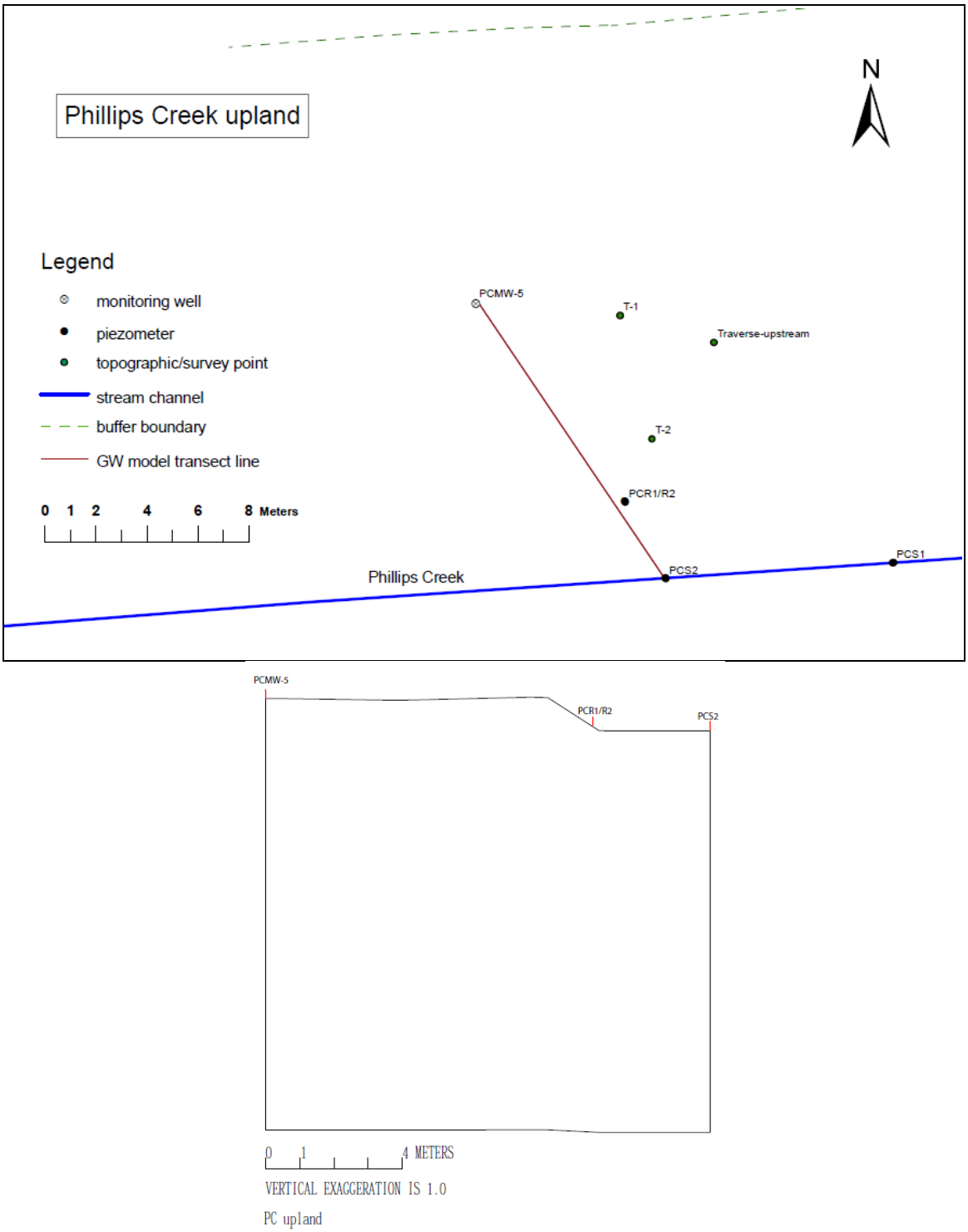

Figure 13. Phillips Creek upland site with surveyed points. The topographic profile of the groundwater model transect line is shown to the right, along with piezometers that are on the transect line.

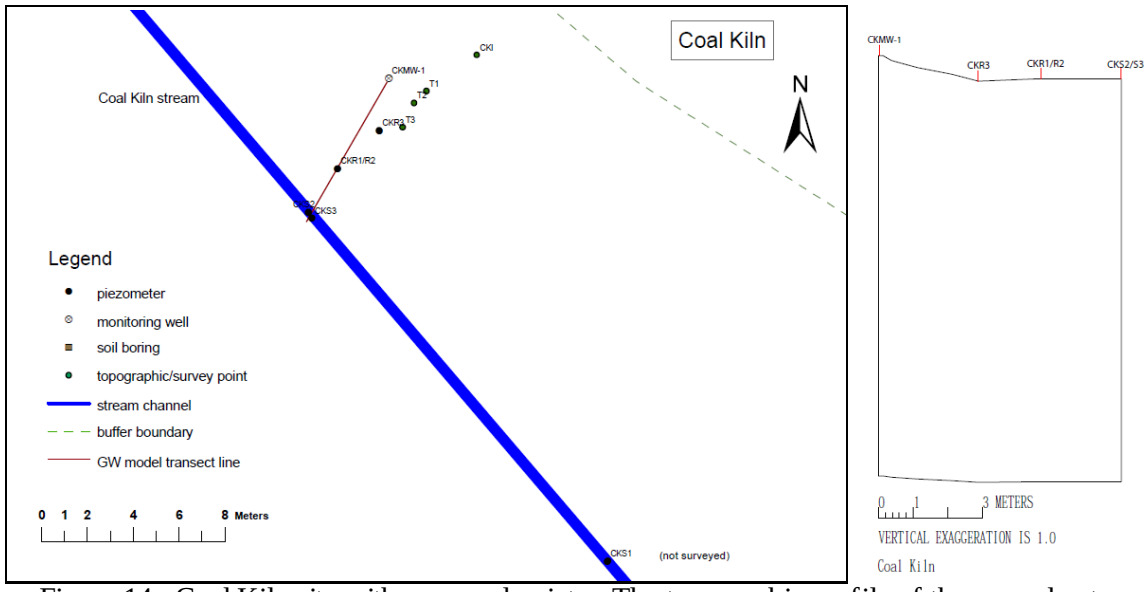

Figure 14. Coal Kiln site with surveyed points. The topographic profile of the groundwater model transect line is shown to the right, along with piezometers that are on or near the transect line.

Table 4. Buffer slopes.

Site	Average slope (%)
CMC hillslope	19.7
CMC floodplain	7.8
PC upland	7.2
PC floodplain	4.1
CK	9.8

the land surface at the N1 piezometer (Figure 10), divided by the distance normal to topography between these two points.

The surveyed topography of each site includes hillslope and riparian floodplain landscapes that comprise a varying proportion of the total buffer width. At the CMC hillslope site, the hillslope covers the entire buffer width, while at Coal Kiln the hillslope represents less than half of the buffer width. A flat upland zone is present in the buffer at the PC upland site, which transitions sharply to a hillslope near the stream channel. The floodplains are shown by the relatively flat portions of each buffer profile adjacent to the

stream channels, with the land surface generally sloping slightly downward toward the stream channel. An exception can be seen at Coal Kiln, where a slight upward land surface slope was observed between PCR3 and the PCR1/R2 cluster. The upland landscape type noted at the PC upland site was grouped with the hillslope landscape type, as both of these environments hydrologically are locations with a relatively thick vadose zone compared to riparian floodplain environments.

Piezometers installed in the buffer portion of each site were categorized by landscape type, with each piezometer assigned to either a riparian floodplain or hillslope landscape (Table 5). The location of a piezometer within the buffer topographic profile, and the color and texture of soils encountered during piezometer installation (Appendix B) were used to determine the landscape type for a given piezometer.

Table 5. Landscape categorization of buffer piezometers.

Site	Riparian floodplain	Hillslope
CMC hillslope	----------	N1A, N1B, N1C, N3A, N3B, N3C, N4A, N4B, N4C, N5A, N5B, N5C, N6A, N6B, N6C, N7A, N7B, N9A, N10A
CMC floodplain	N17A, N17B	----------
PC upland	PCR1, PCR2	----------
PC floodplain	PCR3, PCR3D, PCR4, PCR4D	PCR5
CK	CKR1, CKR2, CKR3	----------

3.4 Hydraulic conductivities determined from slug tests

Data provided by slug tests at ten monitoring wells/piezometers installed at the CMC floodplain, PC upland, PC floodplain and CK sites enabled hydraulic conductivity values to be determined for sediments surrounding these monitoring points (Appendix D). Slug tests were attempted at other piezometers and monitoring wells

installed in the buffer portion of each site, but hydraulic conductivity values could not be determined due to either the static water level not being attained during the test, or the number of level measurements obtained during the rising-head portion of the test being insufficient for data analysis. Among the CMC floodplain, PC upland, PC floodplain and CK sites, hydraulic conductivity values ranged from 10^{-5} to 10^{-3} cm s^{-1} (Table 6). Relatively low hydraulic conductivity values (10^{-4} to 10^{-5} cm s^{-1}) were measured at the riparian floodplain piezometers PCR2, PCR3 and CKR2. Relatively high hydraulic conductivity values (10^{-3} cm s^{-1}) were also observed in the riparian floodplain based on values from piezometers N17A, N17B, PCR4 and CKR1. Based on these results, hydraulic conductivity values of riparian floodplain sediments within the 0.77 to 1.43 m bgs interval can vary from site to site by more than an order of magnitude. A depth effect in hydraulic conductivity was observed at Coal Kiln, where hydraulic conductivity increased from 7.4×10^{-5} cm s^{-1} at a depth of 1.35 m bgs to 2.6×10^{-3} cm s^{-1} at a depth of 2.38 m bgs.

Table 6. Hydraulic conductivities determined by slug tests.

Site	Piezometer/MW	Depth of inlet bgs (m)	K (cm s^{-1})
CMC floodplain	N17A	0.77	1.1×10^{-3}
	N17B	1.25	1.7×10^{-3}
	S17	0.94	3.9×10^{-3}
PC upland	PCMW-5	1.21 - 2.12	1.4×10^{-3}
	PCR2	1.27	4.5×10^{-4}
PC floodplain	PCR5	2.83	3.3×10^{-3}
	PCR4	1.57	3.5×10^{-3}
	PCR3	1.43	5.6×10^{-5} to 1.2×10^{-4}
CK	CKR1	2.38	2.6×10^{-3}
	CKR2	1.35	7.4×10^{-5}

3.5 Groundwater and surface water NO_3^--N

Mean NO_3^--N concentrations for individual piezometers and monitoring wells were greater than 2 mg/L for all piezometers installed in the buffer and streambed locations at the CMC hillslope, CMC floodplain and PC upland sites (Table 7). For piezometers from these three sites, mean NO_3^--N ranged from 2.4 mg/L in buffer piezometer N5A to 12.4 mg/L in streambed piezometer S1B, both of which are located at the CMC hillslope site. Mean NO_3^--N concentrations for a riparian floodplain piezometer cluster installed at the CMC floodplain site were generally similar to mean NO_3^--N concentrations observed in groundwater at the CMC hillslope site. At the CMC floodplain site, the shallow and deep piezometers in the riparian floodplain cluster had mean NO_3^--N concentrations of 6.3 and 8.2 mg/L, respectively. Relatively low mean NO_3^--N concentrations (< 0.6 mg/L) occurred at the riparian floodplain piezometers (CKR1, PCR3 and PCR4) and streambed piezometers (PCS0, CKS2 and CKS3) located at the Phillips Creek floodplain and Coal Kiln sites. A complete separation in mean NO_3^--N concentrations between riparian floodplain and hillslope/upland landscapes is not apparent, as shown by the presence of elevated NO_3^--N in the riparian floodplain piezometers CKR2, PCR3-D and PCR4-D, which are adjacent to and at different depths than the riparian floodplain piezometers CKR1, PCR3 and PCR4, respectively. Mean NO_3^--N concentrations in groundwater samples collected from the latter group of piezometers indicate elevated NO_3^--N is generally absent, with mean NO_3^--N concentrations ranging from less than half the method detection limit to 0.6 mg/L.

Table 7. Average NO_3^--N concentrations at groundwater and surface water sampling locations.

Site	Location	Depth bgs (m)	# of times sampled	Mean NO_3^--N (mg/L)	Std. Dev. NO_3^--N (mg/L)
CMC hillslope	N1A	0.82	10	5.2	1.8
	N1B	1.05	10	7.8	2.0
	N1C	1.39	10	11.1	2.1
	N3A	1.07	10	5.8	2.4
	N3B	1.23	11	7.8	3.1
	N3C	1.41	11	9.7	2.4
	N4A	0.98	11	3.9	1.8
	N4B	1.17	11	4.3	3.1
	N4C	1.38	11	3.5	3.2
	N5A	0.85	11	2.4	3.1
	N5B	1.00	11	3.7	3.4
	N5C	1.21	11	7.0	3.5
	N6A	0.76	12	4.8	2.8
	N6B	0.94	12	6.9	2.9
	N6C	1.11	12	8.3	3.3
	N7A	2.03	12	7.7	3.9
	N7B	2.33	12	11.3	2.8
	N9A	2.36	10	2.7	2.0
	N10A	2.33	12	6.8	3.3
	S1A	0.60	12	12.1	1.5
	S1B	0.88	12	12.4	1.4
	SW	N/A	10	2.6	0.7
	HT well	0 - 10.02	6	4.6	1.1
CMC floodplain	N17A	0.77	7	6.3	0.7
	N17B	1.25	7	8.2	1.4
	S17	0.94	7	5.8	1.9
	SW	N/A	5	3.9	2.0
PC upland	PCR1	2.37	3	4.5	1.0
	PCR2	1.27	2	5.7	1.5
	PCS1	1.00	3	5.5	0.6
	PCS2	1.00	2	2.9	4.0
	PCMW-5	1.21 - 2.12	1	7.1	N/A
	SW	N/A	3	0.8	0.3
PC floodplain	PCS0	1.00	7	0.3	0.4
	PCS3	2.00	5	5.2	2.6
	PCR3	1.43	6	*0.24*	0.2
	PCR3D	2.52	1	4.1	N/A
	PCR4	1.57	4	0.4	0.5
	PCR4D	2.55	1	3.6	N/A
	PCR5	2.83	4	6.4	0.9
	PCMW-4	0 - 3.79	3	4.5	2.3
	SW	N/A	8	1.1	0.6
CK	CKR1	2.38	6	0.6	1.3

	CKR2	1.35	6	2.5	1.7
	CKR3	1.39	4	6.0	0.8
	CKS1	1.00	4	*0.13*	0.2
	CKS2	1.00	6	*0.13*	0.1
	CKS3	2.00	2	*0.02*	0.0
	Tile Drain	N/A	1	5.8	N/A
	CKMW-1	0 - 5.79	1	0.0	N/A
	SW	N/A	7	2.4	0.3

Notes: Mean and standard deviation values were determined using NO_3^--N data obtained from each sampling event completed at a location (Appendix E). For aqueous samples collected between the 5 March 2007 and 3 February 2008 sampling events, the method detection limit (MDL) was 0.26 mg/L. The MDL for aqueous samples collected between the 31 July 2008 and 22 August 2008 sampling events was 0.04 mg/L, and the MDL for aqueous samples collected between the 30 January 2009 and 19 July 2009 sampling events was 0.48 mg/L. Italicized concentrations represent samples where NO_3^--N occurred at a concentration less than one-half the MDL – the one-half value of the MDL is shown.

Mean NO_3^--N concentration in surface water samples collected at the five sites ranged from 0.8 mg/L to 3.9 mg/L (Table 7). The higher mean and standard deviation of NO_3^--N observed at the CMC floodplain site compared to the CMC hillslope site partially reflects the higher maximum value of NO_3^--N in a surface water sample from the CMC floodplain site. A maximum surface water NO_3^--N of 6.7 mg/L occurred at the CMC floodplain site, while maximum surface water NO_3^--N detected at the CMC hillslope site was 4.0 mg/L.

Differences in mean groundwater NO_3^--N occurrences between the CMC hillslope and the four other sites are shown in Figure 15. A semi-normal distribution for mean NO_3^--N over the 2 to 12 mg/L concentration interval occurs for buffer and streambed piezometers at the CMC hillslope site, while a bimodal distribution of mean NO_3^--N can be seen at other sites. The data from the other sites shows a normal distribution of NO_3^--N over the 2 to 8 mg/L concentration interval, and a separate group of piezometers with mean NO_3^--N concentrations less than 0.6 mg/L.

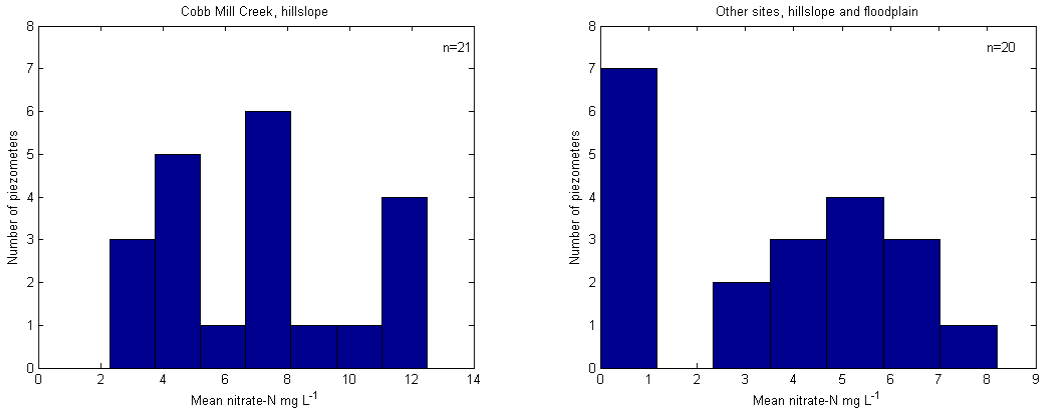

Figure 15. Mean piezometer-based NO_3^--N concentration distributions for the Cobb Mill Creek hillslope site and the four other sites investigated in this study.

The landscape and depth-based distributions of mean NO_3^--N for piezometers located in the buffer portion of each site are shown in Figure 16. Mean NO_3^--N concentrations observed at locations within a hillslope/upland landscape have a normal distribution, consistent with the general distribution of NO_3^--N observed at the CMC hillslope site. This type of distribution contrasts with observations from a riparian floodplain landscape, where a bimodal NO_3^--N distribution occurs (Figure 16). In the depth-based distributions, a similar pattern is observed for mean NO_3^--N at both shallow (< 2 m bgs) and deep (≥ 2 m bgs) locations.

3.6 Phillips Creek floodplain site DOC results

Dissolved organic carbon analytical results for groundwater samples collected from the PC floodplain site on 30 January 2009 are shown in Table 8. For the 30 January 2009 sampling event, DOC concentrations ranged from 0.5 mg/L at the in-stream piezometer PCS3 to 4.2 mg/L at the hillslope piezometer PCR5. Within the riparian floodplain, DOC was measured at a higher concentration at a piezometer located near the

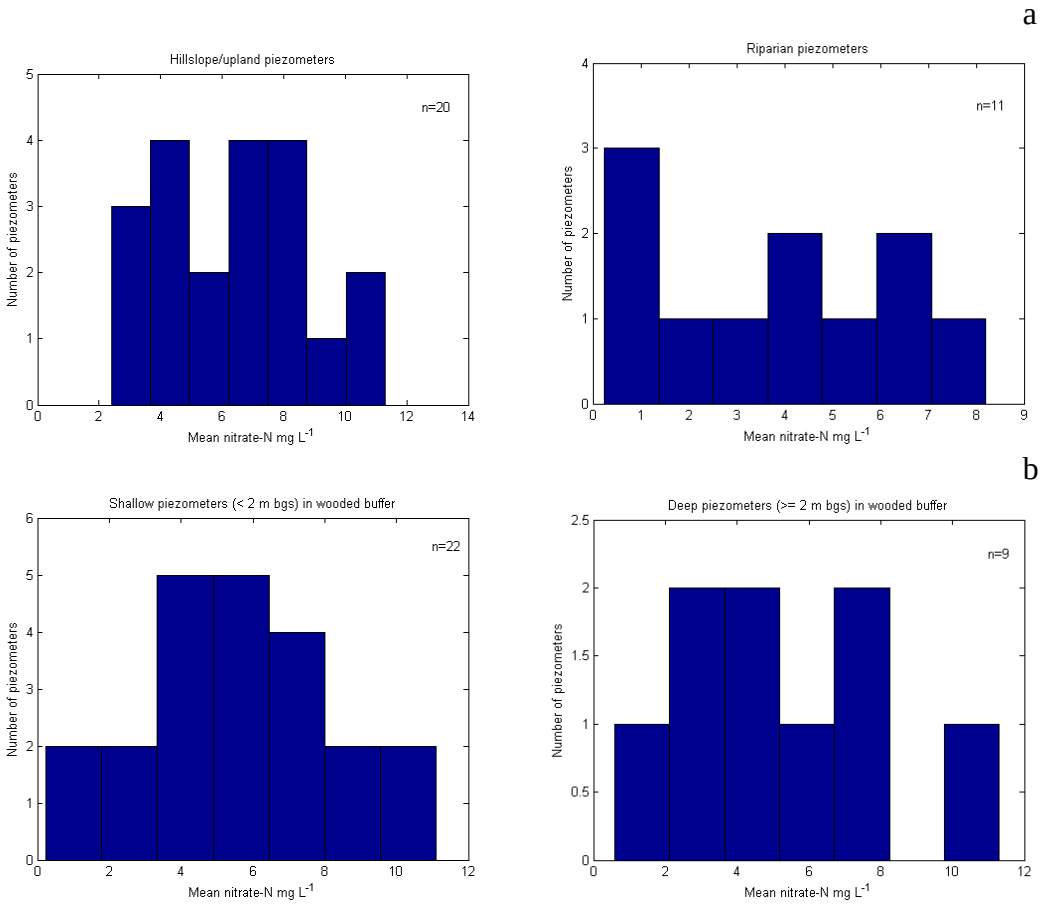

Figure 16. Mean NO_3^--N distributions for piezometers by (a) landscape and (b) depth.

stream channel (PCR3) than at a piezometer located in the outer portion of the riparian floodplain (PCR4) (Table 8).

Table 8. DOC analytical results for PC floodplain site groundwater samples collected on 30 January 2009.

Piezometer	Depth bgs (m)	DOC (mg/L)
PCS0	1.00	1.3
PCS3	2.00	0.5
PCR3	1.43	2.1
PCR4	1.57	0.9
PCR5	2.83	4.2

3.7 Groundwater dissolved oxygen, sulfide and NO_3^--N field analytical results

Dissolved oxygen concentrations measured in the field at the PC floodplain and CK sites were relatively low, while dissolved oxygen varied from ≤ 1 to 4-5 mg/L at the PC upland groundwater-surface water interface (Appendix F). At the PC floodplain site, dissolved oxygen was ≤ 1 mg/L at the hillslope piezometer PCR5 on 31 July 2008, even though NO_3^--N was observed at a mean concentration of 7.2 mg/L at the PCR5 piezometer on this same date. The presence of anaerobic groundwater conditions in shallow floodplain and streambed sediments is supported, however, by the detection of sulfide and low dissolved oxygen concentrations at the PCR3 and PCS0 piezometers on 31 July 2008. At Coal Kiln, dissolved oxygen concentrations in riparian floodplain piezometers ranged from < 1 to 1-2 mg/L, and in streambed piezometers ranged from 1-2 mg/L.

3.8 Groundwater modeling results

Steady-state, groundwater flow was simulated for each site, and plots of the 2-D groundwater flow paths and flow vectors are shown in Figures 17-21. Elevation and distance values along the y-axes of Figures 17-21 are relative to arbitrary, defined reference points and do not reflect actual elevations above sea level. From the model output, general groundwater flow at each site is predominantly horizontal from the upgradient constant head boundary, with a gradual convergence of flow paths at the stream channel. At the CMC floodplain, PC floodplain and CK sites, the reduced hydraulic conductivity values of the floodplain sediments cause a downward deflection of flow paths at the hillslope-floodplain boundary (Figs. 18, 20, 21), which is not simulated

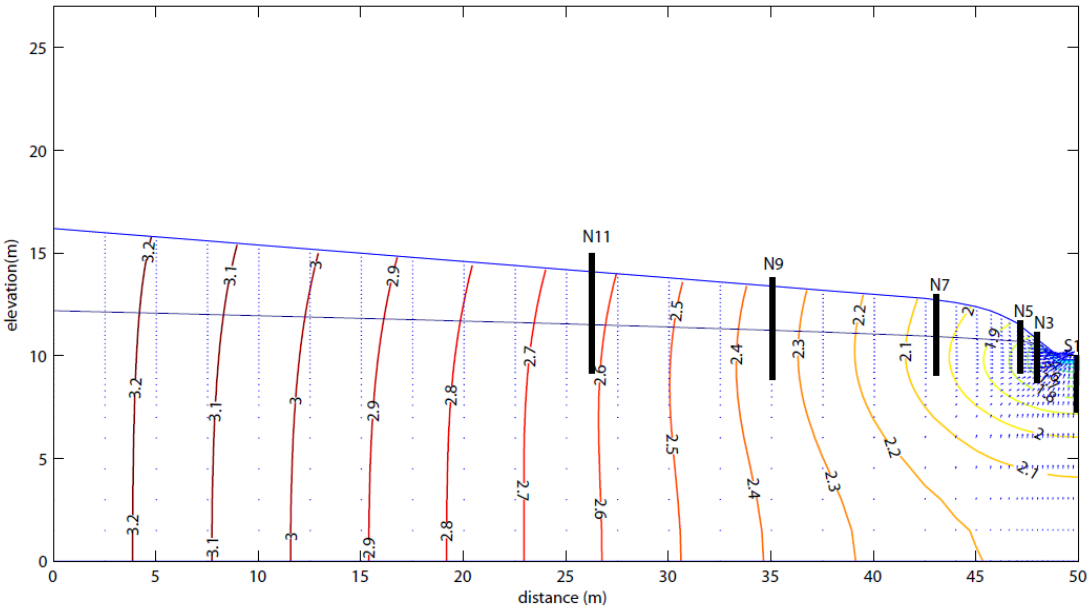

Figure 17. Steady-state, hydraulic head contours of subsurface at CMC hillslope site. The upper surface of the figure is defined by the transect line in Figure 10. Figure is from Gu (2007). Note: Hydraulic head contours should end at water table line and not the land surface line.

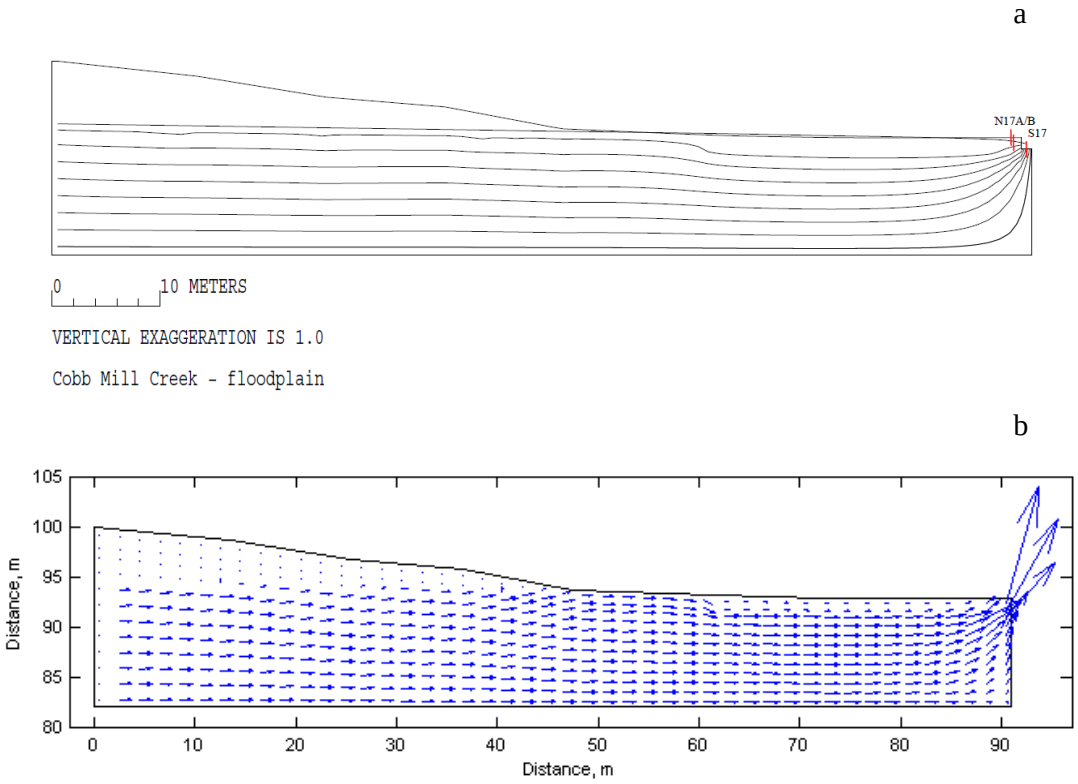

Figure 18. Steady-state, groundwater flow paths determined from MODFLOW and MODPATH (a), and groundwater flow vectors based on MODFLOW output for the CMC floodplain site (b).

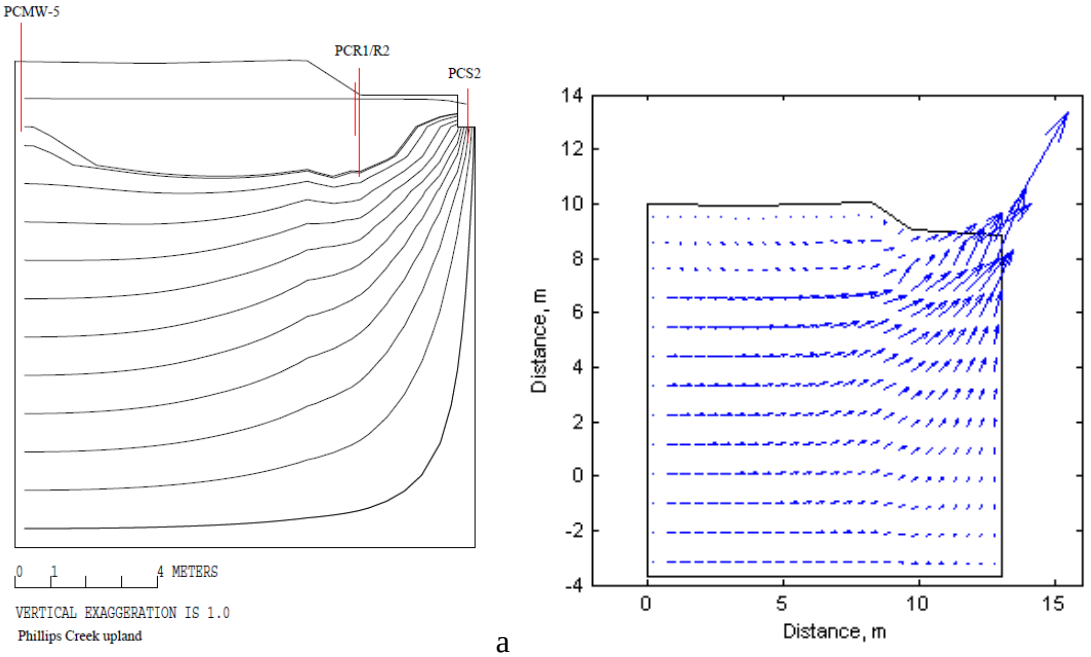

a b

Figure 19. Steady-state, groundwater flow paths determined from MODFLOW and MODPATH (a), and groundwater flow vectors based on MODFLOW output for the PC upland site (b).

a

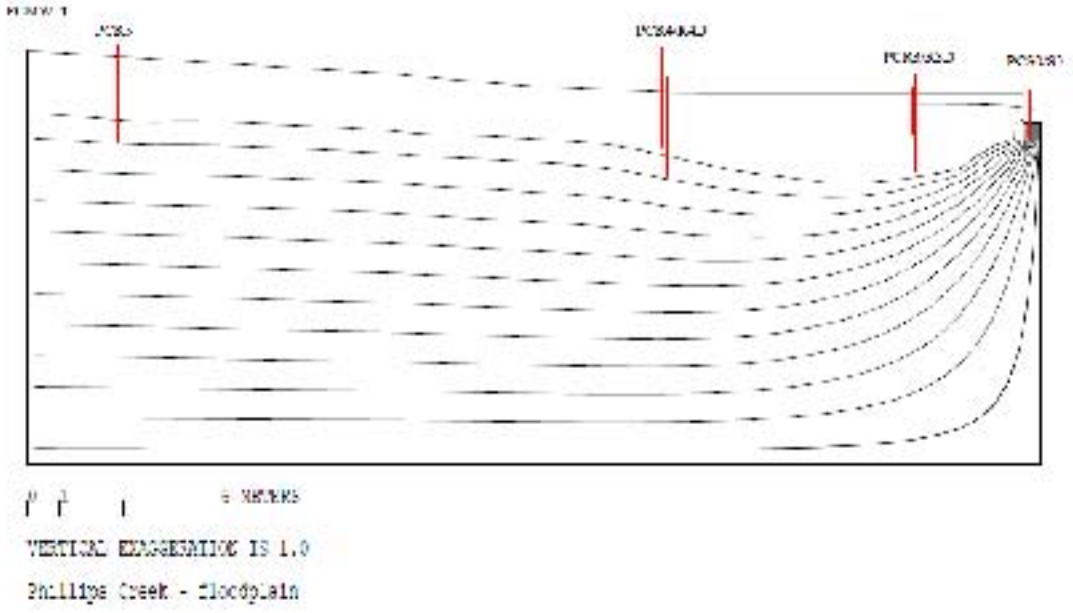

b

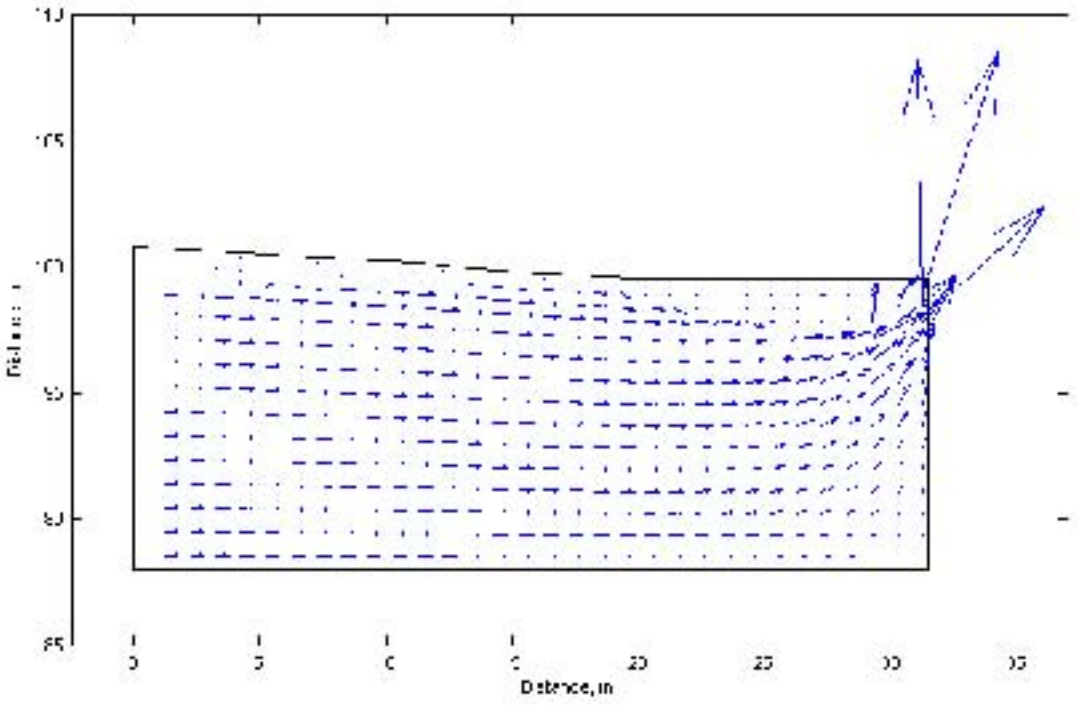

Figure 20. Steady-state, groundwater flow paths determined from MODFLOW and MODPATH (a), and groundwater flow vectors based on MODFLOW output for the PC floodplain site (b).

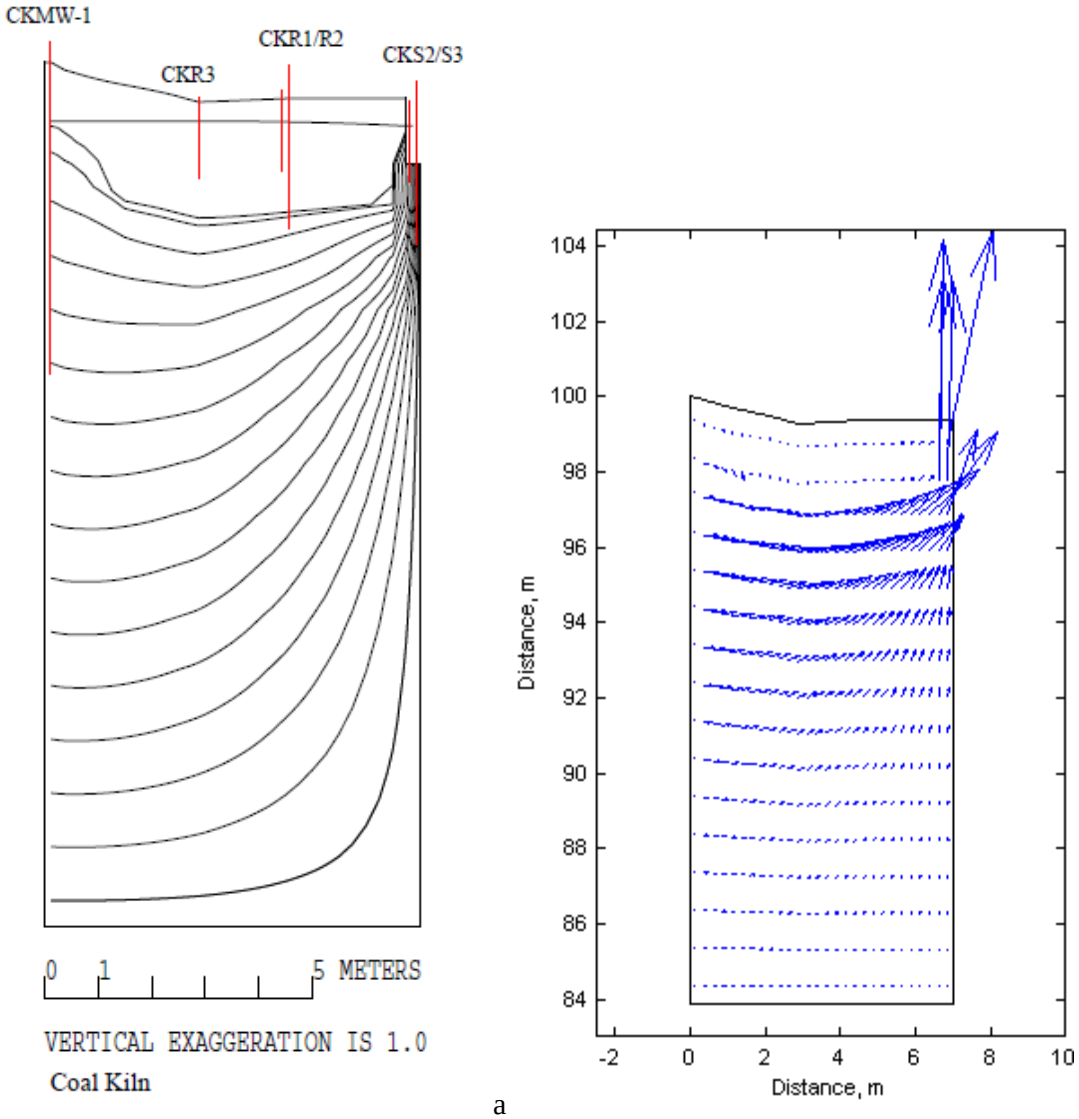

a b

Figure 21. Steady-state, groundwater flow paths determined from MODFLOW and MODPATH (a), and groundwater flow vectors based on MODFLOW output for the CK site (b).

under steady-state conditions at a hillslope-only site (Fig. 17). With the exception of the PC upland site, groundwater flow within the floodplain sediments has a noticeably lower magnitude than flow in the underlying sediments located approximately 2 m or greater below the ground surface, where the hydraulic conductivity was observed or is inferred to be greater than the hydraulic conductivity of the floodplain sediments. The modeled

groundwater flow paths are sensitive to hydraulic conductivity differences in the vertical direction, as seen in plots of flow at the PC upland site. At the upgradient boundary of this site, a downward deflection of the shallow groundwater flow paths was simulated with an increase with depth in hydraulic conductivity from 1.4×10^{-3} cm s^{-1} to 5.5×10^{-3} cm s^{-1}. The inflow - outflow volumetric percent discrepancies of the MODFLOW-based groundwater models, which provide an indication of how well a model is constructed, were $\leq \sim 5\%$ for each site (Table 9).

Table 9. Volumetric percent discrepancies computed by MODFLOW for each site groundwater flow simulation. Note: positive values indicate greater inflow than outflow at model boundaries.

Site	% volumetric discrepancy
CMC floodplain	1.72
PC upland	1.48
PC floodplain	5.08
CK	3.92

3.9 In-stream piezometer vertical hydraulic gradients observations

Vertical hydraulic gradients were computed using depth-to-water and depth-to-stream measurements from in-stream piezometers (Table 10). Data for in-stream piezometers indicate that on average, upward groundwater flow into the stream channel, indicated by positive gradient values, occurred at each site. Noticeably lower vertical hydraulic gradient values occur at the Phillips Creek sites and Coal Kiln than the Cobb Mill Creek floodplain site. This difference reflects the greater topographic relief of the buffer at Cobb Mill Creek compared to the buffers at Phillips Creek and Coal Kiln.

Table 10. Vertical hydraulic head gradients of in-stream piezometers.

Site	Location	Date	Vertical head gradient
CMC floodplain	S17-stream channel	3/6/2007	0.155
		7/13/2007	0.177
		2/3/2008	0.148
		7/16/2009	0.165
			mean = 0.161
PC upland	PCS1-stream channel	7/12/2007	0.152
		8/8/2007	0.066
		7/19/2009	-0.016
			mean = 0.067
	PCS2-stream channel	8/8/2007	0.082
		7/19/2009	-0.007
			mean = 0.038
PC floodplain	PCS0-stream channel	3/6/2007	0.215
		8/8/2007	0.006
		1/30/2009	0.050
		7/19/2009	0.030
			mean = 0.075
CK	CKS1-stream channel	6/3/2007	0.050
		7/13/2007	0.078
		8/8/2007	0.046
			mean = 0.058
	CKS2-stream channel	7/13/2007	0.048
		8/8/2007	0.050
		10/9/2007	0.034
		7/18/2009	-0.009
			mean = 0.031

4 Discussion

In comparison to the natural background concentration of NO_3^--N in shallow groundwater of the Delmarva Peninsula (0.4 mg/L, (Hamilton et al., 1993)), elevated NO_3^--N was observed in groundwater and surface water at each site in this study. The occurrences of NO_3^--N in groundwater within the buffer portion of each site had, however, some noticeable variations. At the CMC floodplain site, elevated NO_3^--N was observed in groundwater one meter below the streambed at this site, which is consistent with observations at the downstream hillslope site. The groundwater entering the forested buffer of the CMC floodplain site was not sampled in this study, but it is likely to have a similar NO_3^--N composition as groundwater sampled at the hilltop well of the CMC hillslope site, which has a mean NO_3^--N concentration of 4.6 mg/L. Moreover, the hilltop well at the CMC hillslope site is screened within the upper portion of the unconfined aquifer at this site, and groundwater sampled from this monitoring well may not reflect the relatively high NO_3^--N concentrations that occur at greater depths in the unconfined aquifer at this site. From the steady-state groundwater modeling results for the Cobb Mill Creek hillslope site (Figure 17), shallow and deep groundwater flow paths converge at the in-stream piezometer S1B, where NO_3^--N has been observed at a mean concentration of 12.4 mg/L.

At Phillips Creek, elevated NO_3^--N was observed in monitoring wells located near the agricultural field-buffer boundary at the upland and floodplain sites, indicating the forested buffers at both of these sites receive inputs of elevated NO_3^--N in groundwater. The buffer at Coal Kiln also receives NO_3^--N inputs based on observations from shallow (< 2 m bgs) piezometers at this site. Unlike other sites, however, NO_3^--N was not

detected in groundwater samples from the outer monitoring well located near the agricultural field-buffer boundary at Coal Kiln, and secondly, was not detected in groundwater sampled from an in-stream piezometer installed at a depth of two meters below the streambed at this site.

Based on NO_3^--N and hydraulic head observations from in-stream piezometers installed at the CMC floodplain, PC upland and PC floodplain sites, groundwater with agriculturally-derived NO_3^--N flows through organic-rich streambed sediments prior to discharging to the stream channel at these sites. The porewater NO_3^--N and sediment organic matter profile obtained from the PC upland site on 11 July 2007 (Figure 6d) is similar to NO_3^--N and organic matter profiles observed in sediment cores from the CMC hillslope site, where nitrate removal by denitrification occurs in the upper 20-40 cm of the streambed sediments (Galavotti, 2004; Gu et al., 2007). In three other profiles from the CMC floodplain, PC upland and PC floodplain sites, NO_3^--N occurred at a concentration < 0.3 mg/L at the base of the porewater profiles (40 cm depth), in contrast to observations at the CMC hillslope site. The elevated NO_3^--N measured in groundwater samples collected at depths $\geq$ 1 m below the streambed at the CMC floodplain and Phillips Creek sites, combined with the relatively low NO_3^--N concentrations observed in shallower porewater samples indicates nitrate attenuation does occur in streambed sediments at these two stream sites, and is due to either mixing with groundwaters absent of elevated NO_3^--N, and/or removal of NO_3^--N by microbial activity, which presumably is denitrification. Occurrences of NO_3^--N in surface water samples from Phillips Creek and Coal Kiln at concentrations greater than natural background concentration indicate

agriculturally-derived NO_3^--N is able to transported to the stream channel at both sites through natural groundwater discharge and/or engineered drainage.

The buffer topographic profiles in this study show differences are present among the five sites in their relative proportion of hillslope and riparian floodplain landscapes. From a geomorphic standpoint, landscape differences within the topographic profile are also supported by differences in subsurface soil and sediment composition, which were observed at the PC upland and PC floodplain. Soil and subsurface sediment characteristics at these two sites reveal a decrease in sand content and corresponding increases in organic matter and fine-grained sediment content between outer, hillslope/upland points (PCR5, PCMW5) and riparian points near the stream channel (PCR1/R2, PCR3) (Appendix B). This fining pattern in soils from the outer upland/hillslope portion of the buffer to the riparian floodplain portion of the buffer was not observed at Coal Kiln, where soils from approximately 0 to 40 cm observed in cores collected at the agricultural field-buffer boundary were generally similar to soils and sediments at this same depth interval encountered during installation of the piezometers in the riparian floodplain portion of this site (Appendix B). The lack of marked differences in soil and sediment characteristics across the topographic profile at Coal Kiln indicates buffer topography does not have as much of an effect on the soil and subsurface sediment texture at this site compared to Phillips Creek.

Where subsurface sediments were not able to be observed through coring or augering, differences in their texture within the buffer portions of each site were indicated by differences in their subsurface hydraulic conductivity values determined from slug

tests. At both the PC upland and floodplain sites, hydraulic conductivity values of the sediments surrounding piezometer or monitoring well points decreased by an order of magnitude between the hillslope/upland and floodplain landscapes (Table 6). The decrease in hydraulic conductivity from the hillslope to riparian floodplain landscape at both Phillips Creek sites indicates the general fining in sediment texture observed in soils and shallow sediments collected during augering and coring also occurs in the shallow sediments (< 2 m bgs) where groundwater samples were collected.

The slug test results also indicate subsurface hydraulic conductivity values differ with depth within the riparian floodplain landscapes investigated in this study. At the CMC floodplain and CK sites, greater hydraulic conductivity values were observed at the deep piezometer compared to the shallow piezometer in clusters installed in the riparian floodplains at these sites (Table 6). Although the hydraulic conductivity of sediments surrounding the deep piezometers in clusters installed in this same landscape setting could not be quantified at the Phillips Creek sites, an increase in hydraulic conductivity with depth can qualitatively be seen in slug test data from the Phillips Creek floodplain site. Specifically, the slug test water level data from PCR3D (2.52 m bgs) shows a greater rate of water level increase during the rising head portion of the slug test than the rate of water level increase recorded during the rising head portion of the slug test at PCR3 (1.43 m bgs) (Appendix D). Additional support for a textural, and likewise hydraulic conductivity transition in floodplain sediments within the depth interval of PCR3 and PCR3D can be found in observations of floodplain lithology at Walls Landing Creek in the Eastern Shore of Virginia. Subsurface sediments at two well clusters

installed in the floodplain along Walls Landing Creek "… consisted of dark brown, organic rich, fine-grained sand, silt and clay" in the upper three to four feet (0.91 to 1.22 m), and below this depth, were a "… fine-grained to coarse-grained, tan to light-tan sand and contain abundant gravel …" (Speiran, 1996).

Using measured and literature values for hydrologic boundary conditions and aquifer properties, groundwater flow was simulated at each site using MODFLOW. The volumetric percent discrepancies of the site-specific groundwater flow models, which provide an indication of how well the model is constructed, ranged from 1.48 to 5.08%. The 5.08% discrepancy obtained for the PC floodplain site model may be due to a greater down-valley direction of groundwater flow toward the stream channel than the direction of flow indicated by the groundwater model transect line. If the groundwater model transect line was also oriented in a more down-valley direction, a lower stream constant head boundary would be obtained, which may reduce volumetric flow discrepancy in the model. While a groundwater model transect line that was more oriented differently may have a lower flow discrepancy for the PC floodplain site, the flow paths shown in such a model would likely be very similar to flow paths shown in Figure 20.

The riparian floodplains at the CMC floodplain, PC floodplain and CK sites had an effect on the shallow groundwater flow paths at these sites based on the groundwater modeling results. Close-up images of the groundwater flow vectors in the floodplain portions of these sites reveal a downward deflection of flow paths at the hillslope-floodplain transitions at these sites (Figure 22(a-c)). A downward deflection of groundwater flow was not observed, however, at the PC upland site (Figure 22(d)). The

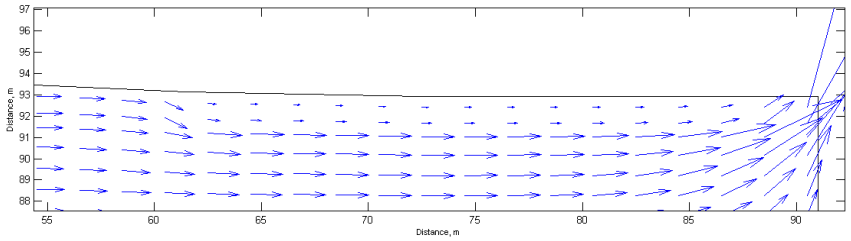

a

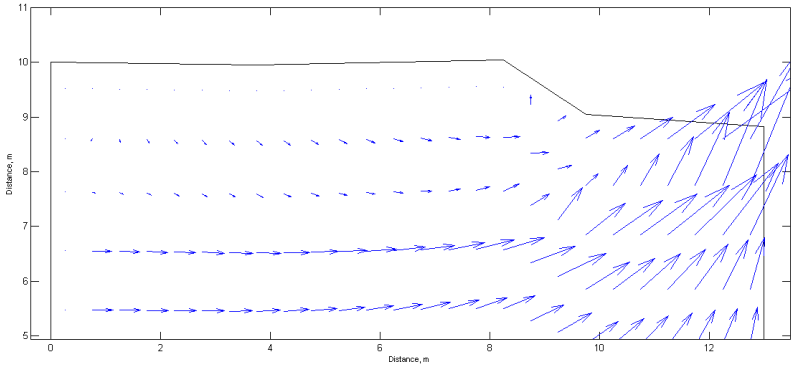

b

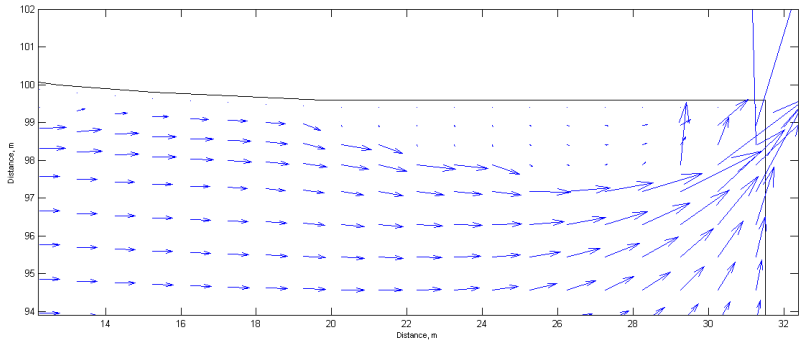

c

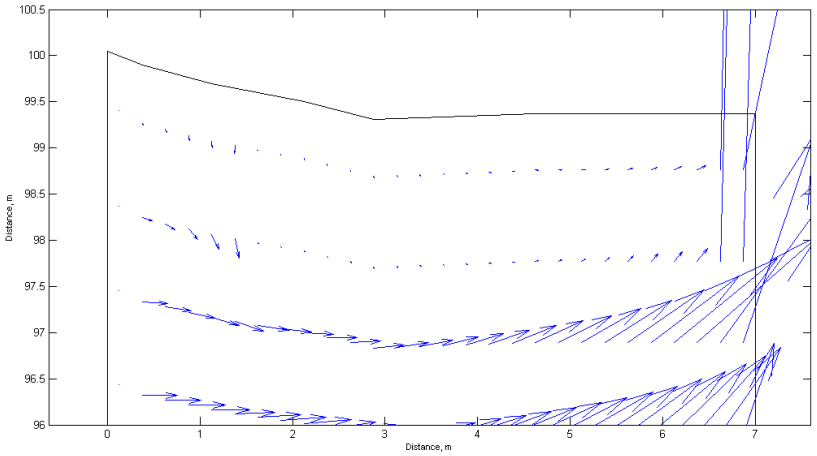

d

Figure 22. Close-up view of groundwater flow vectors in and near floodplain sediments at (a) CMC floodplain, (b) PC upland, (c) PC floodplain and (d) CK.

lack of flow path deflection at the PC upland site is attributed to the presence of less permeable streambed sediments at this site compared to the CMC and CK sites, and to more permeable floodplain sediments at this site compared to the floodplain sediments located at the PC floodplain site. At the sites where a groundwater flow path deflection was modeled, the pattern of deflection and area of low groundwater flow follows the zones of low hydraulic conductivity in each model (Appendix A).

The distances between the upgradient constant head boundaries and the stream head boundaries represented in the PC upland and CK site groundwater flow models are relatively small compared to the distances between these same points in the other groundwater flow models in this study. The relative proximity of the constant head boundary to the stream head boundary in the PC upland and CK site models may be the cause for at least some of the downward deflection of the groundwater flow paths near the upgradient end of each model (Figures 19 and 21). A downward direction of groundwater flow paths at an upgradient head boundary, followed by an upward direction of groundwater flow paths toward a stream head boundary, can occur in relatively small, localized flow systems (Toth, 1963). By setting the upgradient constant head boundary relatively close to the stream head boundary, localized flow systems that are unrepresentative of the actual groundwater hydrology may be present in the uppermost layers of the PC upland and CK site groundwater flow models.

For sites where a floodplain comprises half or nearly half of the total buffer width (*i.e.*, CMC floodplain, PC floodplain, CK), deflection of groundwater flow paths beneath floodplain sediments enables the potential for elevated NO_3^--N in shallow groundwater to

by-pass the floodplain sediments. The groundwater modeling results, and observations of NO_3^--N in piezometers at the PC floodplain site indicate the absence of elevated NO_3^--N in shallow floodplain sediments (< 2 m bgs) is due to this by-pass flow process. The groundwater modeling results from the CMC floodplain site indicate differences in vertical hydraulic conductivity that are less than an order of magnitude can cause flow paths to be deflected downward beneath the floodplain sediments, although additional data on groundwater NO_3^--N in the outer portion of the floodplain at this site is needed to confirm a by-pass flow mechanism at this site. At Coal Kiln, the modeled groundwater flow and observations of NO_3^--N at this site are not in agreement, with modeled flow paths indicating elevated NO_3^--N should occur in the relatively deep groundwater sampled at this site, and not in the shallow groundwater where it was observed. Comparison of this site to others in this study has added difficulty, however, due to the lack of elevated NO_3^--N in groundwater that is deeper than ~2 m below the ground surface or streambed at this site.

Similar observations on the ability of groundwater with elevated NO_3^--N to by-pass floodplain sediments were reported by Burt et al. (1999) for a riparian floodplain adjacent to the River Thame in England. At their study site, the presence of a gravel layer beneath the fine-grained floodplain sediment was considered to act as a preferential pathway for agriculturally-derived nitrate to enter the river channel. The mechanism for NO_3^--N in groundwater to by-pass floodplain sediments identified by Burt et al. (1999) differs from the conceptual model for the occurrence of by-pass flow identified by Lowrance et al. (1997) for outer coastal plain unconfined aquifers, where the presence of

relatively thick aquifers allows deep flow paths to discharge directly to stream channels. At the PC floodplain site, both the stratigraphy of sediments in the floodplain and the aquifer thickness appear to allow groundwater with elevated NO_3^--N to by-pass any nitrate removal that would occur in the shallow (< 2 m bgs) floodplain sediments.

The modeled groundwater flow paths and observations of NO_3^--N from sites in this study indicate the effect of riparian floodplains on shallow groundwater NO_3^--N is more apparent at buffers where the floodplain is a relatively extensive landscape feature. The downward deflection of groundwater flow paths at the CMC floodplain and PC floodplain sites is clearly shown by the steady-state groundwater modeling results (Fig. 22a, 22c). The groundwater NO_3^--N observations from the PC floodplain site support a by-pass flow mechanism for the occurrence of low to non-detected concentrations of NO_3^--N in shallow floodplain groundwater at this site. This by-pass flow is not seen at the PC upland and CK sites, where the relatively narrow floodplains at these sites (~3 to 4 m length) do not have a clear effect on shallow groundwater NO_3^--N. In consideration of these site differences, it appears that a minimum floodplain length (normal to the stream channel) is needed to cause NO_3^--N to be transported beneath the floodplain in the study region. The lengths of the floodplains at the PC floodplain and CMC floodplain sites are approximately 12 and 30 m, respectively, which suggest that outer coastal plain buffer-stream sites with thick riparian floodplains that are at least 12 m in length will have low or non-detectable concentrations of NO_3^--N in the shallow floodplain groundwater.

A key criterion in the occurrence of a by-pass flow mechanism for groundwater NO_3^--N is not the width of the floodplain alone, but the presence of permeable sediments (*e.g.* sands, gravels) that function as a preferential flow path beneath the less permeable, fine-grained floodplain sediments (Burt, 1997). The floodplains on the Eastern Shore of Virginia that are relatively wide (>12 m in length) may facilitate better sorting of silt from the sandy soils and streambed sediments than stream reaches with a relatively narrow or non-existent floodplain. The silt that is deposited in the floodplain would cause the development of a relatively low permeability layer over the permeable sediments that comprise the Columbia aquifer. The development of a distinct floodplain deposit would subsequently allow groundwater to preferentially flow beneath the floodplain and by-pass its nitrate removal ability.

In the conceptual model for nitrate removal in riparian zones developed by Vidon and Hill (2004c), the critical controls identified in the model are buffer topography, aquifer thickness and soil/sediment texture. Based on their model, the sites in this study with slopes >5% (CMC hillslope, CMC floodplain, PC upland and Coal Kiln) would be small N sinks, while the PC floodplain site, which has an average slope of 4.1%, would function as a small to medium N sink. The by-pass flow mechanism identified at the PC floodplain site prevents significant nitrate removal from occurring at this site; therefore, the PC floodplain site cannot be considered a greater N sink than the other four sites in this study. The ability of groundwater with elevated NO_3^--N to by-pass floodplain sediments indicates an understanding of groundwater hydrology at buffers with slopes <5% is necessary to categorize their importance as locations for nitrate removal.

In summary, the results from this study indicate riparian floodplains along streams in the Eastern Shore of Virginia can affect NO_3^--N concentrations in shallow (< 2 m bgs) groundwater. The absence of elevated NO_3^--N in shallow groundwater in a riparian floodplain landscape is caused by a downward deflection of groundwater flow at the hillslope-floodplain transition, which limits the capacity for nitrate to be removed in riparian floodplain sediments. This by-pass flow mechanism was more apparent at a site with a relatively extensive floodplain (12 m length), indicating a minimal floodplain length is needed to have a clear effect on shallow groundwater NO_3^--N. Occurrences of elevated NO_3^--N in groundwater beneath the streambed was observed at four of the five buffer-stream sites in this study. The varying proportions of hillslope and floodplain landscapes at these four sites indicate elevated NO_3^--N can be transported to streambed sediments regardless of buffer topography and landscape. Denitrification in streambed sediments remains, therefore, a critical mechanism for reducing nitrate delivery to stream channels in this region.

Bibliography

Angier, J., et al. (2005). "Hydrology of a first-order riparian zone and stream, mid-Atlantic coastal plain, Maryland." Journal of Hydrology **309**: 149-166.

Bohlke, J. and J. Denver (1995). "Combined use of groundwater dating, chemical, and isotopic analyses to resolve the history and fate of nitrate contamination in two agricultural watersheds, Atlantic coastal plain, Maryland." Water Resources Research **31**(9): 2319-2339.

Bouwer, H. (1989). "The Bouwer and Rice slug test - an update." Ground Water **27**(3): 304-309.

Bouwer, H. and R. C. Rice (1976). "A slug test for determining hydraulic conductivity of unconfined aquifers with completely or partially penetrating wells." Water Resources Research **12**(3): 423-428.

Bricker, S., et al. (2007). Effects of Nutrient Enrichment in the Nation's Estuaries: A Decade of Change. NOAA Coastal Ocean Program Decision Analysis Series No. 26. National Centers for Coastal Ocean Science, Silver Spring, MD. **:** 328 pp.

Burger, R. L. and K. Belitz (1997). "Measurement of anisotropic hydraulic conductivity in unconsolidated sands: a case study from a shoreface deposit, Oyster, Virginia." Water Resources Research **33**(6): 1515-1522.

Burt, T., et al. (1999). "Denitrification in riparian buffer zones: the role of floodplain hydrology." Hydrological Processes **13**(10): 1451-1463.

Burt, T. P. (1997). The hydrological role of floodplains within the drainage basin system. Buffer zones: their processes and potential in water protection. N. E. Haycock, T. P. Burt, K. W. T. Goulding and G. Pinay. Hertfordshire, UK, Quest Environmental.

Denver, J., et al. (2004). "Water quality in the Delmarva Peninsula: Delaware, Maryland, and Virginia, 1999-2001." United States Geological Survey **Circular 1228**: 36 pp.

Domagalski, J. L., et al. (2008). "Influences of the unsaturated, saturated, and riparian zones on the transport of nitrate near the Merced River, California, USA." Hydrogeology Journal **16**(4): 675-690.

Fetter, C. W. (1994). Applied Hydrogeology. Upper Saddle River, NJ, Prentice-Hall, Inc.

Freeze, R. A. and J. A. Cherry (1979). Groundwater. Englewood Cliffs, NJ, Prentice-Hall, Inc.

Galavotti, H. (2004). Spatial profiles of sediment denitrification at the ground water - surface water interface in Cobb Mill Creek on the Eastern Shore of Virginia. Environmental Sciences. Charlottesville, VA, University of Virginia. **M.S.:** 94.

Gold, A. J., et al. (1998). "Patchiness in groundwater nitrate removal in a riparian forest." Journal of Environmental Quality **27**: 146-155.

Gregory, S. V., et al. (1991). "An ecosystem perspective of riparian zones." Bioscience **41**(8): 540-551.

Groffman, P., et al. (1992). "Nitrate dynamics in riparian forests: microbial studies." Journal of Environmental Quality **21**: 666-671.

Gu, C. (2007). Hydrological control on nitrate delivery through the groundwater-surface water interface. Department of Environmental Sciences. Charlottesville, VA, University of Virginia. **Ph.D:** 250.

Gu, C., et al. (2007). "Nitrate reduction in streambed sediments: effects of flow and biogeochemical kinetics." Water Resources Research **43**: W12413, doi:10.1029/2007WR006027.

Gu, C., et al. (2008). "Influence of stream-groundwater interactions in the streambed sediments on NO_3^- flux to a low-relief coastal stream." Water Resources Research **44**: W11432, doi:10.1029/2007WR006739.

Hamilton, P. A., et al. (1993). Water-quality assessment of the Delmarva peninsula, Delaware, Maryland, and Virginia - effects of agricultural activities on, and distribution of, nitrate and other inorganic constituents in the surficial aquifer, USGS Open File Report 93-40.

Hamilton, P. A. and D. R. Helsel (1995). "Effects of agriculture on ground-water quality in five regions of the United States." Ground Water **33**(2): 217-226.

Harbaugh, A. W. (2005). MODFLOW-2005, The U.S. Geological Survey modular ground-water model - the Ground-Water Flow Process: U.S. Geological Survey Techniques and Methods 6-A16, variously p.

Hill, A. (1990). "Ground water flow paths in relation to nitrogen chemistry in the near-stream zone." Hydrobiologia **206**: 39-52.

Hill, A. (1996). "Nitrate removal in stream riparian zones." Journal of Environmental Quality **25**(4): 743-755.

Hill, A. R. (2000). Stream chemistry and riparian zones. Streams and Ground Waters. J. B. Jones and P. J. Mulholland. San Diego, CA, Academic Press**:** pp. 83-110.

Hornberger, G. and P. Wiberg (2005). Numerical methods in hydrological science, American Geophysical Union.

Hubbard, S., et al. (2001). "Hydrogeological characterization of the South Oyster Bacterial Transport Site using geophysical data." Water Resources Research **37**(10): 2431-2456.

Lowrance, R. (1992). "Groundwater nitrate and denitrification in a coastal plain riparian forest." Journal of Environmental Quality **21**: 401-405.

Lowrance, R., et al. (1997). "Water quality functions of riparian forest buffers in Chesapeake Bay watersheds." Environmental Management **21**(5): 687-712.

Lowrance, R., et al. (1984). "Riparian forests as nutrient filters in agricultural watersheds." BioScience **34**(6): 374-377.

McClain, M., et al. (2003). "Biogeochemical hot spots and hot moments at the interface of terrestrial and aquatic ecosystems." Ecosystems **6**: 301-312.

Meng, A. A. and J. H. Harsh (1988). Hydrogeologic framework of the Virginia coastal plain, USGS. **Professional Paper 1404-C**.

Mixon, R. B. (1985). Stratigraphic and geomorphic framework of uppermost Cenozoic deposits in the southern Delmarva peninsula, Virginia and Maryland. Washington, D.C., USGS.

NOAA (2004). Climatography of the United States No. 20 Monthly Station Climate Summaries, 1971-2000 National Climatic Data Center.

Paerl, H. W. (1997). "Coastal eutrophication and harmful algal blooms: importance of atmospheric deposition and groundwater as "new" nitrogen and other nutrient sources." Limnology and Oceanography **42**(5): 1154-1165.

Peterjohn, W. T. and D. L. Correll (1984). "Nutrient dynamics in an agricultural watershed: observations on the role of a riparian forest." Ecology **65**(5): 1466-1475.

Pollock, D. W. (1994). "User's Guide for MODPATH/MODPATH-Plot, Version 3: A particle tracking post-processing package for MODFLOW, the U.S. Geological Survey finite-difference ground-water flow model: U.S. Geological Survey Open-File Report 94-464." 234 pp.

Puckett, L. J., et al. (2002). "Using chemical, hydrologic, and age dating analysis to delineate redox processes and flow paths in the riparian zone of a glacial outwash aquifer-stream system." Water Resources Research **38**(8): 10.1029/2001WR000396.

Remson, I., et al. (1971). Numerical methods is subsurface hydrology. New York, John Wiley & Sons, Inc.

Richardson, D. L. (1994). Hydrogeology and analysis of the ground-water flow system of the Eastern Shore, Virginia USGS Water-Supply Paper 2401. USGS.

Speiran, G. K. (1996). Geohydrology and geochemistry near coastal ground-water-discharge areas of the Eastern Shore, Virginia. USGS. **Water Supply Paper 2479**.

Tesoriero, A. J., et al. (2000). "Mechanism and rate of denitrification in an agricultural watershed: electron and mass balance along groundwater flow paths." Water Resources Research **36**(6): 1545-1559.

Toth, J. (1963). "A theoretical analysis of groundwater flow in small drainage basins." Journal of Geophysical Research **68**(16): 4795-4812.

Vidon, P. and A. R. Hill (2004a). "Denitrification and patterns of electron donors and acceptors in eight riparian zones with contrasting hydrogeology." Biogeochemistry **71**(2): 259-283.

Vidon, P. G. F. and A. R. Hill (2004b). "Landscape controls on the hydrology of stream riparian zones." Journal of Hydrology **292**: 210-228.

Vidon, P. G. F. and A. R. Hill (2004c). "Landscape controls on nitrate removal in stream riparian zones." Water Resources Research **40**(3).

Winston, R. B. (2009). "ModelMuse - A graphical user interface for MODFLOW-2005 and PHAST: U.S. Geological Survey Techniques and Methods 6-A29." 52 pp.

Winter, T. C., et al. (1999). Ground water and surface water: a single resource. US Geological Survey Circular 1139, United States Geological Survey.

Appendix A – Groundwater model input parameters

Site: Cobb Mill Creek floodplain

Hydrologic boundary conditions

Upgradient constant head boundary: 94.213 m
Stream constant head boundary: 92.374 m
Recharge: 8×10^{-9} m s^{-1}

Horizontal hydraulic conductivity (K_x) values

Zone 1 K_x: 1.1×10^{-3} cm s^{-1}, slug test measurement
Zone 2 K_x: 1.7×10^{-3} cm s^{-1}, slug test measurement
Zone 3 K_x: 3.9×10^{-3} cm s^{-1}, slug test measurement
Zone 4 K_x: 5.5×10^{-3} cm s^{-1}, literature

SIP solver seed value for iteration variables: 2.1449×10^{-4}

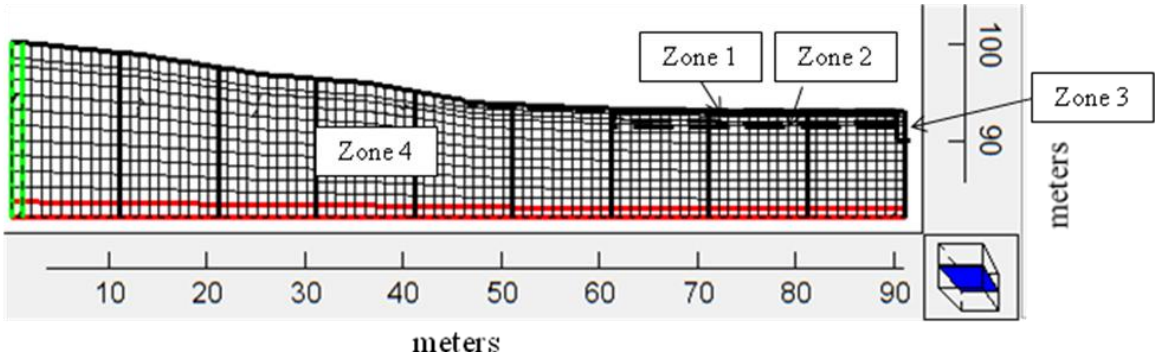

Figure A.1. CMC floodplain hydraulic conductivity zones.

Note: The source of the hydraulic conductivity value is included for each hydraulic conductivity zone.

Site: Phillips Creek upland

Hydrologic boundary conditions

Upgradient constant head boundary: 8.9 m
Stream constant head boundary: 8.164 m
Recharge: 4×10^{-9} m s^{-1}

Horizontal hydraulic conductivity (K_x) values

Zone 1 K_x: 1.4×10^{-3} cm s^{-1}, slug test measurement
Zone 2 K_x: 4.5×10^{-4} cm s^{-1}, slug test measurement
Zone 3 K_x: 7.6×10^{-5} cm s^{-1}, laboratory permeameter measurement
Zone 4 K_x: 5.5×10^{-3} cm s^{-1}, literature

SIP solver seed value for iteration variables: 4.44882×10^{-4}

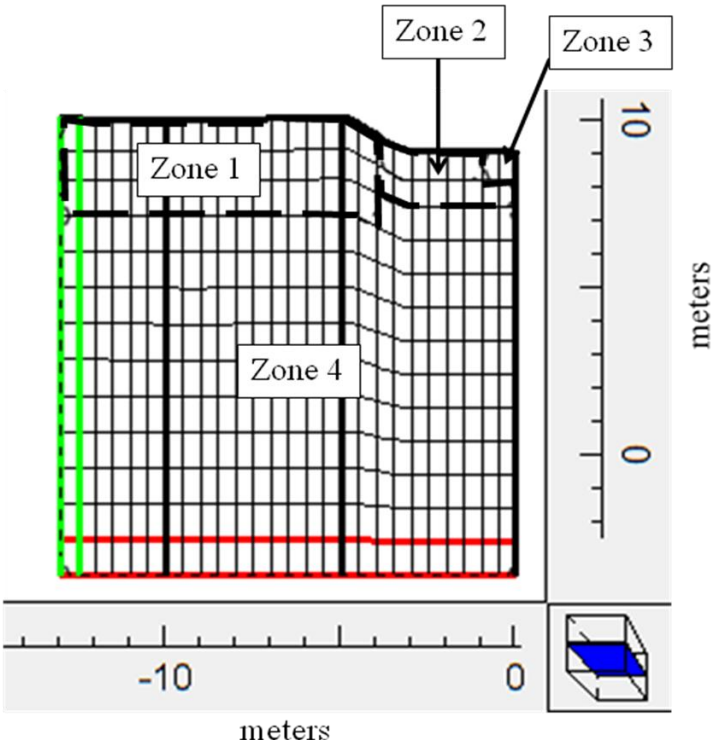

Figure A.2. PC upland hydraulic conductivity zones.

Site: Phillips Creek floodplain

Hydrologic boundary conditions

Upgradient constant head boundary: 99.28 m

Stream constant head boundary: 99.082 m

Recharge: 3×10^{-9} m s^{-1}

Horizontal hydraulic conductivity (K_x) values

Zone 1 K_x: 3.4×10^{-3} cm s^{-1}, slug test measurement

Zone 2 K_x: 8.8×10^{-5} cm s^{-1}, slug test measurement

Zone 3 K_x: 5.5×10^{-3} cm s^{-1}, literature

SIP solver seed value for iteration variables: 1.30827×10^{-4}

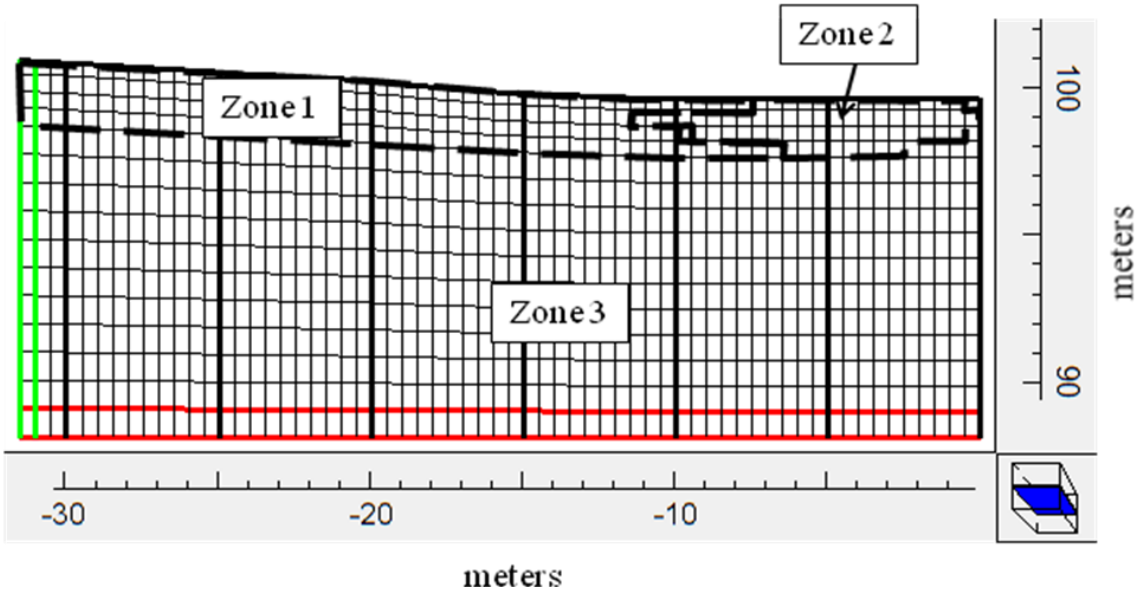

Figure A.3. PC floodplain hydraulic conductivity zones.

Site: Coal Kiln

Hydrologic boundary conditions

Upgradient constant head boundary: 98.947 m

Stream constant head boundary: 98.863 m

Recharge: 8×10^{-9} m s^{-1}

Horizontal hydraulic conductivity (K_x) values

Zone 1 K_x: 1.2×10^{-2} cm s^{-1}, laboratory permeameter measurement

Zone 2 K_x: 7.4×10^{-5} cm s^{-1}, slug test measurement

Zone 3 K_x: 2.6×10^{-3} cm s^{-1}, slug test measurement

Zone 4 K_x: 5.5×10^{-3} cm s^{-1}, literature

SIP solver seed value for iteration variables: 2.4281×10^{-4}

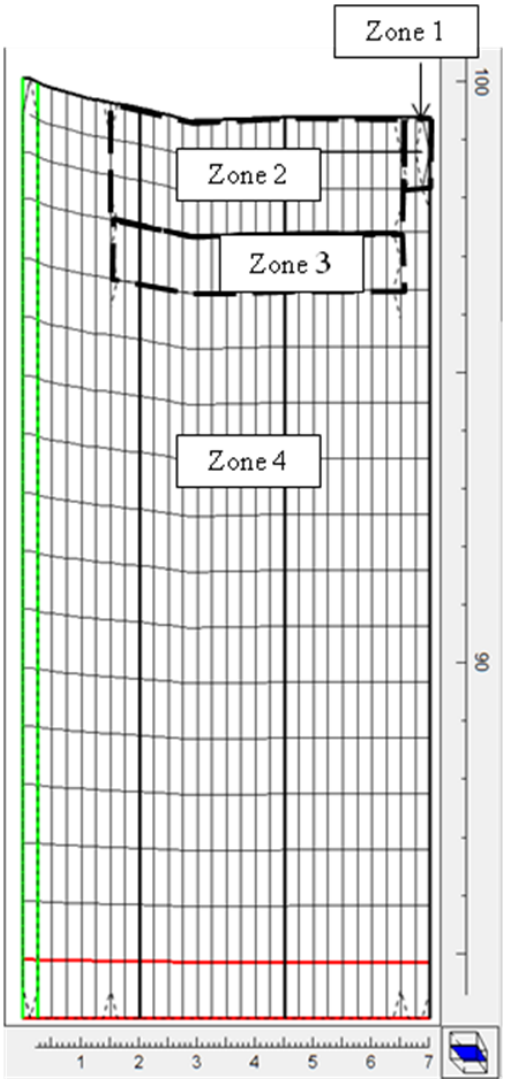

Figure A.4. Coal Kiln hydraulic conductivity zones.

Appendix B – Soil and sediment core logs

Sediment core: CMC 3/5/07
Date collected: 5 March 2007
Site: CMC floodplain

Length of core advanced: Not recorded
Length of core recovered: 47.0 cm

Depth (cm)	Description
0 – 7.6	Brown fine SAND with some organic matter
7.6 – 15.2	Dk. brown fine SAND and ORGANIC MATTER
15.2 – 27.9	Dk. tan medium to coarse SAND with traces of fine quartz gravel and organic matter
27.9 – 30.4	Tan-gray fine to medium SAND with trace organic matter
30.4 – 35.6	Brown fine to medium SAND with trace organic matter; oxidized iron staining surrounding particulate organic matter at 35.6 cm
35.6 – 47.0	Tan fine SAND with traces of fine quartz gravel and thin organic matter lenses

Sediment core: PC 3/5/07
Date collected: 5 March 2007
Site: PC floodplain

Length of core advanced: Not recorded
Length of core recovered: 58.4 cm

Depth (cm)	Description
0 – 12.7	Dk. tan fine to coarse SAND with little particulate plant detritus and organic matter
12.7 – 33.0	Tan fine to coarse SAND with trace organic matter, organic matter lenses present at approximately 20 cm and 28 cm depths
33.0 – 41.9	Dk. fine to medium SAND with trace organic matter
41.9 – 44.5	Tan to slight gray fine SAND with trace organic matter
44.5 – 58.4	Dk. brown PEAT with little particulate wood detritus

Note: Depth is distance from top of sediment in core.

Sediment core: Coal Kiln 6/2/07
Date collected: 2 June 2007
Site: Coal Kiln

Length of core advanced: Not recorded
Length of core recovered: 60 cm

Depth (cm)	Description
5	Tan fine to medium SAND, clean, with traces of dark mineral sands and fine gravel
10	Tan fine SAND, clean with trace dark mineral sands
20	Brown fine to medium SAND with traces of silt and organic matter
30	Same as 20 cm depth
40	Tan-brown very fine to fine SAND with traces of fine gravel, organic matter and dark mineral sands
50	Tan very fine to fine SAND with trace of dark minerals
60	Same as 50 cm depth

Sediment core: PCPW2
Date collected: 11 July 2007
Site: Phillips Creek upland

Length of core advanced: Not recorded
Length of core recovered: 57 cm

Depth (cm)	Description
0 – 6	Dk. brown PEAT with trace plant fragments
6 – 20	Dk. brown PEAT and fine to medium SAND with trace of woody plant fragments
20 – 28	Brown to tan-brown fine to coarse SAND with little organic matter, trace plant fragments
28 – 34	Dk. brown fine SAND with some organic matter, trace silt
34 – 57	Brown SILT with little organic matter, traces of fine to coarse sand and clay

Sediment core: CKPW2
Date collected: 12 July 2007
Site: Coal Kiln

Length of core advanced: Not recorded
Length of core recovered: 73.7 cm

Depth (cm)	Description
0 – 55.9	Tan medium to coarse SAND, traces of organic lenses from 0 to 46 cm, oxidized iron lens at 23 cm, brown patchy organic matter with oxidized iron from 46 to 55.9 cm
55.9 – 73.7	Lt. gray to tan fine SAND with oxidized iron staining present from 64.8 to 67.3 cm

Sediment core: PCPW3
Date collected: 8 August 2007
Site: Phillips Creek upland

Length of core advanced: Not recorded
Length of core recovered: 59 cm

Depth (cm)	Description
0 – 4	Dk. brown organic PEAT with trace plant fragments
4 – 21	Dk. brown organic PEAT with some fine to coarse sand, silt and trace woody plant fragments
21 – 50	Dk. brown fine to medium SAND with little organic matter, traces of silt and plant fragments
50 – 59	Tan fine to medium SAND with trace organic matter

Sediment core: CKPW3
Date collected: 8 October 2007
Site: Coal Kiln

Length of core advanced: Not recorded
Length of core recovered: 60 cm

Depth (cm)	Description
5	Dk. tan fine SAND, clean
10	Tan fine to medium SAND, clean
20	Lt. brown fine to coarse SAND with trace organic matter
30	Tan-brown fine to coarse SAND with trace organic matter
40	Tan fine SAND with trace organic matter
50	Tan-gray very fine to fine SAND with trace mica grains
60	Tan very fine to fine SAND, clean

Sediment core: PC 2/2/08
Date collected: 2 February 2008
Site: Phillips Creek floodplain

Length of core advanced: 173 cm
Length of core recovered: 143 cm

Depth (cm)	Description
0 – 1	Tan-brown fine to medium SAND with little fine gravel, trace particulate plant matter
1 – 7	Brown fine SAND with trace organic matter
7 – 16	Tan-brown fine SAND with trace organic matter
16 – 34	Tan fine to medium SAND with trace of coarse sand and organic matter
34 – 69	Brown PEAT
69 – 71	Brown woody PLANT DEBRIS
71 – 78	Tan fine SAND with traces of fine gravel and organic matter
78 – 90	Tan-brown fine to coarse SAND with little fine gravel, trace organic matter
90 – 102	Tan very fine to fine SAND with little silt, trace woody plant debris
102 – 108	Tan very fine to fine SAND with trace fine gravel
108 – 112	Tan-brown very fine to fine SAND with trace woody plant debris
112 – 136	Tan very fine to fine SAND with trace silt
136 – 143	Tan very fine to medium SAND with trace coarse sand

Sediment core: CK 2/2/08
Date collected: 2 February 2008
Site: Coal Kiln

Length of core advanced: 173 cm
Length of core recovered: 118 cm

Depth (cm)	Description
0 – 2	Woody PLANT DEBRIS with little fine sand
2 – 11	Tan fine to medium SAND with trace organic matter
11 – 18	Tan fine to medium SAND with approximately 6 cm diameter. patch of organic matter, trace particulate plant debris
18 – 29	Tan fine to medium SAND
29 – 35	Tan fine to coarse SAND with little fine gravel and approximately 4 cm diameter. patch of organic matter
35 – 46	Greenish-tan fine SAND
46 – 60	Tan fine to medium SAND
60 – 81	Greenish-tan fine SAND
81 – 96	Tan medium to coarse SAND with trace fine gravel
96 – 110	Greenish-tan fine to medium SAND with little silt
110 – 118	Tan fine to coarse SAND with trace fine gravel

Soil Boring: PCSB-1, 0 to 5 ft core
Date collected: 20 August 2008
Site: PC floodplain

Length of core advanced: 150 cm
Length of core recovered: 85 cm

Depth (cm)	Description
0 – 2	Dk. brown fine to medium SAND with little organic matter
2 – 11	Dk. brown to brown fine SAND with traces of organic matter and silt
11 – 17	Lt. brown fine SAND with little silt, trace of organic matter
17 – 70	Yellowish-tan fine SAND with little silt, trace fine gravel and ~1 cm diameter. organic patch at 30 cm
70 – 85	Tan fine to medium SAND with traces of fine gravel and silt

Soil Boring: PCSB-2, 0 to 5 ft core
Date collected: 20 August 2008
Site: PC floodplain

Length of core advanced: 150 cm
Length of core recovered: 78 cm

Depth (cm)	Description
0 – 7	Dk. Brown fine to medium SAND and OM, traces of leaf and woody plant fragments
7 – 14	Brown fine to medium SAND with little organic matter, trace woody plant fragments
14 – 20.5	Lt. brown fine to medium SAND with trace organic matter
20.5 – 24	Dk. Tan fine to medium SAND with traces of silt and organic matter
24 – 28.5	Lt. to dk. brown fine to medium SAND with traces of organic matter and fine root fragments
28.5 – 50	Tan-brown fine to medium SAND with traces of silt, fine gravel and organic matter
50 – 56	Yellowish-brown fine to medium SAND with trace of dk. brown decomposed wood patches, traces of silt and fine gravel
56 – 63	Yellowish-brown fine to medium SAND with traces of silt and fine gravel
63 – 78	Tan fine to medium SAND with traces silt and fine gravel

Notes: Depth is distance below top of soil/sediment in core for both the initial and second core collected at each boring location. For the 5 to 10 ft. cores, sediments that originated from the 0 to 5 ft depth and fell into borehole were excluded from the logs.

Soil Boring: PCSB-2, 5 to 10 ft core
Date collected: 20 August 2008
Site: PC floodplain

Length of core advanced: 150 cm
Length of core recovered: 103 cm

Depth (cm)	Description
0 – 18	Tan-gray fine to medium SAND with traces silt, fine gravel
18 – 25	Tan-brown fine SAND, trace silt
25 – 50	Tan fine to coarse SAND, trace fine gravel
50 – 64	Tan-brown fine to coarse SAND, trace fine gravel
64 – 75	Tan-brown medium to coarse SAND, little fine gravel
75 – 99	Orangish-brown medium to coarse SAND, trace fine gravel
99 – 103	Tan-brown very fine to fine SAND, trace fine gravel

Soil Boring: PCSB-4, 0 to 5 ft core
Date collected: 20 August 2008
Site: PC floodplain

Length of core advanced: 150 cm
Length of core recovered: 100 cm

Depth (cm)	Description
0 – 4	Dk. brown fine to medium SAND with some organic matter
4 – 15	Brown fine to medium SAND with little silt, trace of organic matter
15 – 21	Lt. brown fine to medium SAND with little silt, trace organic matter
21 – 31	Tan-brown fine to medium SAND with traces of silt and organic matter
31 – 38	Tan-brown fine to medium SAND with little silt and trace of organic matter
38 – 47	Tan fine to medium SAND with traces of silt, patchy organic matter
47 – 67	Tan fine SAND, trace silt
67 – 80	Tan to reddish-tan fine SAND with traces of silt and ~1-2 mm diameter reddish-brown stains
80 – 87	Reddish-brown fine to medium SAND with trace fine gravel
87 – 93	Reddish-brown fine to coarse SAND, trace fine gravel
93 – 100	Reddish-brown fine to medium SAND, trace fine gravel

Soil Boring: PCSB-5, 0 to 5 ft core
Date collected: 20 August 2008
Site: PC floodplain

Length of core advanced: 150 cm
Length of core recovered: 103 cm

Depth (cm)	Description
0 – 6	Dk. brown fine to medium SAND with little silt and organic matter
6 – 12	Brown fine to medium SAND with little silt, trace organic matter
12 – 20	Tan-brown fine to medium SAND with little silt, trace organic matter
20 – 40	Brown to tan fine to medium SAND with some silt, trace organic matter, ~1 cm diameter patch of organic matter at 34 cm
40 – 82	Lt. gray fine to medium SAND with some silt, traces of patchy organic matter and dense clay
82 – 95	Tan-gray very fine to fine SAND, trace silt
95 – 103	Tan fine to medium SAND

Soil Boring: PCSB-5, 5 to 10 ft core
Date collected: 20 August 2008
Site: PC floodplain

Length of core advanced: 150 cm
Length of core recovered: 125 cm

Depth (cm)	Description
0 – 15	Tan-brown fine to medium SAND with trace fine gravel
15 – 45	Orangish-brown medium to coarse SAND with trace fine gravel
45 – 52	Tan-brown fine to coarse SAND with trace fine gravel
52 – 73	Tan fine to medium SAND with trace fine gravel
73 – 95	Lt. tan fine to medium SAND with traces of coarse sand and fine gravel
95 – 125	Tan-brown fine to medium SAND with trace fine gravel

Soil Boring: PCSB-6, 5 to 7 ft core
Date collected: 20 August 2008
Site: PC floodplain

Length of core advanced: 80 cm
Length of core recovered: 80 cm

Depth (cm)	Description
0 – 19	Tan-brown fine to coarse SAND with trace fine gravel
19 – 23	Tan fine to medium SAND
23 – 29	Tan to tan-brown fine to coarse SAND, trace fine gravel
29 – 50	Tan fine to medium SAND, trace fine gravel
50 – 60	Tan fine to medium SAND, trace organic matter
60 – 70	Dk. brown fine to medium SAND, trace organic matter and silt
70 – 80	Grayish-tan to dk. brown fine to medium SAND with some silt, trace organic matter

Note: Top of core suspected to have been mislabeled in field.

Soil Boring: PCSB-7, 5 to 6 ft core
Date collected: 20 August 2008
Site: PC floodplain

Length of core advanced: 60 cm
Length of core recovered: 60 cm

Depth (cm)	Description
0 – 41	Tan-brown fine to coarse SAND with trace fine gravel
41 – 60	Tan-brown fine to medium SAND with trace fine gravel

Soil Boring: PCSB-9, 0 to 5 ft core
Date collected: 20 August 2008
Site: PC floodplain

Length of core advanced: 150 cm
Length of core recovered: 81 cm

Depth (cm)	Description
0 – 7	Brown fine SAND with traces of silt and organic matter
7 – 20	Yellowish-tan fine SAND with traces of silt and organic matter
20 – 43	Orangish-brown fine SAND with traces of silt and organic matter
43 – 50	Orangish-brown fine SAND with reddish-brown staining and traces of silt and organic matter
50 – 81	Yellowish-tan fine to medium SAND with trace fine gravel

Soil Boring: PCSB-9, 5 to 10 ft core
Date collected: 20 August 2008
Site: PC floodplain

Length of core advanced: 150 cm
Length of core recovered: 106 cm

Depth (cm)	Description
0 – 35	Tan fine SAND
35 – 45	Tan-brown fine to medium SAND
45 – 58	Orangish-brown medium to coarse SAND, trace fine gravel
58 – 62	Orangish-brown fine to medium SAND, trace fine gravel
62 – 83	Tan fine to coarse SAND, trace fine gravel
83 – 88.5	Orangish-tan very fine to fine SAND
88.5 – 96	Tan-brown fine to coarse SAND, little fine gravel
96 – 106	Orangish-brown medium to coarse SAND with little fine gravel

Soil Boring: PCSB-10, 0 to 5 ft core
Date collected: 20 August 2008
Site: PC floodplain

Length of core advanced: 150 cm
Length of core recovered: 95 cm

Depth (cm)	Description
0 – 5	Dk. brown fine to medium SAND with little organic matter and fine root fragments
5 – 9	Dk. brown fine SAND with trace of organic matter
9 – 20	Brown fine SAND with trace of organic matter and fine root fragments
20 – 40	Slightly orangish-brown fine to medium SAND with trace of organic matter
40 – 49	Tan-brown fine to medium SAND with trace fine root fragments
49 – 55	Brown fine SAND, trace organic matter
55 – 59	Lt. brown fine to medium SAND
59 – 80	Tan-brown fine to medium SAND with traces of patchy particulate organic matter and fine gravel
80 – 85	Yellow-brown fine SAND with traces of patchy organic matter and reddish-brown staining
85 – 90	Tan-brown very fine to fine SAND with trace of reddish-brown staining
90 – 91	Slightly orange-brown fine SAND with trace silt
91 – 95	Orange-brown fine SAND with trace silt

Soil Boring: PCSB-10, 5 to 10 ft core
Date collected: 20 August 2008
Site: PC floodplain

Length of core advanced: 150 cm
Length of core recovered: 84 cm

Depth (cm)	Description
0 – 14	Gray to orangish-brown fine SAND with traces of silt and fine gravel
14 – 26	Orangish-brown fine to medium SAND with traces of silt and fine gravel
26 – 31	Tan-gray fine to medium SAND
31 – 48	Tan-gray medium to coarse SAND with trace fine gravel
48 – 53	Tan-gray fine to coarse SAND with trace fine gravel
53 – 66	Tan fine to coarse SAND with trace fine gravel
66 – 81	Tan very fine to fine SAND with trace fine gravel
81 – 84	Tan fine to coarse SAND with trace fine gravel

Soil Boring: PCSB-11, 0 to 4 ft core
Date collected: 20 August 2008
Site: PC floodplain

Length of core advanced: 120 cm
Length of core recovered: 80 cm

Depth (cm)	Description
0 – 12	Dk. brown fine to medium SAND with little organic matter
12 – 20	Brown fine to medium SAND with trace organic matter
20 – 32	Brown to lt. brown fine to medium SAND with traces of silt, organic matter and fine gravel
32 – 42	Brown fine to medium SAND with traces of silt and organic matter
42 – 48	Lt. brown fine to medium SAND with traces of silt and fine gravel
48 – 65	Tan fine to medium SAND with trace silt
65 – 80	Lt. tan very fine to fine SAND

Soil Boring: PCSB-11, 4 to 9 ft core
Date collected: 20 August 2008
Site: PC floodplain

Length of core advanced: 150 cm
Length of core recovered: 128 cm

Depth (cm)	Description
0 – 5	Tan fine SAND, trace silt
5 – 49	Lt. tan very fine to medium SAND, trace fine gravel
49 – 79	Lt. tan medium to coarse SAND, trace fine gravel
79 – 91	Lt. brown fine to medium SAND with traces of coarse sand and fine gravel
91 – 115	Orangish-brown medium to coarse SAND with trace fine gravel
115 – 128	Tan-brown very fine to fine SAND with trace fine gravel

Soil Boring: PCSB-12, 0 to 4 ft core
Date collected: 20 August 2008
Site: PC floodplain

Length of core advanced: 120 cm
Length of core recovered: 103 cm

Depth (cm)	Description
0 – 8	Dk. brown fine to medium SAND with little organic matter
8 – 17	Brown fine to medium SAND with traces of silt and organic matter
17 – 31	Lt. brown fine to medium SAND with trace silt
31 – 43	Brown fine to medium SAND with little silt, patch of organic matter at 37 cm
43 – 57	Tan to yellowish-brown fine to medium SAND with little silt. Woody plant fragment at 48 cm.
57 – 92	Tan very fine to fine SAND
92 – 97	Tan fine to coarse SAND
97 – 103	Tan fine to medium SAND

Soil Boring: PCSB-12, 4 to 9 ft core
Date collected: 20 August 2008
Site: PC floodplain

Length of core advanced: 150 cm
Length of core recovered: 101 cm

Depth (cm)	Description
0 – 26	Tannish-gray fine SAND
26 – 50	Tannish-gray fine to coarse SAND with trace of fine gravel
50 – 56	Orangish-brown fine to coarse SAND with trace of fine gravel
56 – 71	Tan-brown fine to medium SAND with trace of fine gravel
71 – 92	Orangish-brown fine to coarse SAND with trace of fine gravel
92 – 101	Yellowish-brown very fine to fine SAND

Soil Boring: PCSB-13, 0 to 3 ft core
Date collected: 20 August 2008
Site: PC floodplain

Length of core advanced: 90 cm
Length of core recovered: 79 cm

Depth (cm)	Description
0 – 10	Dk. brown fine SAND with traces of silt and organic matter
10 – 18	Lt. brown fine SAND with traces of silt and organic matter
18 – 39	Tan-brown fine to medium SAND with traces of silt and organic matter
39 – 48	Yellowish-brown fine to medium SAND with traces of silt and fine gravel
48 – 60	Tan-gray fine SAND with some silt, little orange-colored staining and trace clay
60 – 79	Tan-gray fine SAND with some silt, trace clay, dense

Soil Boring: PCSB-13, 3 to 8 ft core
Date collected: 20 August 2008
Site: PC floodplain

Length of core advanced: 150 cm
Length of core recovered: 118 cm

Depth (cm)	Description
0 – 12	Tannish-brown fine SAND
12 – 54	Tan very fine to fine SAND
54 – 64	Tan fine to coarse SAND with trace fine gravel
64 – 77	Lt. brown fine to coarse SAND with trace fine gravel
77 – 98	Lt. brown fine to medium SAND
98 – 118	Orangish-brown medium to coarse SAND with trace fine gravel

Soil Boring: PCSB-14, 0 to 5 ft core
Date collected: 20 August 2008
Site: PC floodplain

Length of core advanced: 150 cm
Length of core recovered: 115.8 cm

Depth (cm)	Description
0 – 5	Dk. brown PEAT with trace plant material, trace of fine to medium sand
5 – 12	Dk. brown fine to medium SAND with some organic matter, trace plant roots
12 – 15	Lt. brown fine to medium SAND with trace of organic matter, plant fragments
15 – 25	Tan-brown fine to medium SAND with trace of silt, patchy organic matter
25 – 35	Tan fine to medium SAND with trace of silt, patchy organic matter
35 – 55.5	Tan fine SAND with traces of silt and organic matter
55.5 – 70	Tan-gray fine SAND with some silt and clay, moderately cohesive
70 – 80	Tan fine to medium SAND, trace silt
80 – 92	Tan-gray fine to coarse SAND with little silt
92 – 99	Tan fine to coarse SAND with trace silt
99 – 115.8	Tan fine to medium SAND, trace silt, laminations present

Soil Boring: PCSB-14, 5 to 10 ft core
Date collected: 20 August 2008
Site: PC floodplain

Length of core advanced: 150 cm
Length of core recovered: 140 cm

Depth (cm)	Description
0 – 33	Tan fine to medium SAND
33 – 68	Tannish-brown fine to medium SAND, trace fine gravel
68 – 91	Orangish-tan medium to coarse SAND with little fine gravel
91 – 98	Orangish-tan fine to coarse SAND with trace fine gravel
98 – 109	Tan fine to medium SAND with trace fine gravel
109 – 126	Orangish-tan fine to coarse SAND with little fine gravel
126 – 130	Tan-brown fine SAND with trace fine gravel
130 – 140	Olive-tan very fine to fine SAND

Soil Boring: PCSB-15, 0 to 5 ft core
Date collected: 20 August 2008
Site: PC floodplain

Length of core advanced: 150 cm
Length of core recovered: 103.8 cm

Depth (cm)	Description
0 – 5	Dk. brown PEAT with trace plant roots
5 – 15	Dk. brown fine SAND with some organic matter, trace silt and plant root fragments
15 – 18.6	Tan fine SAND with traces of silt and organic matter
18.6 – 22.1	Tan-brown fine to medium SAND, trace silt
22.1 – 26.1	Tan fine to medium SAND, traces of silt and plant stems
26.1 – 35.6	Lt. brown fine to medium SAND, traces of silt, organic matter and plant roots
35.6 – 39.6	Tan fine SAND, traces of silt and coarse sand
39.6 – 45.6	Yellow-tan fine SAND and SILT, trace coarse sand
45.6 – 54.6	Lt. tan fine SAND with some silt, trace oxidized iron staining
54.6 – 61.8	Tan-gray fine SAND with little silt and clay, moderately cohesive, trace fine plant roots
61.8 – 69.0	Tan-gray fine SAND, trace silt
69.0 – 76.2	Tan-brown fine SAND, traces of silt and ~1 mm diameter. particulate organic matter
76.2 – 83.4	Tan-brown fine SAND, trace silt
83.4 – 97.8	Tan-brown fine to medium SAND, traces of dk. mineral laminations and silt
97.8 – 103.8	Tan fine to coarse SAND, trace fine gravel

Soil Boring: PCSB-15, 5 to 10 ft core
Date collected: 20 August 2008
Site: PC floodplain

Length of core advanced: 150 cm
Length of core recovered: 130 cm

Depth (cm)	Description
0 – 30	Tan fine to medium SAND with trace fine gravel
30 – 37	Tan fine SAND
37 – 46	Tan-brown fine SAND
46 – 51	Tan-brown fine to coarse SAND
51 – 66	Tan-brown fine SAND with trace fine gravel
66 – 113	Orangish-tan medium to coarse SAND with some fine gravel
113 – 130	Tannish-gray very fine to fine SAND with trace fine gravel

Soil Boring: PCSB-16, 0 to 5 ft core
Date collected: 20 August 2008
Site: PC floodplain

Length of core advanced: 150 cm
Length of core recovered: 104.2 cm

Depth (cm)	Description
0 – 5	Lt. brown fine-medium SAND with trace silt, organic matter
5 – 11	Tan fine SAND with little silt, trace organic matter
11 – 27	Tan to lt. brown fine to medium SAND with traces of organic matter, silt, and root fragments
27 – 32	Tan fine to medium SAND with little silt, trace root fragments
32 – 50.4	Tan fine SAND with little silt, traces of root fragments and fine gravel
50.4 – 57.6	Tan-brown fine to medium SAND with little silt and clay, moderately cohesive, slight oxidized iron
57.6 – 64.8	Tan-brown fine to medium SAND with traces of silt, clay, and organic matter, slightly cohesive
64.8 – 72	Tan fine SAND with traces of silt and organic matter
72 – 79.2	Tan fine SAND with trace silt
79.2 – 93.6	Tan fine SAND with traces of silt and dark brown organic matter patches (1-2 mm diameter.)
93.6 – 100.8	Light tan medium SAND with trace of dark mineral laminations
100.8 – 104.2	Tan fine to medium SAND

Soil Boring: PCSB-16, 5 to 7 ft core
Date collected: 20 August 2008
Site: PC floodplain

Length of core advanced: 60 cm
Length of core recovered: 59 cm

Depth (cm)	Description
0 – 10	Tan fine to medium SAND
10 – 30	Tan fine to coarse SAND with trace fine gravel
30 – 49	Tan fine SAND
49 – 59	Tan fine to medium SAND with trace fine gravel

Soil Boring: PCSB-16, 5 to 10 ft core*
Date collected: 20 August 2008
Site: PC floodplain

Length of core advanced: 95 cm
Length of core recovered: 95 cm

Depth (cm)	Description
0 – 50	Tan fine to medium SAND with slight fine gravel
50 – 65	Orangish-tan fine to medium SAND with slight fine gravel
65 – 95	Orangish-tan medium to coarse SAND with little fine gravel

*Core collected from same borehole as PCSB-16, 5 to 7 ft core. The materials described above are likely to be representative of the 7 to 10 ft depth interval.

Soil Boring: CKSB-1, 0 to 5 ft core
Date collected: 21 August 2008
Site: Coal Kiln

Length of core advanced: 150 cm
Length of core recovered: 105 cm

Depth (cm)	Description
0 – 8	Brown fine SAND with trace silt and organic matter
8 – 40	Dk. brown fine to medium SAND with little silt, trace organic matter and fine gravel
40 – 53	Tan to dk. brown fine to medium SAND with trace silt, organic matter, and fine gravel
53 – 75	Tan to dk. brown fine SAND, trace of woody debris and silt – dk. brown sand caused by dk. mineral laminations
75 – 90	Tan to dk. brown fine to medium SAND with reddish-brown staining around dk.-colored sands
90 – 105	Tan fine SAND

Soil Boring: CKSB-1, 5 to 10 ft core
Date collected: 21 August 2008
Site: Coal Kiln

Length of core advanced: 150 cm
Length of core recovered: 135 cm

Depth (cm)	Description
0 – 8	Dk. brown to tan fine SAND with trace silt and organic matter (material suspected to have fallen into borehole from shallower depth)
8 – 38	Dk. tan very fine to fine SAND with trace patchy organic matter
38 – 73	Tan to grayish-tan fine to medium SAND
73 - 89	Grayish-tan very fine to fine SAND with specks of shiny, gold-colored sand-sized grains
89 – 94	Tan fine to medium SAND
94 – 111	Grayish-tan fine SAND with specks of shiny, gold-colored sand-sized grains
111 – 118	Tan fine to medium SAND
118 – 135	Tan medium to coarse SAND

Soil Boring: CKSB-2, 0 to 5 ft core
Date collected: 21 August 2008
Site: Coal Kiln

Length of core advanced: 150 cm
Length of core recovered: 105 cm

Depth (cm)	Description
0 – 5	Dk. brown loose ORGANIC MATTER and fine SAND with trace silt
5 – 30	Dk. brown fine SAND with little silt and organic matter
30 – 38	Dk. brown to tan fine to medium SAND with traces of silt, organic matter and fine gravel
38 – 49	Tan fine to coarse SAND with patch of organic matter at 43-45 cm, patchy reddish-brown staining
49 – 60	Tan fine to medium SAND with patch of organic matter at 53.5-54.5 cm, patchy reddish-brown staining
60 – 93	Dk. tan fine SAND with patch of reddish-brown staining from 65-66 cm
93 – 102	Tan fine to medium SAND
102 – 105	Dk. tan fine to medium SAND

Soil Boring: CKSB-2, 5 to 10 ft core
Date collected: 21 August 2008
Site: Coal Kiln

Length of core advanced: 150 cm
Length of core recovered: 100 cm

Depth (cm)	Description
0 – 5	Dk. brown fine to medium SAND with little silt and organic matter (material suspected to have fallen into borehole from shallower depth)
5 – 30	Tan to grayish-tan fine to medium SAND with patches of reddish-brown staining
30 – 45	Orangish-tan to lt. tan fine to coarse SAND
45 – 47	Grayish-tan fine SAND
47 – 49	Orangish-tan fine to coarse SAND
49 – 53	Grayish-tan fine SAND with specks of shiny, sand-sized gold-colored minerals
53 – 55	Lt. tan fine to medium SAND with specks of shiny, gold-colored minerals
55 – 60	Grayish-tan fine SAND with trace of gold-colored, sand-sized mineral grains
60 – 65	Tan fine to medium SAND with trace of gold-colored, sand-sized mineral grains
65 – 72	Grayish-tan very fine to fine SAND with trace of gold-colored, sand-sized mineral grains
72 – 74	Tan fine to medium SAND with trace of gold-colored, sand-sized mineral grains
74 – 77	Greenish-tan fine SAND with trace of mica flakes
77 – 90	Tan fine to medium SAND with trace of gold-colored, sand-sized mineral grains
90 – 100	Grayish-tan fine SAND with trace of gold-colored, sand-sized mineral grains

Soil Boring: PCR1
Date advanced: 11 July 2007
Site: PC upland

Depth (cm)	Description
0 – 30	Dk. brown moist PEAT

Soil Boring: PCR2
Date advanced: 7 August 2007
Site: PC upland

Depth (cm)	Description
0 – 15	Brown PEAT with trace particulate plant debris
15 – 30	Brown PEAT and FINE SAND with trace particulate plant debris

Soil Boring: PCMW5
Date advanced: 14 July 2009
Site: PC upland

Depth (cm)	Description
0 – 10	Brown fine to medium SAND and SILT, little organic matter
10 – 21	Brown fine to medium SAND and SILT, little organic matter with traces of root and leaf fragments
21 – 32	Brown fine to medium SAND with little silt and trace organic matter
32 – 60	Brown fine to medium SAND with little silt and trace organic matter, root fragments
60 – 65	Dk. brown PEAT with some fine to medium sand
65 – 74	Dk. brown fine to medium SAND with little organic matter
74 – 85	Dk. tan fine to medium SAND with traces of silt and organic matter
85 – 104	Dk. brown fine to medium SAND with traces of clay, silt and organic matter, slightly cohesive
104 – 115	Brown fine to medium SAND with traces of silt and organic matter

Soil Boring: PCR3
Date advanced: 8 October 2007
Site: PC floodplain

Depth (cm)	Description
0 – 35	Dk. brown PEAT with trace silt and clay

Soil Boring: PCR3D
Date advanced: 13 July 2009
Site: PC floodplain

Depth (cm)	Description
0 – 30	Dk. brown PEAT
30 – 50	Dk. brown PEAT with trace silt and fine sand

Soil Boring: PCR4
Date advanced: 29 July 2008
Site: PC floodplain

Depth (cm)	Description
0 – 30	Dk. brown fine to medium SAND with some silt and organic matter
30 – 45	Tan-brown fine to medium SAND with little silt, trace organic matter
45 – 60	Not recorded
60 – 85	Tan-gray fine SAND with some silt and clay, cohesive
85 – 100	Brown-gray SILT, SAND and CLAY, cohesive
100 – 125	Tan medium to coarse SAND, clean

Soil Boring: PCMW2
Date advanced: 30 July 2008
Site: PC floodplain

Depth (cm)	Description
0 – 45	Brown fine to medium SAND with little silt and trace organic matter
45 – 95	Dk. tan medium SAND with trace silt
95 – 135	Tan fine to medium SAND

Soil Boring: PCR4-D
Date advanced: 13 July 2009
Site: PC floodplain

Depth (cm)	Description
0 – 10	Dk. brown PEAT
10 – 17.5	Brown ORGANIC MATTER and SILT, cohesive
17.5 – 30	Brown-gray medium SAND with little silt
30 – 40	Yellowish-tan medium SAND with little silt
40 – 50	Yellowish-tan medium SAND with some silt and clay, cohesive
50 – 60	Yellowish-tan fine to medium SAND with some silt and clay, cohesive
60 – 75	Grayish-brown fine SAND, SILT and CLAY, cohesive
75 – 80	Grayish-brown fine to medium SAND with trace silt and clay
80 – 90	Gray fine to medium SAND with little silt

Soil Boring: PCR5
Date advanced: 29 July 2008
Site: PC floodplain

Depth (cm)	Description
0 – 35	Brown fine to medium SAND with traces of silt and organic matter
35 – 180	Yellow-brown fine to medium SAND with trace silt

Soil Boring: CKR1/R2
Date advanced: 12 July 2007
Site: Coal Kiln

Depth (cm)	Description
0 – 46	Dk. brown fine to medium SAND with trace organic matter and silt

Soil Boring: CKR3
Date advanced: 8 October 2007
Site: Coal Kiln

Depth (cm)	Description
0 – 20	Dk. brown fine to medium SAND with little organic matter, trace silt
20 – 35	Tan-brown medium SAND with trace organic matter

Appendix C – Photographs of soil and sediment cores

Note: The top of sediment/soil for each core photographed in this appendix is on the left side of the photograph.

Sediment core: CMC 3/5/07 Site: CMC floodplain, streambed

Sediment core: PC 3/5/07 Site: PC floodplain, streambed

Sediment core: Coal Kiln 6/2/07 Site: Coal Kiln, streambed

Sediment core: PCPW2 Site: Phillips Creek upland, streambed

Sediment core: CKPW2 Site: Coal Kiln, streambed

Sediment core: PCPW3 Site: Phillips Creek upland, streambed

Sediment core: PC 2/2/08 Site: Phillips Creek floodplain, streambed

Sediment core: CK 2/2/08 Site: Coal Kiln, streambed

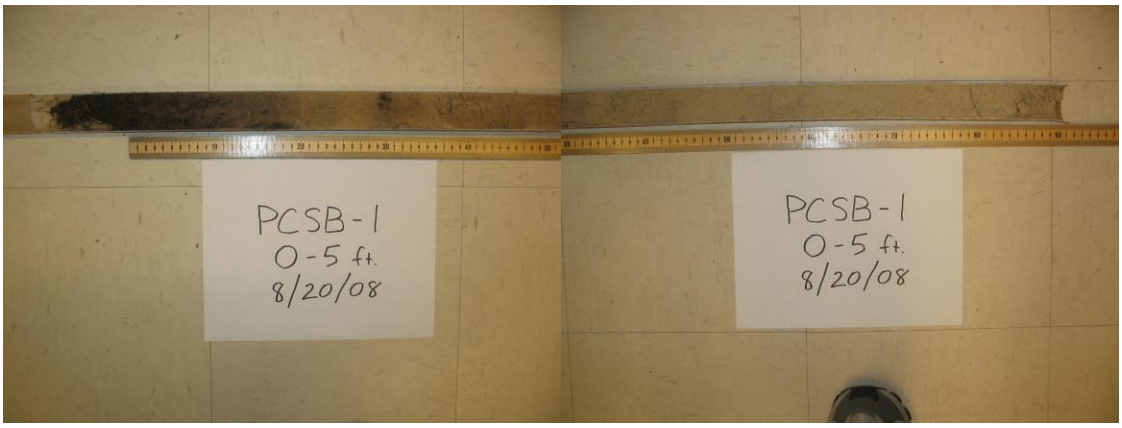

Soil Boring: PCSB-1, 0 to 5 ft core Site: PC floodplain, buffer

Soil Boring: PCSB-2, 0 to 5 ft core Site: PC floodplain, buffer

Soil Boring: PCSB-2, 5 to 10 ft core Site: PC floodplain, buffer

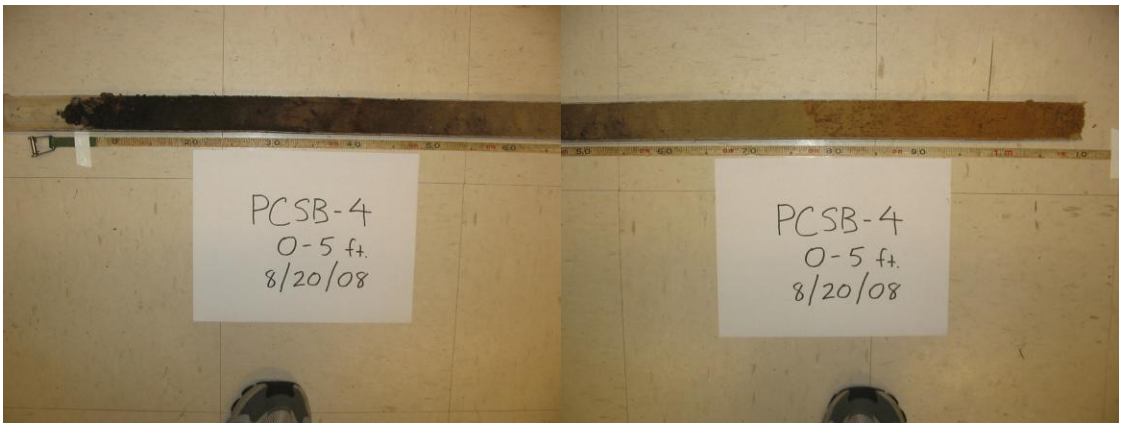

Soil Boring: PCSB-4, 0 to 5 ft core Site: PC floodplain, buffer

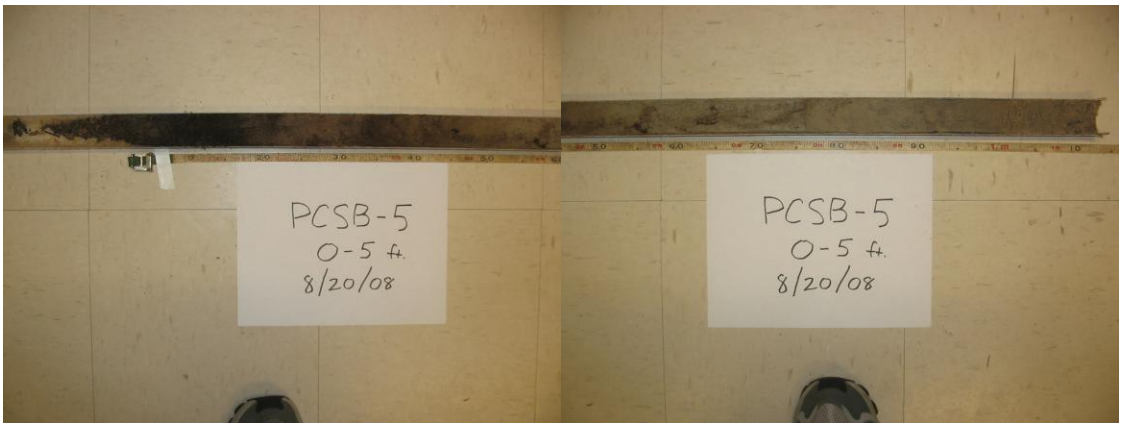

Soil Boring: PCSB-5, 0 to 5 ft core Site: PC floodplain, buffer

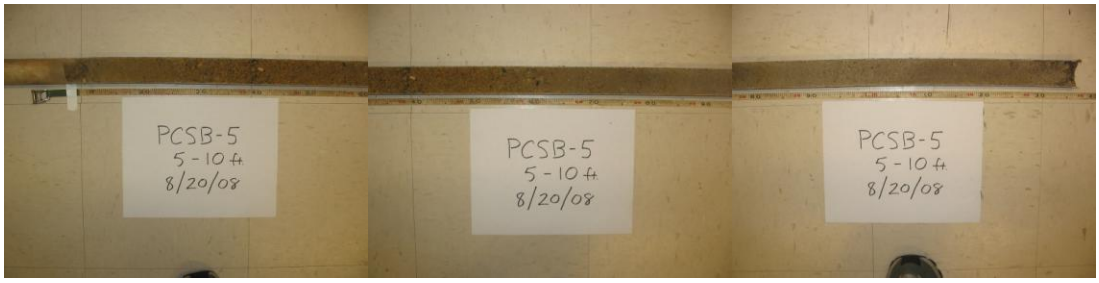

Soil Boring: PCSB-5, 5 to 10 ft core Site: PC floodplain, buffer

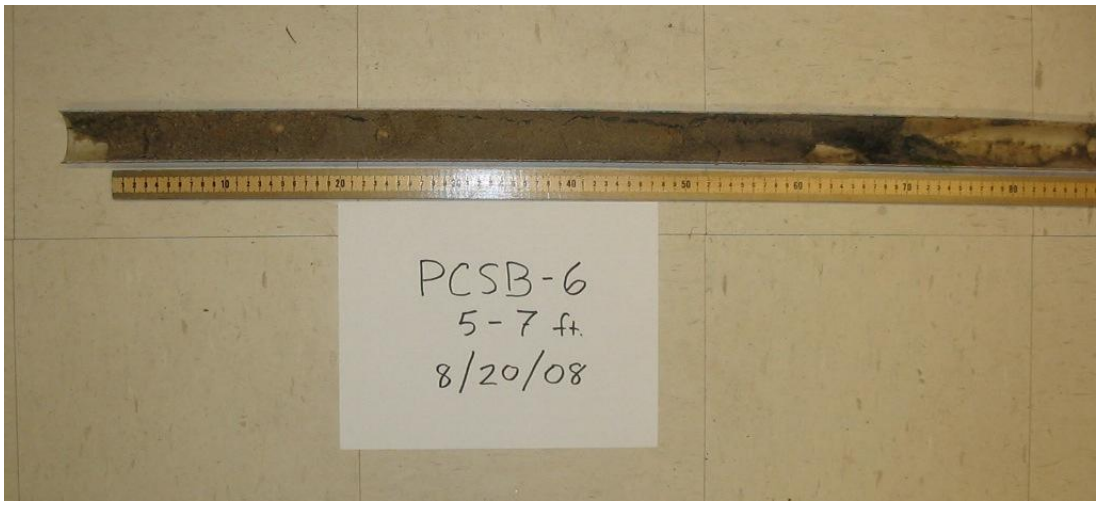

Soil Boring: PCSB-6, 5 to 7 ft core Site: PC floodplain, buffer

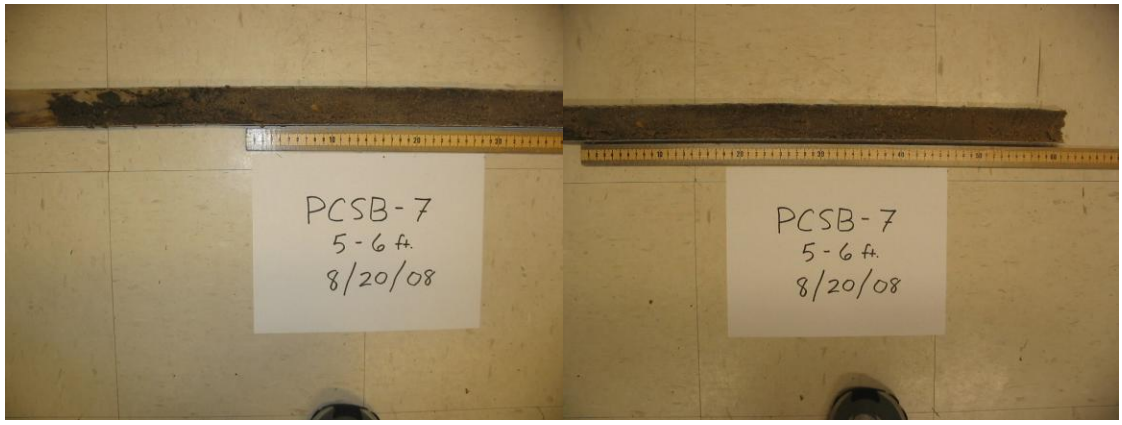

Soil Boring: PCSB-7, 5 to 6 ft core Site: PC floodplain, buffer

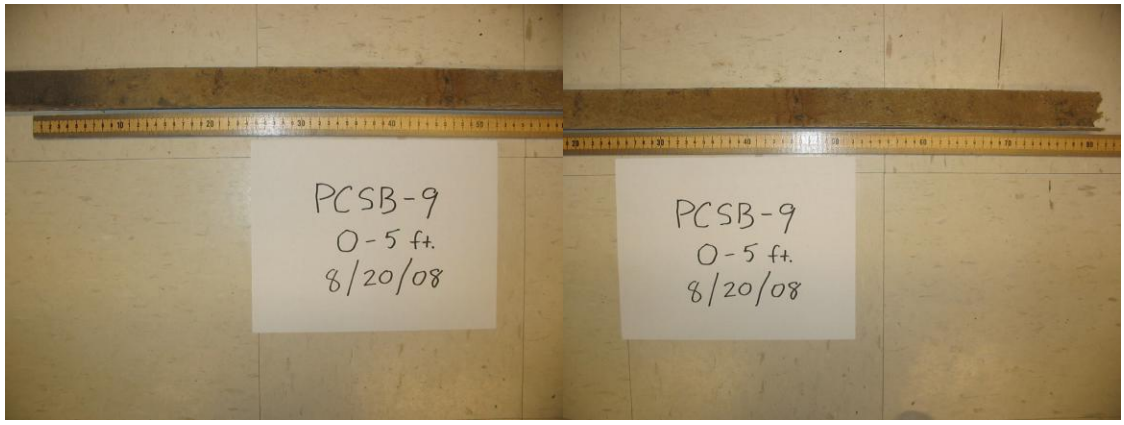

Soil Boring: PCSB-9, 0 to 5 ft core Site: PC floodplain, buffer

Soil Boring: PCSB-9, 5 to 10 ft core Site: PC floodplain, buffer

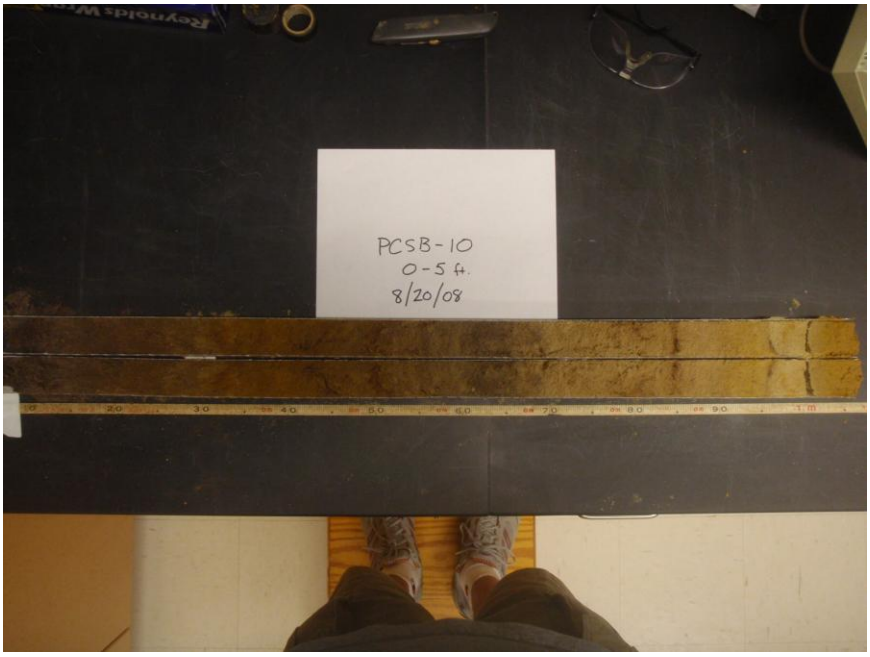

Soil Boring: PCSB-10, 0 to 5 ft core Site: PC floodplain, buffer

Soil Boring: PCSB-10, 5 to 10 ft core Site: PC floodplain, buffer

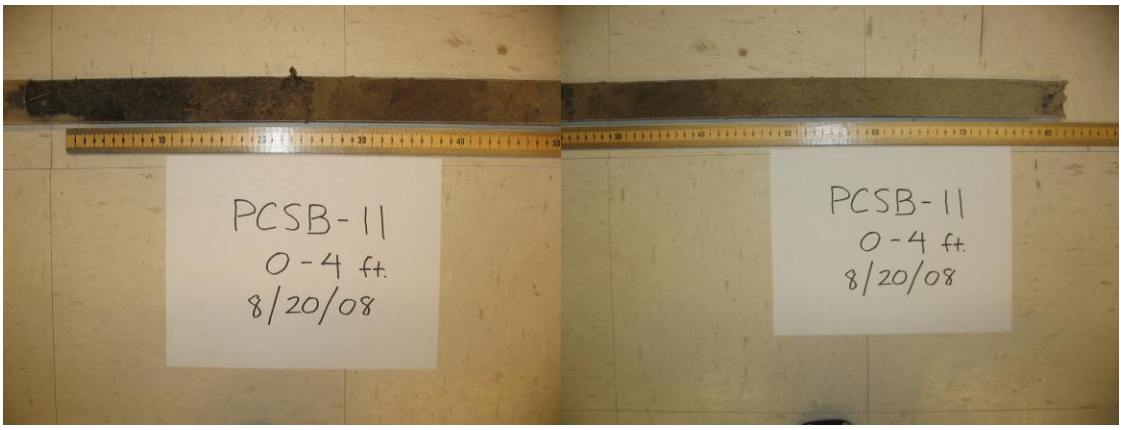

Soil Boring: PCSB-11, 0 to 4 ft core Site: PC floodplain, buffer

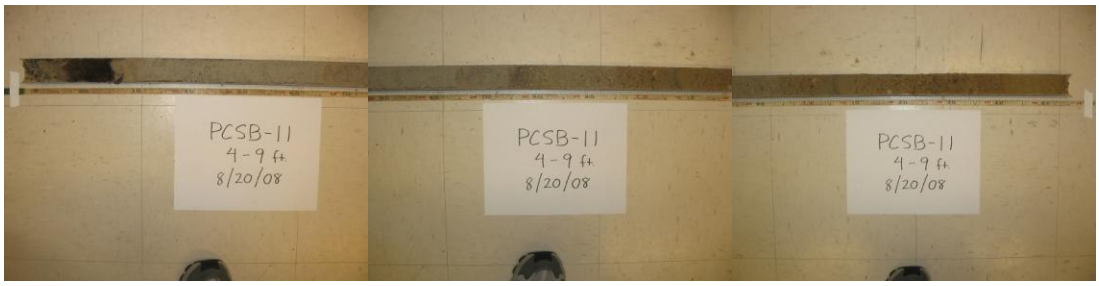

Soil Boring: PCSB-11, 4 to 9 ft core Site: PC floodplain, buffer

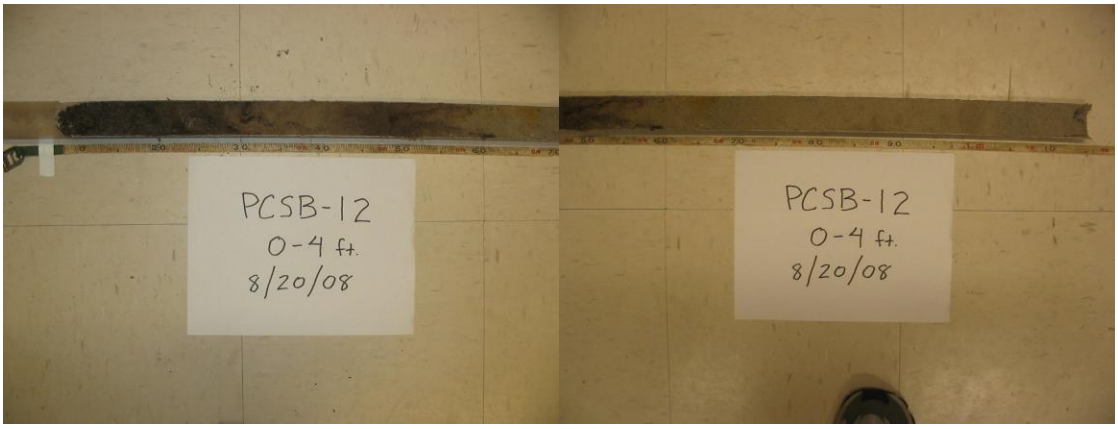

Soil Boring: PCSB-12, 0 to 4 ft core Site: PC floodplain, buffer

Soil Boring: PCSB-12, 4 to 9 ft core Site: PC floodplain, buffer
Top of sediment in this core is on the right-hand end.

Soil Boring: PCSB-13, 0 to 3 ft core Site: PC floodplain, buffer

Soil Boring: PCSB-13, 3 to 8 ft core Site: PC floodplain, buffer

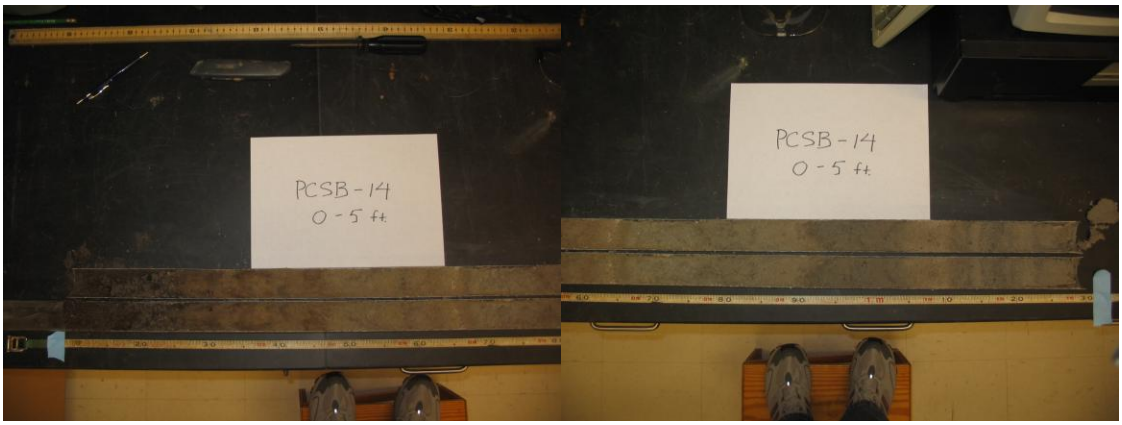

Soil Boring: PCSB-14, 0 to 5 ft core Site: PC floodplain, buffer

Soil Boring: PCSB-14, 5 to 10 ft core Site: PC floodplain, buffer

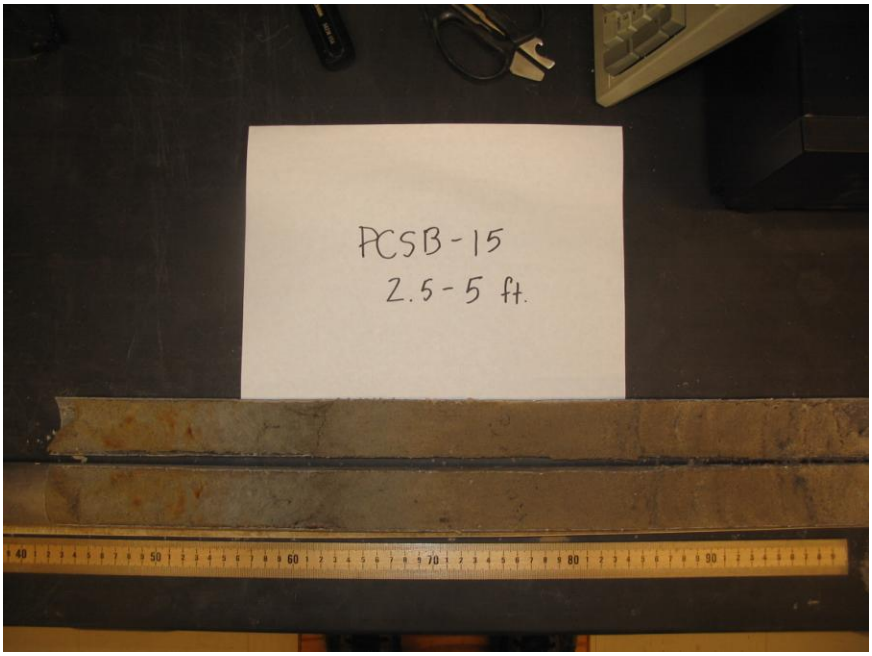

Soil Boring: PCSB-15, 2.5 to 5 ft core Site: PC floodplain, buffer

Soil Boring: PCSB-15, 5 to 10 ft core Site: PC floodplain, buffer

Soil Boring: PCSB-16, 5 to 7 ft core Site: PC floodplain, buffer

Soil Boring: PCSB-16, 5 to 10 ft core* Site: PC floodplain, buffer
*Core collected from same borehole as PCSB-16, 5 to 7 ft core. The materials shown above are likely to be representative of the 7 to 10 ft depth interval.

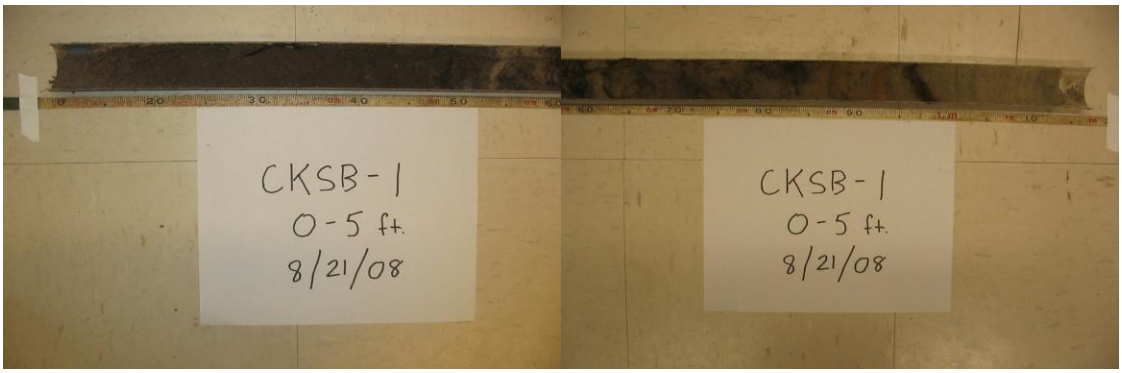

Soil Boring: CKSB-1, 0 to 5 ft core Site: Coal Kiln, buffer

Soil Boring: CKSB-1, 5 to 10 ft core Site: Coal Kiln, buffer

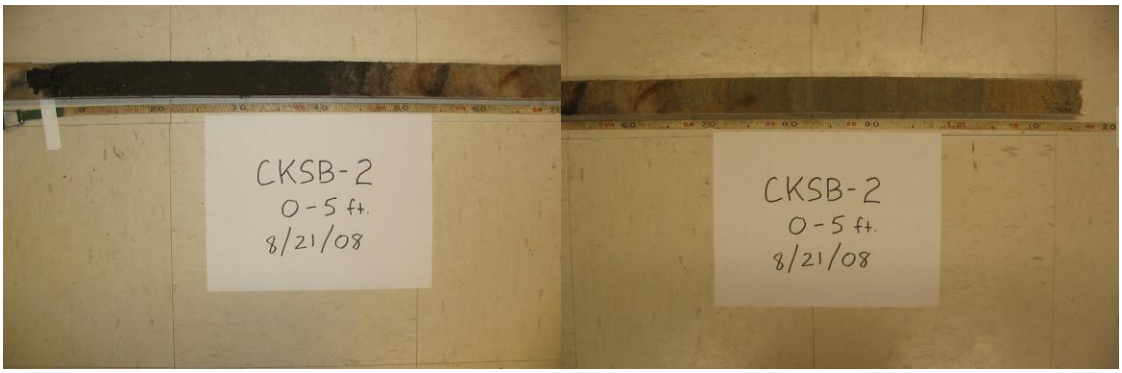

Soil Boring: CKSB-2, 0 to 5 ft core Site: Coal Kiln, buffer

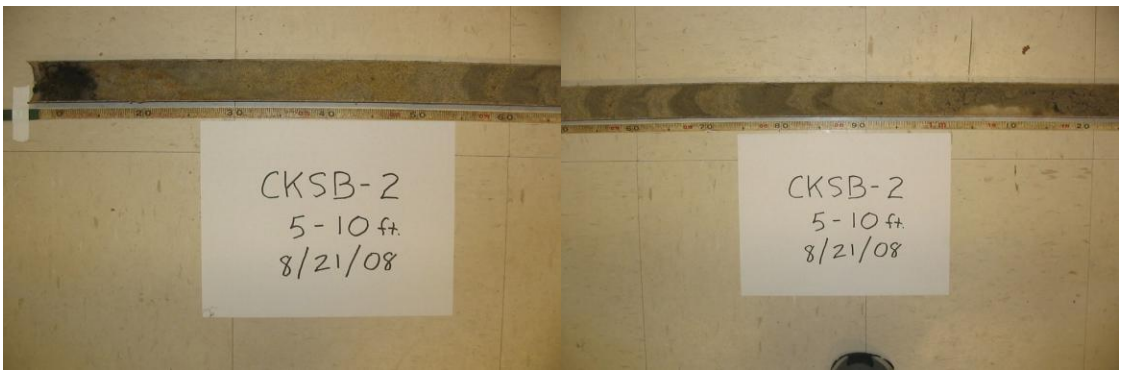

Soil Boring: CKSB-2, 5 to 10 ft core Site: Coal Kiln, buffer

Appendix D – Piezometer and monitoring well slug test water level recordings

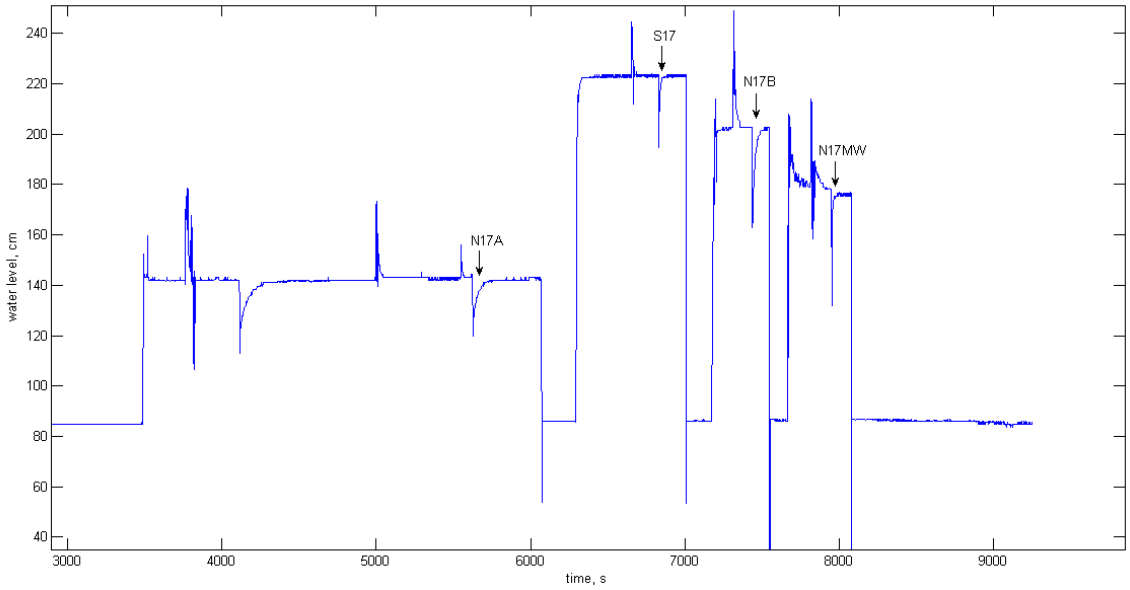

Figure D.1. Water level recording of slug tests completed at CMC floodplain on 14 July 2009.

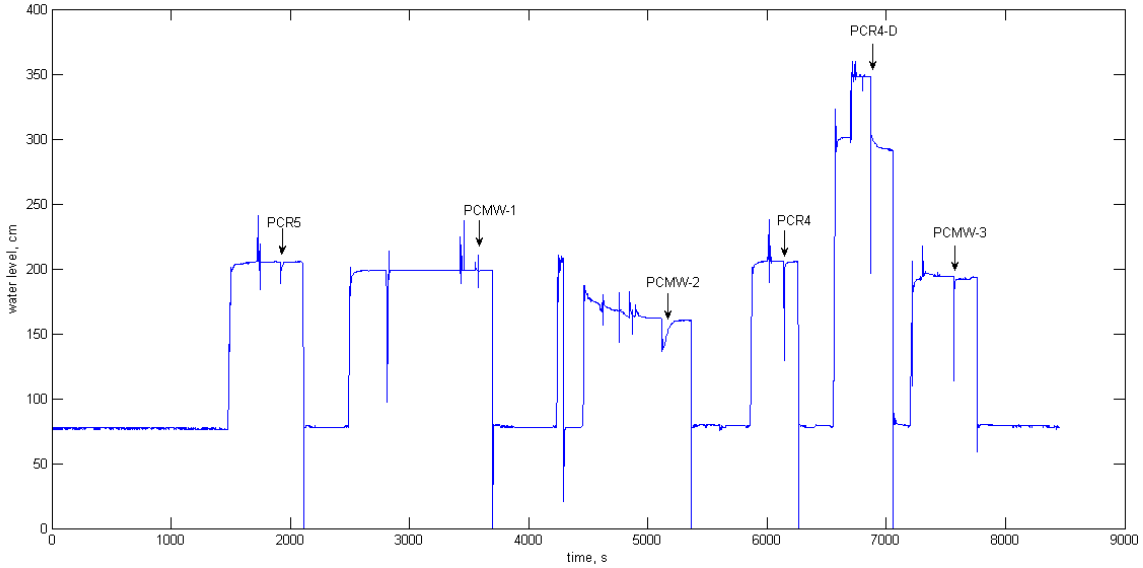

Figure D.2. Water level recording of slug tests completed at PC floodplain site on 16 July 2009.

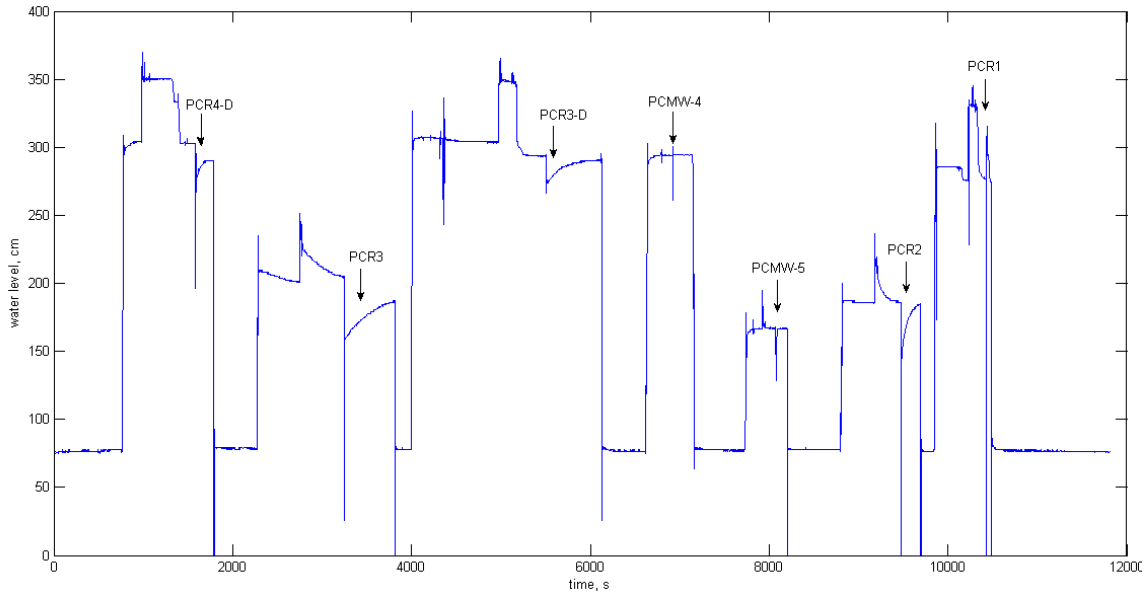

Figure D.3. Water level recording of slug tests completed at PC floodplain and upland sites on 16 July 2009.

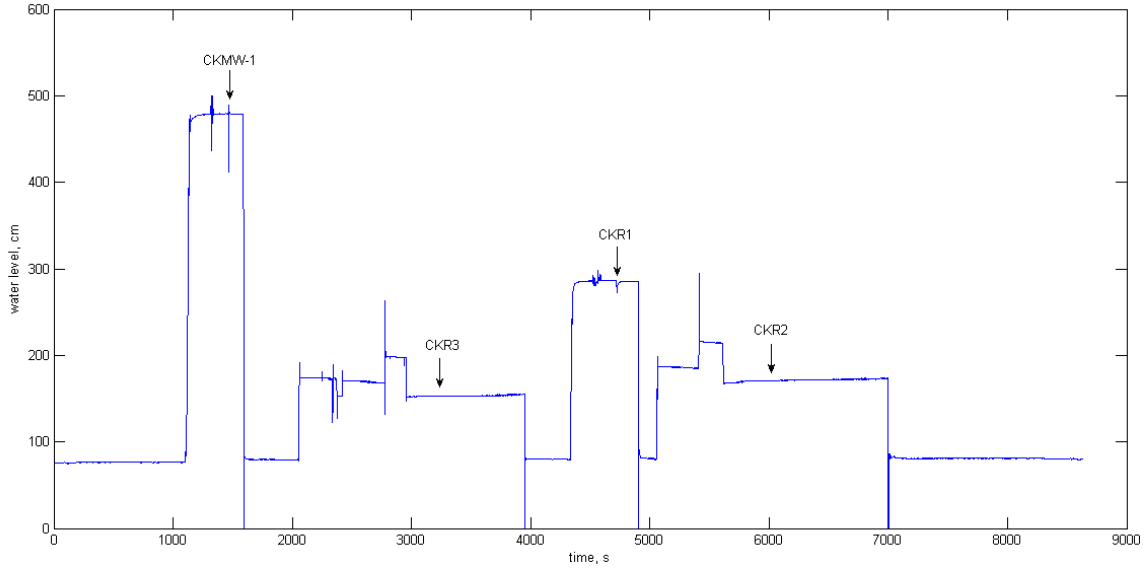

Figure D.4. Water level recording of slug tests completed at Coal Kiln on 18 July 2009.

Appendix E – Groundwater and surface water NO_3^--N results

Table E.1. Cobb Mill Creek floodplain groundwater and surface water NO_3^--N (mg/L).

		6 March 2007			13 July 2007		
		replicates	mean	std. dev.	replicates	mean	std. dev.
buffer piez.	N17A	6.8	6.8	0.1	6.3	6.4	0.1
		6.7			6.4		
		6.9			6.6		
	N17B	7.2	7.1	0.0	8.1	8.1	0.1
		7.1			8.1		
		7.1			8.3		
in-stream piez.	S17	3.5	3.5	0.0	6.6	6.6	0.0
		3.5			6.6		
		3.5			6.6		
surface water	SW	2.1	-----	-----	4.3	-----	-----
		-----			-----		
		-----			-----		

		26 July 2007			2 August 2007		
		replicates	mean	std. dev.	replicates	mean	std. dev.
buffer piez.	N17A	6.8	6.3	0.4	6.9	6.9	-----
		6.0			6.9		
		6.0			-----		
	N17B	8.0	8.0	0.0	8.3	8.3	-----
		8.0			8.3		
		8.0			-----		
in-stream piez.	S17	6.4	6.3	0.0	6.4	6.4	-----
		6.3			6.4		
		6.3			-----		
surface water	SW	-----	-----	-----	-----	-----	-----
		-----			-----		
		-----			-----		

Note: Replicates are field replicate samples. The mean of the replicates for a sampling event was used to compute the mean NO_3^--N concentration for a sampling location.

		3 February 2008			19 August 2008		
		replicates	mean	std. dev.	replicates	mean	std. dev.
buffer piez.	N17A	6.4	6.5	0.1	6.3	6.3	0.0
		6.6			6.2		
		6.4			6.3		
	N17B	6.8	6.9	0.1	8.0	8.0	0.0
		7.1			8.0		
		6.9			8.0		
in-stream piez.	S17	2.8	2.9	0.1	6.8	6.8	0.0
		2.9			6.8		
		3.0			6.8		
surface water	SW	1.9	2.0	0.0	6.7	6.7	0.0
		2.0			6.7		
		1.9			6.7		

		7/16/2009		
		replicates	mean	std. dev.
buffer piez.	N17A	4.8	-----	-----

	N17B	11.2	-----	-----

		-----		
in-stream piez.	S17	8.1	-----	-----

		-----		
surface water	SW	2.7	-----	-----

Table E.2. Phillips Creek upland groundwater and surface water NO_3^--N (mg/L).

		12 July 2007			8 August 2007		
		replicates	mean	std. dev.	replicates	mean	std. dev.
buffer piez.	PCR1	4.8	4.8	0.0	5.4	5.3	0.0
		4.8			5.3		
		4.9			5.3		
	PCR2	Not installed	-----	-----	4.7	4.6	0.0
					4.6		
					4.6		
in-stream piez.	PCS1	6.1	6.0	0.1	5.5	5.5	0.0
		6.0			5.5		
		6.0			5.5		
	PCS2	Not installed	-----	-----	5.7	5.7	0.1
					5.7		
					5.8		
monitoring well	MW-5	Not installed	-----	-----	Not installed	-----	-----
surface water	SW	0.8	-----	-----	0.9	-----	-----
		-----			-----		
		-----			-----		

		19 July 2009		
		replicates	mean	std. dev.
buffer piez.	PCR1	3.4	-----	-----

	PCR2	6.7	-----	-----

		-----		
in-stream piez.	PCS1	4.9	-----	-----

	PCS2	0.1	-----	-----

		-----		
monitoring well	MW-5	7.1	-----	-----

		-----		
surface water	SW	1.3	-----	-----

Table E.3. Phillips Creek floodplain groundwater and surface water NO_3^--N (mg/L).

		6 March 2007			8 August 2007		
		replicates	mean	std. dev.	replicates	mean	std. dev.
buffer piez.	PCR3	Not installed	-----	-----	Not installed	-----	-----
in-stream piez.	PCS0	1.2	1.2	0.0	0.1	0.0	0.0
		1.2			0.0		
		1.2			0.1		
	PCS3	Not installed	-----	-----	Not installed	-----	-----
surface water	SW	2.3	-----	-----	0.8	-----	-----
		-----			-----		
		-----			-----		

		9 October 2007			3 February 2008		
		replicates	mean	std. dev.	replicates	mean	std. dev.
buffer piez.	PCR3	0.1	0.1	0.0	0.2	0.2	0.0
		0.1			0.2		
		0.1			0.2		
in-stream piez.	PCS0	-----	-----	-----	0.2	0.2	0.0
		-----			0.2		
		-----			0.2		
	PCS3	Not installed	-----	-----	0.6	0.6	0.0
					0.6		
					0.6		
surface water	SW	0.6	0.6	0.0	1.0	1.0	0.0
		0.6			1.0		
		0.6			1.0		

		31 July 2008			22 August 2008		
		replicates	mean	std. dev.	replicates	mean	std. dev.
buffer piez.	PCR3	0.2	0.1	0.1	0.0	0.0	0.0
		0.0			0.0		
		0.0			0.0		
	PCR3 D	Not installed	-----	-----	Not installed	-----	-----
	PCR4	0.1	0.1	0.1	0.0	0.0	0.0
		0.1			0.0		
		0.2			0.0		
	PCR4 D	Not installed	-----	-----	Not installed	-----	-----
	PCR5	7.5	7.2	0.2	5.2	5.2	0.0
		7.1			5.2		
		7.1			5.2		
in-stream piez.	PCS0	0.0	0.0	0.0	0.0	0.0	0.0
		0.1			0.0		
		0.0			0.0		
	PCS3	6.8	6.8	0.0	5.8	5.8	0.0
		6.8			5.8		
		6.8			5.8		
monitoring well	MW-4	Not installed	-----	-----	4.2	4.2	0.0
					4.2		
					4.2		
surface water	SW	1.0	1.0	0.0	0.7	0.7	0.0
		1.1			0.7		
		1.0			0.7		

		30 January 2009			19 July 2009		
		replicates	mean	std. dev.	replicates	mean	std. dev.
buffer piez.	PCR3	0.3	-----	-----	0.4	-----	-----
		-----			-----		
		-----			-----		
	PCR3D	Not installed	-----	-----	4.1	-----	-----

	PCR4	0.3	-----	-----	1.2	-----	-----
		-----			-----		
		-----			-----		
	PCR4D	Not installed	-----	-----	3.6	-----	-----

	PCR5	6.5	-----	-----	6.8	-----	-----
		-----			-----		
		-----			-----		
in-stream piez.	PCS0	0.3	-----	-----	0.7	-----	-----
		-----			-----		
		-----			-----		
	PCS3	7.1	-----	-----	5.5	-----	-----
		-----			-----		
		-----			-----		
monitoring well	MW-4	2.5	-----	-----	7.0	-----	-----
		-----			-----		
		-----			-----		
surface water	SW	2.0	-----	-----	0.7	-----	-----
		-----			-----		
		-----			-----		

Table E.4. Coal Kiln groundwater and surface water NO_3^--N (mg/L).

		2 June 2007			12 July 2007		
		replicates	mean	std. dev.	replicates	mean	std. dev.
buffer piez.	CKR1	Not installed	-----	-----	0.0 0.0 0.0	0.0	0.0
	CKR2	Not installed	-----	-----	4.6 4.5 4.6	4.6	0.0
	CKR3	Not installed	-----	-----	Not installed	-----	-----
in-stream piez.	CKS1	ND ND ND	-----	-----	0.0 0.0 0.0	0.0	0.0
	CKS2	Not installed	-----	-----	0.0 0.0 0.0	0.0	0.0
surface water	SW	2.4 ----- -----	-----	-----	2.5 2.4 -----	2.4	-----

ND: not detected

		8 August 2007			9 October 2007		
		replicates	mean	std. dev.	replicates	mean	std. dev.
buffer piez.	CKR1	0.1 0.0 0.0	0.0	0.0	0.1 0.1 0.1	0.1	0.0
	CKR2	3.5 3.5 3.4	3.5	0.1	1.3 0.8 0.4	0.9	0.5
	CKR3	Not installed	-----	-----	4.8 4.7 4.8	4.8	0.1
in-stream piez.	CKS1	0.4 0.4 0.2	0.4	0.1	----- ----- -----	-----	-----
	CKS2	0.2 0.1 0.0	0.1	0.1	0.5 0.4 0.2	0.3	0.1
surface water	SW	2.6 ----- -----	-----	-----	2.8 2.7 2.8	2.8	0.0

		3 February 2008			1 August 2008		
		replicates	mean	std. dev.	replicates	mean	std. dev.
buffer piez.	CKR1	3.2	3.3	0.1	0.0	0.0	0.0
		3.3			0.0		
		3.3			0.0		
	CKR2	0.2	0.2	0.0	2.1	2.2	0.0
		0.2			2.1		
		0.2			2.2		
	CKR3	6.4	6.2	0.2	6.5	6.4	0.1
		6.0			6.3		
		6.3			6.4		
in-stream piez.	CKS1	-----	-----	-----	0.0	0.0	0.0
		-----			0.0		
		-----			0.0		
	CKS2	0.2	0.2	0.0	0.0	0.0	0.0
		0.2			0.0		
		0.2			0.0		
	CKS3	Not installed	-----	-----	0.0	0.0	0.0
					0.0		
					0.0		
surface water	SW	1.8	1.8	0.0	2.1	2.1	0.0
		1.8			2.1		
		1.8			2.1		

		22 August 2008		
		replicates	mean	std. dev.
buffer piez.	CKR1	0.0	0.0	0.0
		0.0		
		0.0		
	CKR2	3.8	3.8	0.0
		3.8		
		3.7		
	CKR3	6.6	6.6	0.0
		6.7		
		6.6		
in-stream piez.	CKS1	-----	-----	-----

	CKS2	0.0	0.0	0.0
		0.0		
		0.0		
	CKS3	0.0	0.0	0.0
		0.0		
		0.0		
monitoring well	MW-1	0.0	0.0	0.0
		0.0		
		0.0		
surface water	SW	2.5	2.5	0.1
		2.4		
		2.5		

Appendix F – Field dissolved oxygen, nitrate-N and sulfide data

Table F.1. Field DO, NO_3^--N and S^{2-} analytical results.

Site	Piezometer	Date	DO (mg/L)	NO_3^--N (mg/L)	S^{2-} (mg/L)
PCF	PCR4	29 July 2008	-----	0 – 0.25	-----
		31 July 2008	≤ 1	-----	0
	PCR5	29 July 2008	-----	1.25 – 1.5	-----
		31 July 2008	≤ 1	-----	-----
	PCS0	31 July 2008	≤ 1	-----	0.4
	PCS3	31 July 2008	1 – 2	-----	0
	PCR3	31 July 2008	1	-----	2
	PCR3D	19 July 2009	≤ 1	-----	-----
	PCR4D	19 July 2009	1 – 2	-----	-----
CK	CKS2	1 Aug 2008	1	-----	-----
	CKS3	1 Aug 2008	1 – 2	0	-----
	CKR1	1 Aug 2008	< 1	-----	-----
	CKR2	1 Aug 2008	1 – 2	-----	-----
	CKR3	1 Aug 2008	1 – 2	-----	-----
PCU	PCR1	19 July 2009	4 - 5	-----	-----
	PCR2	19 July 2009	4 - 5	-----	-----
	PCS2	19 July 2009	≤ 1	-----	-----

Notes: PCF – Phillips Creek floodplain
CK – Coal Kiln
PCU – Phillips Creek upland